ARMY SBIR FINAL REPORT

SEPTEMBER 1996

PHASE SIGNATURE ANTENNA DRIVE DIAGNOSTICS SYSTEM

ARMY CONTRACT NO. DASG60-96-C-0045

PREPARED FOR

U.S. ARMY SPACE AND STRATEGIC DEFENSE COMMAND
CONTRACT & ACQUISITION MANAGEMENT OFFICE
CSSD-CM-CK
P.O. BOX 1500
HUNTSVILLE, ALABAMA 35807-3801

BY

AI SIGNAL RESEARCH, INC.
3322 SOUTH MEMORIAL PARKWAY, SUITE 67
HUNTSVILLE, AL 35801
(205)880-1968

AI SIGNAL RESEARCH TECHNICAL REPORT TR-4021-96-09

AI SIGNAL RESEARCH
PROGRAM MANAGER: JEN JONG

ARMY
CONTRACT MONITOR: RICHARD RODGERS
CONTRACTING OFFICER: JOE W. WARD

DISCLAIMER NOTICE

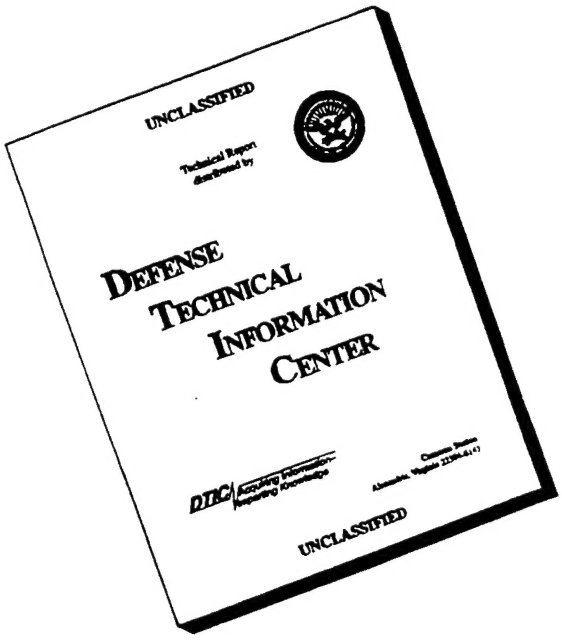

THIS DOCUMENT IS BEST QUALITY AVAILABLE. THE COPY FURNISHED TO DTIC CONTAINED A SIGNIFICANT NUMBER OF PAGES WHICH DO NOT REPRODUCE LEGIBLY.

REPORT DOCUMENTATION PAGE

Form Approved
OMB No. 0704-0188

1. AGENCY USE ONLY *(Leave blank)*	2. REPORT DATE	3. REPORT TYPE AND DATES COVERED
	September 1, 1996	Final Report/September 1996

4. TITLE AND SUBTITLE
Phase Signature Antenna Drive Diagnostics System

5. FUNDING NUMBERS
C
DASG60-96-C-0045

6. AUTHOR(S)
Dr. Jen-Yi, Jong

7. PERFORMING ORGANIZATION NAME(S) AND ADDRESS(ES)
AI SIGNAL RESEARCH, INC.
3322 South Memorial Parkway, Suite 67
Huntsville, AL 35801

8. PERFORMING ORGANIZATION REPORT NUMBER
TR-4021-96-09

9. SPONSORING/MONITORING AGENCY NAME(S) AND ADDRESS(ES)
SBIR Contracting Officer
U.S. Army Space and Strategic Defense Command
Contract & Acquisition Management Office
CSSD-CM-CK
P.O. Box 1500
Huntsville, Alabama 35807-3801

10. SPONSORING/MONITORING AGENCY REPORT NUMBER

11. SUPPLEMENTARY NOTES

12a. DISTRIBUTION/AVAILABILITY STATEMENT

12b. DISTRIBUTION CODE

13. ABSTRACT *(Maximum 200 words)*

ASRI proposes to design and demonstrate a Phase Signature Antenna Drive Diagnostics System (PSADDS) for incipient fault detection and diagnostics of drive system bearing/gear train components. The PSADDS utilizes ASRI's innovative Phase Signature Analysis (PSA) techniques developed for the Space Shuttle Main Engine failure detection. During Phase I, ASRI successfully conducted a Proof Of Concept study through a field test of MISA antenna drive-train system. The results demonstrated that the PSADDS can successfully monitor and identify critical bearing/gearbox signatures along with their underlying causes. In addition, several unique requirements and considerations such as interference of air blower noise have been identified, which would be critical to the development of the ALTAIR drive health monitoring system. The Phase I study demonstrated that PSADDS can overcome these inherent problems, reduce mis-interpretation rates and greatly improve system reliability. Phase I identified the best format to represent monitoring signatures for the drive train components. Phase I used real-world data from the MISA antenna to establish feasibility of PSADDS as a reliable ALTAIR health monitoring system. The Phase II SBIR objective is to build PSADDS for demonstration and implementation on the ALTAIR antenna. A commercial system for industrial application will be developed in Phase III.

14. SUBJECT TERMS	15. NUMBER OF PAGES
Bearing/Gearbox Monitoring, Bi-coherence, Rotary Machinery Spectrum Analysis, Radar Antennas, Phase Synchronized Enhancement	64
	16. PRICE CODE

17. SECURITY CLASSIFICATION OF REPORT	18. SECURITY CLASSIFICATION OF THIS PAGE	19. SECURITY CLASSIFICATION OF ABSTRACT	20. LIMITATION OF ABSTRACT
Unclassified	Unclassified	Unclassified	

NSN 7540-01-280-5500

Standard Form 298 (Rev-2-89)
Prescribed by ANSI Std. Z39-18 298-102

PHASE I TECHNICAL SUMMARY

Machinery health monitoring and diagnostics have long provided significant technical challenges in the defense, manufacturing and transportation industries. In Phase I, ASRI assessed and evaluated a diagnostic system designed to provide the Army an early detection capability for antenna drive defects and associated bearing wear problems. Specific application is the U.S. Army ALTAIR. ASRI submitted a Phase II proposal to finalize the design and demonstrate a Phase Signature Antenna Drive Diagnostics System (PSADDS). PSADDS will utilize ASRI's innovative Phase Signature Analysis (PSA) techniques developed for the detection of Space Shuttle Main Engine failure. The primary objective during Phase I was to asses feasibility of PSADDS through the acquisition and analysis of field test data from an operational antenna. Data was obtained by instrumenting an azimuth drive train on the Millstone Hill Steerable Antenna (MISA) located at the MIT Lincoln Laboratory, Haystack Observatory. More than 24-hours of dynamic data were acquired from 13 instrumentation channels that measured characteristic signatures for critical drive train components as shown in Figures 1(a) and 1(b). Phase I demonstrated that PSADDS can successfully monitor and identify critical bearing/gearbox signatures and their underlying causes.

Data analysis focused on: (1) identification of characteristic frequencies associated with the rotordynamic properties of drive system components; (2) identification of spectral contents of the various component dynamic signatures; (3) establishment of causality through comparisons of characteristic frequencies with spectral content; and (4) identification of anomalies that would indicate possible defects in drive system components. Drive train component signatures reveal clean signals with a high density of synchronous and related harmonic content. Correlation with mechanical system characteristic frequencies have been successfully performed to establish causality. In addition, several unique requirements and considerations which would be critical to the development of the ALTAIR drive health monitoring system were identified. These include the following:

(1) RF interference during UHF antenna operation introduces a high level of corruption in the test measurements which, for an operational system, will dictate either: (a) extensive RF shielding; or (b) a requirement for periodic drive system calibration runs with radar turned off.

(2) The measurements across the MISA drive train are subject to strong interference from air blower noise and vibration. Identification of such interference can be effectively achieved using a nonlinear coherence analysis technique to determine whether a spectral component is associated with air blower interference. Due to the lack of phase information among different frequency components, such nonlinear correlation can not be identified through conventional linear spectral/correlation analysis techniques.

(3) The results of MISA antenna test data indicate that, due to non-stationary antenna operation and robust signature detection, the best method to generate a frequency spectrum signature of drive components should be a "Normalized" PSEM PSD with respect to Sync frequency rather than ordinary "Raw" PSD. Figure 2(a) and 2(b) show the raw PSD and PSEM PSD of MISA's inside motor bearing measurement. The PSEM PSD can: (a) identify non-sync-related anomalies due to air blower noise interference, such as the peaks marked "12Nb-N," "12Nb+N," 12Nb+2N," ... "12Nb+4N" with broad bandwidth; and (b) identify sync-related bearing signatures, such as the bearing-related anomalies marked "A1" and "A2."

(4) Computation of bearing characteristic frequencies is straightforward; however, other factors such as nonlinear interaction cause problems in detecting the bearing defect signatures. Such nonlinear phenomenon was observed in the MISA's drive motor bearing test data. Phase I demonstrated that the proposed bi-coherence analysis technique can effectively detect and identify such nonlinear modulation/sideband patterns associated with various bearing defects

A reliable health monitoring system such as PSADDS can prevent catastrophic failures and significantly reduce down-time by flagging potential problems before they occur. Using MISA test data, Phase I has shown that conventional spectral analysis techniques would not be effective either: (a) in representing the best frequency spectrum as diagnostic signature; or (b) in detecting and discriminating the noise from the air blower, due to the lack of phase information among different frequency components. However, phase information of machinery vibration signals can play a significant role for fault diagnostics and better identify well hidden defect symptoms which are often unidentifiable using conventional spectral analysis. Using ASRI's PSA techniques overcomes these limitations associated with the ALTAIR.

Figure 1(a):Picture of the instrumented drive train of the MISA Azimuth Drive

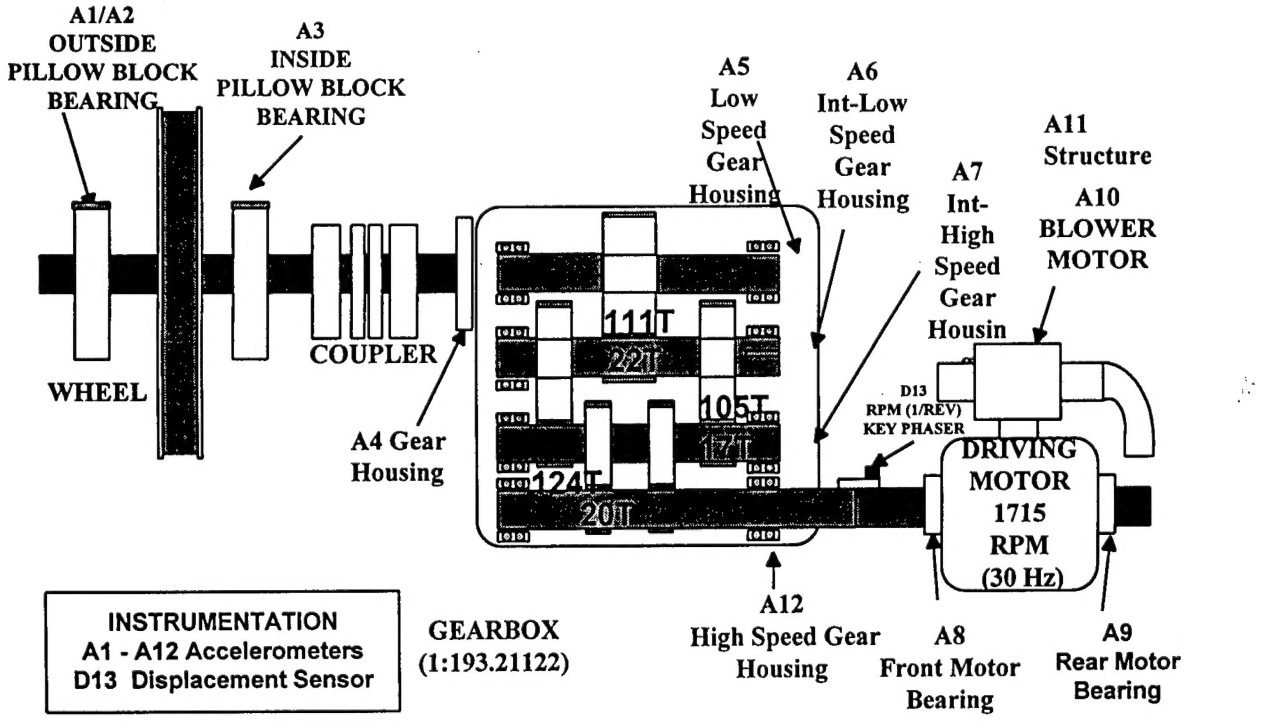

Figure 1(b): Schematic of the MIT Haystack Observatory MISA Azimuth Drive Train Showing Instrumentation Locations for Field Measurements Acquired During Phase I Test Program

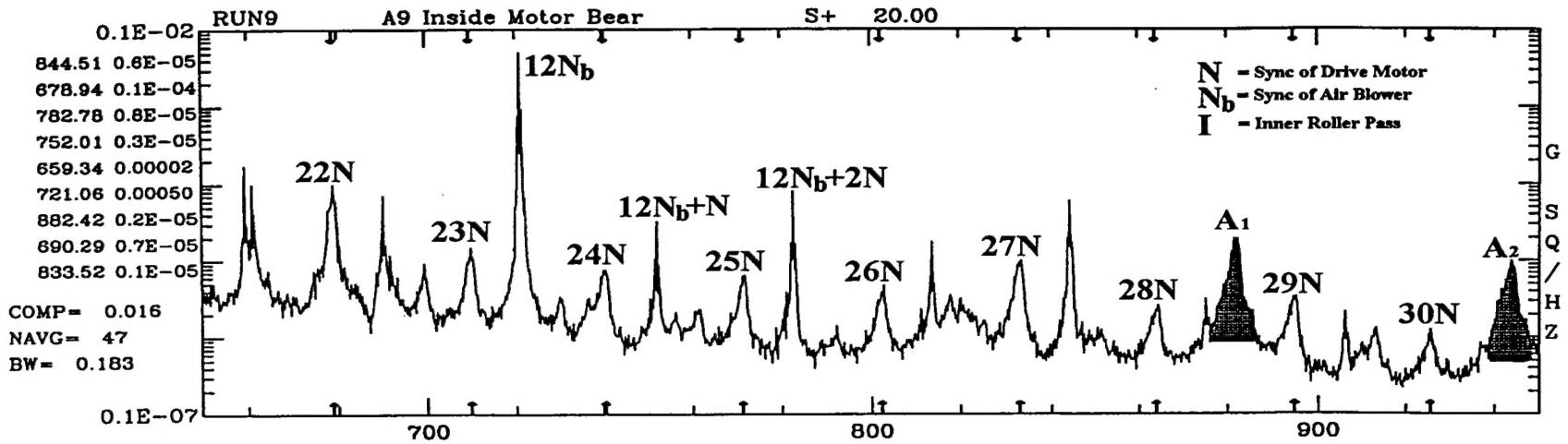

Figure 2(a): Ordinary "Raw" Power Spectral Density (PSD), Inside Motor Bearing

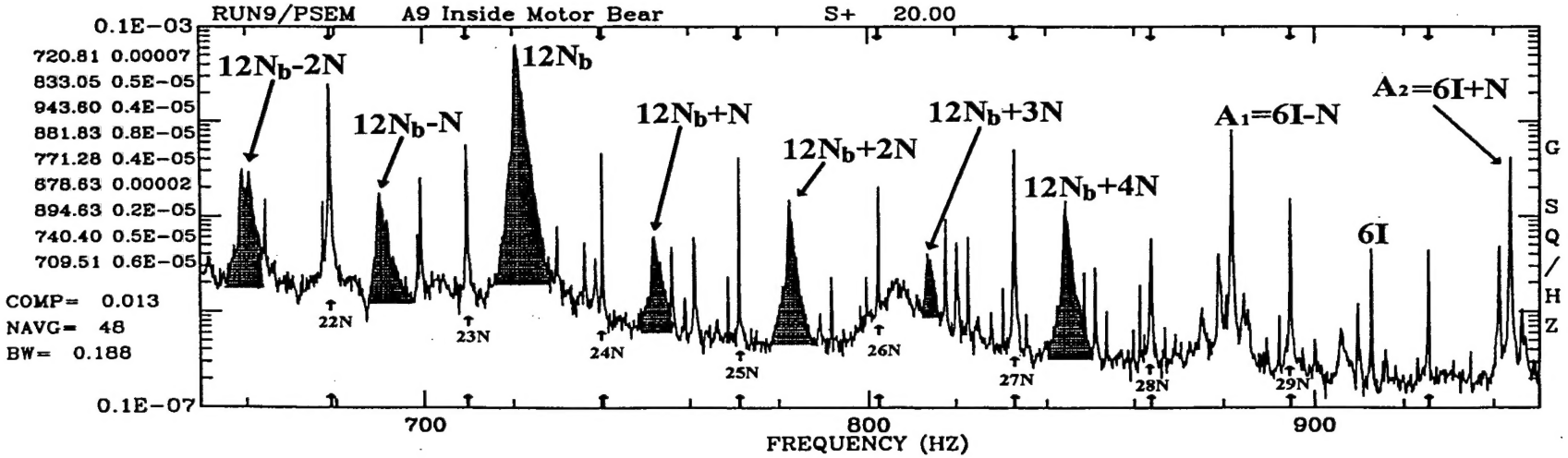

Figure 2(b): PSEM PSD: The Best Format for Antenna Spectum Signature
Discrete Peaks Indicate Drive Train Sync-Related Frequencies
Broad Peaks Indicate Non-Sync-Related (e.g. Due To Air Blower)

TABLE OF CONTENTS

Report Documentation Page (Standard Form 298) 1

Phase I Technical Summary (1 page text, 2 pages Diagram) 2

Table of contents 5

[1] Phase I Tasks Objectives 6

[2] Technical Problems 6

2.1 Phase I Proof-Of-Concept Study Through Field Test of MISA Antenna 7

2.2 Field Tests & Mechanical Assessment of MISA Antenna Drive 7

2.3 Preliminary Test Data Analysis of MISA Antenna Drive Train 8

2.4 Technical Problems and Unique Requirement/Consideration identified from MISA Test 16

[3] General Methodology 16

[4] Technical Approaches and Results 19

4.1 PSADDS System Software Design 19

4.1.1 Base-Line Data base (BLDB) Subsystem 19
4.1.2 Anomaly Detection (AD) Subsystem 20
4.1.3 Anomaly Identification (AI) Subsystem 21

4.2. Proposed Solutions for the Unique Requirement and Consideration of ALTAIR Health Monitoring Based on MISA Field Test Data 23

4.2.1 Interference from RF radiation 23
4.2.2. Interference due to air blower noise and vibration 23
4.2.3. Best method to generate frequency spectrum signatures 30
4.2.4. Detection of Bearing Signature due to Nonlinear Interaction 43
4.2.5. Gearbox Monitoring of MISA Antenna 49

[5] Important Findings and Conclusions 52

[6] Implications for Future Research 55

[7] Significant Hardware Development 60

7.1 Remote Modules 60

7.2 Host Module 63

[8] Special Comments 64

[1] PHASE I TASKS OBJECTIVES

The overall objective of the SBIR program is to develop a Phase Signature Antenna Drive Diagnostics System (PSADDS) utilizing our innovative Synchronous Phase Analysis (SPA) technique for the ALTAIR antenna drive system. Principal Phase I objectives are to investigate optimal drive component signature through a preliminary field testing and demonstrate the relative benefits of Phase Signature Analysis (PSA) techniques along with the detectability study of various types of degradation and failure and their defect signatures. The specific tasks performed in phase I along with their objectives are:

1) Conducted a preliminary field test at the Millstone Hill Steerable UHF Antenna (MISA) located at the MIT Lincoln Laboratory, Haystack Observatory, Westford, MA, by instrumenting one of the two azimuth drive trains. Over 24-hours of dynamic data were acquired for thirteen instrumentation channels that measured characteristic signatures for critical drive train components.

2) Performed detailed test data analysis to investigate the optimal antenna drive component defect signatures along with their detectability associated with various types of degradation/failure modes. **Identified the best method to generate a frequency spectrum signature of antenna drive components for on-line health monitoring.**

3) Demonstrated the effectiveness and relative benefits of phase signature analysis techniques over conventional methods in detecting and identifying defect signatures and false alarm. The measurements across the MISA drive train are subjected to strong interference from air blower noise and vibration. **Investigated the best way to process and identify the noise interference from neighboring air blower and/or lube pump vibration.**

4) Identified the environmental and operational requirements of the PSADDS vibration monitoring system (i.e., the optimal measurement locations, type and number of dynamic sensors, required system analysis bandwidth, signal processing methodology, noise interference, etc.) for ALTAIR antenna.

5) Developed a research plan for Phase II development of a prototype PSADDS system for testing, demonstration and operational implementation.

[2] TECHNICAL PROBLEMS

Bearing/gear train health monitoring and diagnosis has long been a significant technical challenge in the aeronautics, defense and transportation industries. A reliable health monitoring system can prevent catastrophic failures and strategically significant down time by flagging potential problems before failure occurs. Most machinery failures are generally preceded by growing tolerances, imbalance, bearing element wear, and the like, which may manifest themselves through subtle modifications in the waveform observed by vibration or acoustic measurements. As computer information processing technology continues to advance, new and innovative signal analysis methods for intelligent information extraction and interpretation have been developed. As a result, the ability to detect/identify defect signatures and false-alarms has become a major requirement of a reliable health monitoring system. Conventional frequency spectrum signature analysis has been a useful technique for defect signature identification. However, under a complex multi-rotor operational environment, vibration signals are often subjected to noise corruption and signal interference which can cause false detection/identification and greatly reduce the diagnostic reliability. The PSADDS will improve these inherent limitations using a hierarchy of novel Phase Signature analysis techniques for anomaly identification. Phase information of machinery vibration signals can play a significant role for fault diagnostics and better identifies well-hidden defect symptoms which are often unidentifiable using conventional spectral analysis. These techniques have been tested using rocket engine test and flight data, and proven to be highly promising for failure identification in other complex machinery. The significance of the proposed program is attributed to its signature understanding capability in discriminating between true defects or false-alarm signatures and can greatly enhance the power and reliability of the diagnostics system.

2.1 Phase I Proof-Of-Concept Study Through Field Test of MISA Antenna Drive system

This SBIR contract is of primary interest to personnel involved in the operation and maintenance of the ALTAIR antenna in Kwajalein. The ALTAIR's drive system consists of DC motors coupled to the drive pinions in both azimuth and elevation through Falk reduction gear boxes. The antenna rides on 16 wheels, mounted in four pivoting wheel bogies. Including the elevation axis bearings and a pintle bearing, there are 59 major bearings permitting articulation and pointing. Maintaining system operability and availability over extended periods is of significant importance to mission accomplishment. However, this antenna has a heavy operational schedule so it was not readily available to support Phase I field tests without several (4 to 6) months of advance planning. As an alternative to the ALTAIR antenna, discussions with MIT Lincoln Lab led to identification of the Millstone Steerable UHF antenna (MISA) operated by the MIT Haystack Observatory in Westford, MA as a candidate test bed for Phase I. The total weight of the MISA antenna is approximately one-half that of ALTAIR antenna, however, the drive systems are similar with MISA having a much lower drive horsepower. For the Phase I proof of concept study, MISA should serve to adequately replicate the ALTAIR drive system.

In order to develop an effective antenna dive health monitoring system, a detailed "audit" of MISA Antenna drive system components was performed to:

- Define the universe of mechanical components to categorize potential failure modes and associated candidate detection methodologies.
- Estimate kinematic relations associated with component operation over the system performance envelope (e.g. bearing characteristic frequencies, gear train frequencies, etc.).
- Identify candidate measurement locations and ranges.
- Review any available diagnostic measurements and/or existing procedures.
- Identified the best method to generate a frequency spectrum signature of antenna drive components for on-line health monitoring.
- Investigated the best way to process and identify the noise interference from neighboring air blower and/or lube pump vibration.
- Identify the optimal signal processing methodology for on-line ALTAIR antenna health monitoring system.

2.2 Field Tests and Mechanical Assessment of MIT MISA Antenna Drive system

Field tests were successfully conducted during Phase I on May 13 through May 15, 1996. An inspection of MISA was conducted to identify favorable instrumentation locations on the MISA drive system. Sensor locations were selected for each major drive component of one of the two main azimuth drive trains. Sensors were mounted to drive components, cabling and signal conditioning electronics were installed and routed to a 14-channel FM tape recorder, and end-to-end continuity checks were performed. Following shunt calibrations, shakedown test runs of the azimuth drive systems were performed to acquire preliminary data prior to antenna operations. Test measurements were acquired for a total of 12 accelerometer channels and one proximity sensor used as a tachometer. Figure 1(a) shows the drive train of the MISA Azimuth Drive, and the corresponding instrumentation locations within the drive train for the MISA test is shown in Figure 1(b). A detailed "audit" of drive system components was performed. The bearing/gear components within the MISA Azimuth Drive system along with their associated bearing/gearmesh characteristic frequencies have been established. Figure 3 shows the schematic of the Gear Train which includes the low speed gear, the intermediate low speed gear and pinion, intermediate high speed gear and pinion, and high speed pinion. Table 1 lists the three gearmesh frequencies within the gearbox. The roller/ball bearing component characteristics along with the fundamental bearing characteristic frequencies within the MISA Azimuth Drive system are listed in Table 2. Accelerometer and

proximity measurements were taken at the following locations (A1, A2, D13 are denoted as Measurement ID).

Main 36-inch Drive Wheel
- A1 - Outer Pillow Block (90 degree)
- A2 - Outer Pillow Block (180 degree)
- A3 - Inner Pillow Block

Gear Train
- A4 - Low speed Output
- A5 - Low Speed Input
- A6 - Intermediate Low-Speed Gear Train Inputs
- A7 - Intermediate High-Speed Gear Train Inputs
- A12 - High Speed Input

DC Electric Drive Motor
- A8 -Front End Bearing
- A9 -Back End Bearing

Drive Motor Cooling Blower
- A10 - Blower Housing

Antenna Structure
- A11- Lower Structural Arm connected to Drive Assemble

Key Phasor
- D13 - Proximity sensor: one blip per revolution on the motor drive shaft

The proximity sensor provided a key phasor by recording one blip per revolution as triggered by the high speed rotation of a key on the motor drive shaft (nominal 1715 rpm). Approximately 13 hours of test data were first recorded during antenna operation. A preliminary review of the data taken during antenna operations show a high-level of RF interference. Subsequently, approximately 2-hours of azimuth drive system vibration data with the antenna turned off (i.e. no RF interference) were acquired. For these tests, the antenna drive operated continuously through alternating clockwise-counterclockwise, 360 degree azimuth excursions. Test data acquired during field test with the antenna turned off was digitized and stored on computer disk and tape for subsequent detailed signature analysis at ASRI's SUN Workstation computer system.

2.3 Preliminary Test Data Analysis & Review of MISA Antenna Drive Train

Clearly, a comprehensive baseline database of signatures and trends for all critical components is beyond the scope of Phase I investigation since the creation of such a database requires longer period of monitoring effort. In addition, it was not permissible to plant seeded faults into the MISA drive train during the Phase I field test. Instead, the objective of this POC study was to obtain a representative sample of vibration signatures associated with various components within the drive train. Based on this representative information under actual MISA antenna operation environment, a number of unique requirements or considerations that would be critical for the successful development of ALTAIR drive health monitoring system have been identified. These unique requirements and considerations play a significant role in the determination of the best method for generating frequency spectrum signatures for health monitoring. In this section, preliminary test data analysis from the MISA drive train testing will be discussed.

Gear Component	# of Teeth	# of Pinion	Sync (In Test)	RPM	Hz	GearMesh Frequency (Hz)	
High Speed Gear Train	0	20	N1=	1851.17	30.8529	M1=20N1=	617.06
Intermediate High Speed Gear Train	124	17	N2=20/124 N1=	298.576	4.976274194	M2=17N2=	84.60
Intermediate Low Speed Gear Train	105	22	N3=17/105 N2=	48.3409	0.805682488	M3=22N3=	17.73
Low Speed Gear Train	111	0	N4=22/111 N3=	9.58109	0.159684818		

Table 1 GearMesh Frequencies of MISA Azimuth Drive Train

Bearing/Model	Accel	Sync (Hz)	# of Roller	Ball Diam	Pitch Diam	C. Angle	Cage N/Hz	BS N/Hz	IRP N/Hz	ORP N/Hz
Inner Motor Brg	A9/A10	30.8529	8	0.4688	2.1063	0	0.388714808	2.13520031	4.890281536	3.1097185
207SZ							11.9929791	65.8771215	150.8793672	95.943833
Outer Motor Brg	A8/Key	30.8529	7	0.7188	2.8544	0	0.374089126	1.85962593	4.381376121	2.6186239
309SF							11.54173438	57.374853	135.1781593	80.792141
High Speed Gear	A12	30.8529	13	0.6867	3.7409	0	0.408217274	2.63204602	7.693175439	5.3068246
MA1312UV							12.59468673	81.2062526	237.3567725	163.73093
Int High Spd Gea	A7	4.9762742	13	0.6867	3.7409	0	0.408217274	2.63204602	7.693175439	5.3068246
MA1312UV							2.031401086	13.0977827	38.2833504	26.408214
Int Low Spd Gear	A6	0.8056825	14	0.7409	4.0362	0	0.408218126	2.63207216	8.284946237	5.7150538
MA5313TV							0.328894196	2.12061445	6.675036101	4.6045187
Low Speed Gear	A5/A4	0.1596848	19	1.079	7.7619	10.28	0.431609578	3.52730036	10.79941802	8.200582
22228LBCO							0.068921497	0.56325631	1.724503096	1.3095084
Inner Wheel Brg	A3	0.1596848	27	1.1417323	10.96367188	8.35	0.448483077	4.74926647	14.89095692	12.109043
23044KMB							0.071615938	0.75838575	2.377859739	1.9336303
Outer Wheel Brg	A1/A2	0.1596848	24	1	8.570866142	8.35	0.442281245	4.22709939	13.38525011	10.61475
23034							0.0706256	0.67500359	2.137421221	1.6950144

Table 2 Bearing Characteristic Frequencies of MISA Azimuth Drive Train

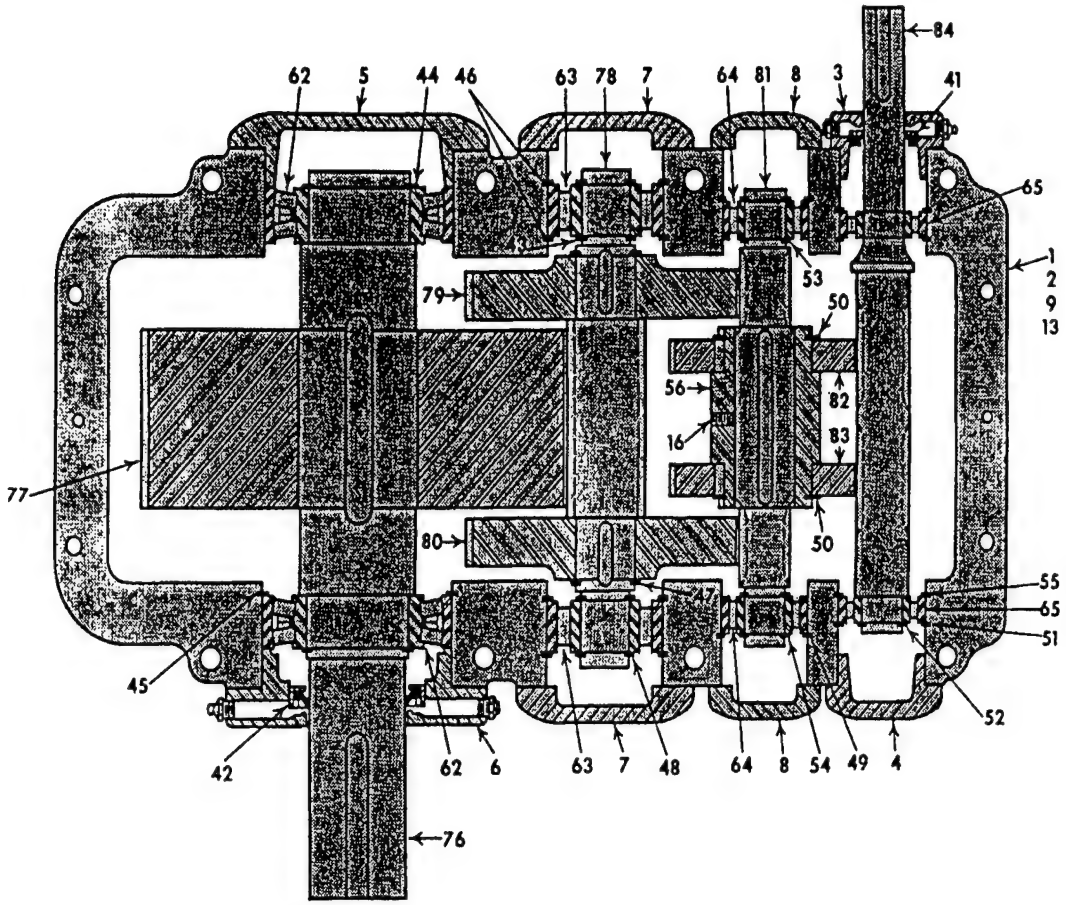

Locator	Description	Quantity required
1-2	Housing (consists of assembled base and cover)	1
3	High speed retainer, open type	1
4	High speed retainer, closed type	1
5	Low speed retainer, closed type	1
6	Low speed retainer, open type	1
7	2nd intermediate speed retainer, closed type	2
8	1st intermediate speed retainer, open type	2
9	Inspection cover	1 or 2
13	Inspection cover gasket	1 or 2
16	Setscrew	1
41	High speed oil seal	1
42	Low speed oil seal	1
43-55	Retaining rings	As req'd
56	Sleeve	1
62	Low speed bearing	2
63	2nd Intermediate speed-bearing	2
64	1st Intermediate speed bearing	2
65	High speed bearing	2
76	Low speed shaft and keys	1
77	Low speed gear	1
78	Low speed pinion with integral shaft, and keys	1
79	Intermediate speed gear (furnished with Locator 80)	1
80	Intermediate speed gear (furnished with Locator 79)	1
81	Intermediate speed pinion with integral shaft and keys	1
82	High speed gear (furnished with Locator 83)	1
83	High speed gear (furnished with Locator 82)	1
84	High speed shaft with integral pinion, and key	1

Figure 3: Schematic of the Gear Train of MISA Azimuth Drive

Figure 4 shows the time history of all the 13 measurements (12 accelerometer and 1 proximity) during a full 360 degree azimuth excursion in the counterclockwise (CCW) direction with the antenna turned off (i.e. no RF interference). These data were digitized at a sampling frequency of 3,000 Hz. The Test ID of this high frequency data is denoted by "RUN9". The measurement ID's (e.g. A1 Outside P. Bearing) are listed on the upper-right portion above each plot. The sync frequency of the drive motor is running at about 1715 RPM (or 30.85 Hz) during steady state operation. The "gap" near the beginning of the proximity measurement (D13) time history indicates the antenna comes to a complete stop after the previous full 360 degree azimuth excursions in the clockwise (CW) direction; while the gap near the end of the plot indicates the stop during the current excursions in the counterclockwise direction. A number of "spikes" are clearly observed in the Outside Pillow Block (A1) which are corresponding to the impact motion between the antenna wheel and the rail gaps on the circular track. The intensity and frequency of such impact motion can be better identified and monitored from the frequency domain spectra of the "envelop" signal which will be discussed in more details in section 4.2.2.

Figure 5 shows the time history of all the 13 measurements over 22.5 full azimuth excursions (360 degree) in alternating (CW and CCW) directions without RF interference. These data were digitized at a lower sampling frequency of 25 Hz. The Test ID of this low frequency data is denoted by "RUN9-LF". The periodic "spikes" in the proximity measurement time history represents the stop times between these 22 alternating-direction runs. These spikes were due to the transient responses of the anti-aliasing low pass filter since the frequency of the major spectral component in this key phasor measurement during steady state operation (ie. 30.85 Hz) is above the cutoff frequency in this low frequency data. It was also observed that several measurements (e.g. A4, A12) show alternating vibration levels as the antenna is rotating in alternating direction.

Figure 6 shows the joint time/frequency spectrogram of the Short Time Fourier Transform (STFT) of Outside Pillow Block Accel measurements (A1) over 22.5 full azimuth excursions from 0 to 1,000 Hz frequency. Each line within this spectrogram represents a discrete PSD spectral component. The peak line marked "GM1" around 610 Hz represents the GearMesh frequency (GM1=20N1, where N1 is the Sync frequency of the drive motor) of the high speed gear train. The frequency of this GearMesh component shows a noticeable discrepancy in RMP between CW and CCW antenna operation. This spectrogram also shows many other sync-related components whose frequencies vary accordingly with the GM1. It should be noted that the frequencies of several spectral components in this figure (such as the peak lines marked "6Nb" and "12Nb" around 360 and 720 Hz) do not change with the GM1. It is anticipated that these two components should represent the harmonic frequencies of the Sync of the air blower (Nb). (The actual schematic of the air blower has not been identified by ASRI during Phase I survey).

Figure 7 shows the Power Spectral Density (PSD) functions of all 13 measurements from 0 to 1,000 Hz frequency over one full azimuth excursion in CCW directions. Figure 8 shows a detailed PSD for Accel measurement A8. The peaks marked "N1", "6*Nb", "GM1" and "GM2" represent the Sync of drive motor, the 6th Harmonic of Sync of the air blower, the GearMesh of the high speed gear train, and the GearMesh of the intermediate high speed gear train respectively. Most of the remaining spectral peaks are due to the Sync and harmonics of the shaft RPM of the drive motor (Sync N1 = 30.85 Hz) , the Sync and harmonics of the air blower (Sync Nb = 60 Hz), the interaction (or modulation) between drive motor (N1) and air blower (Nb), and many anomalous frequency components (anomalies). Some of these anomalies could represent critical defect signatures, while others may be nominal system response signals such as feedthrough from air blower or other elements within the drive system or inherent system structural modes. The complexity of the spectra content presents some difficulty in detecting and identifying defect signatures, especially in a systematic or unsupervised manner.

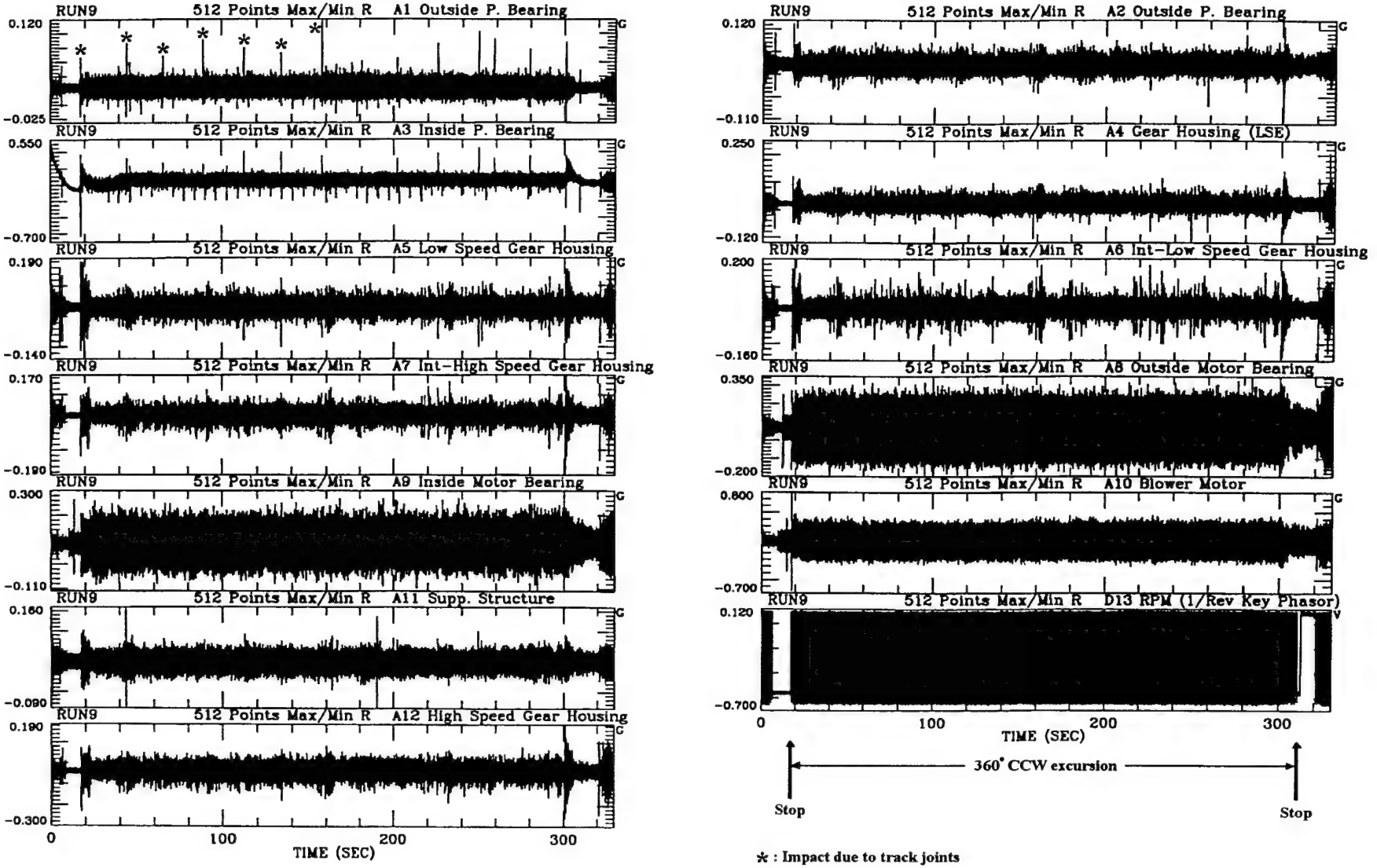

Figure 4: Time histories of 13 MISA Drive Measurements during one full 360 degree azimuth excursion direction without RF interference

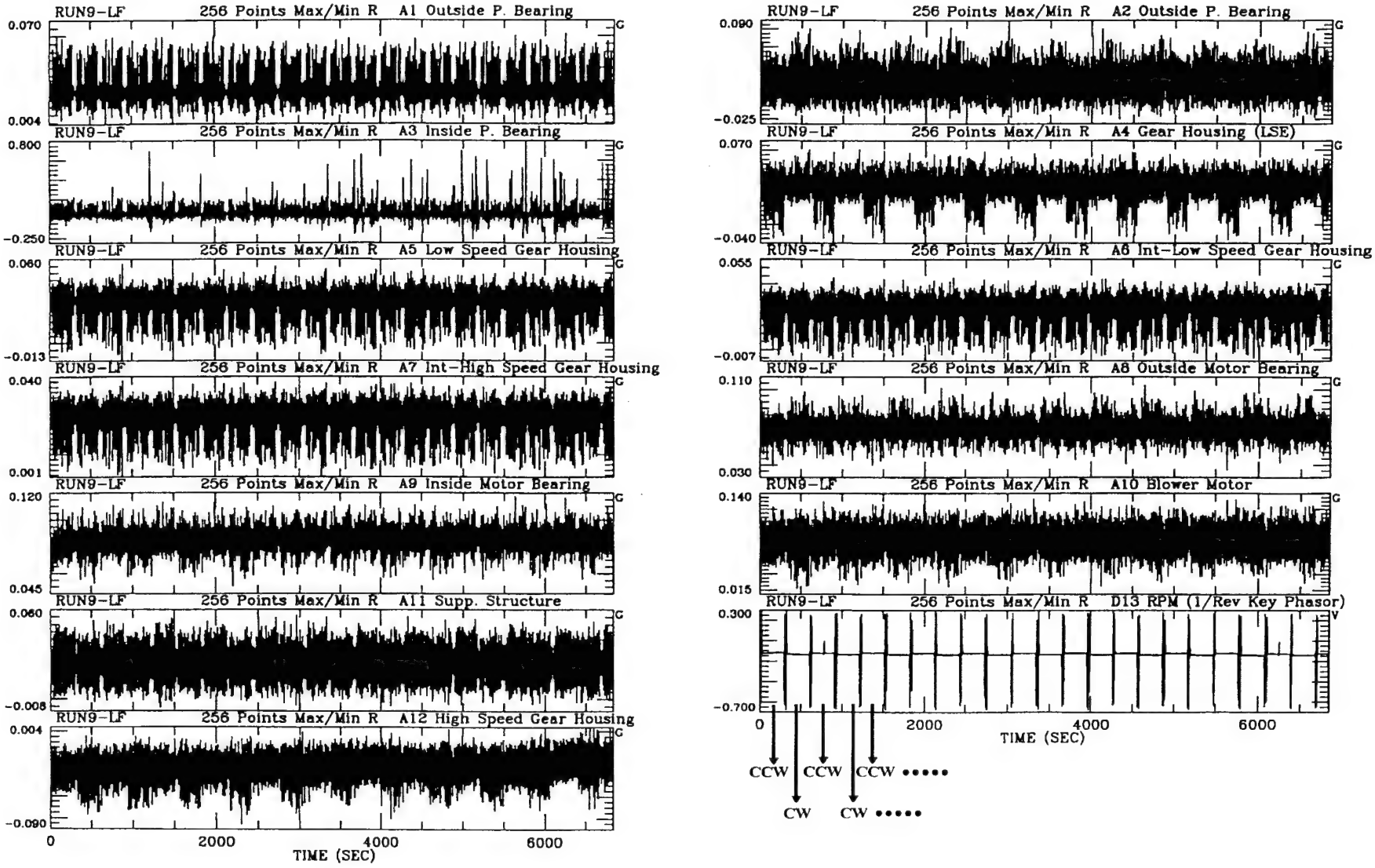

Figure 5: Time history of 13 MISA Drive measurements over 22.5 full azimuth excursions in alternating (CW and CCW) directions without RF interference

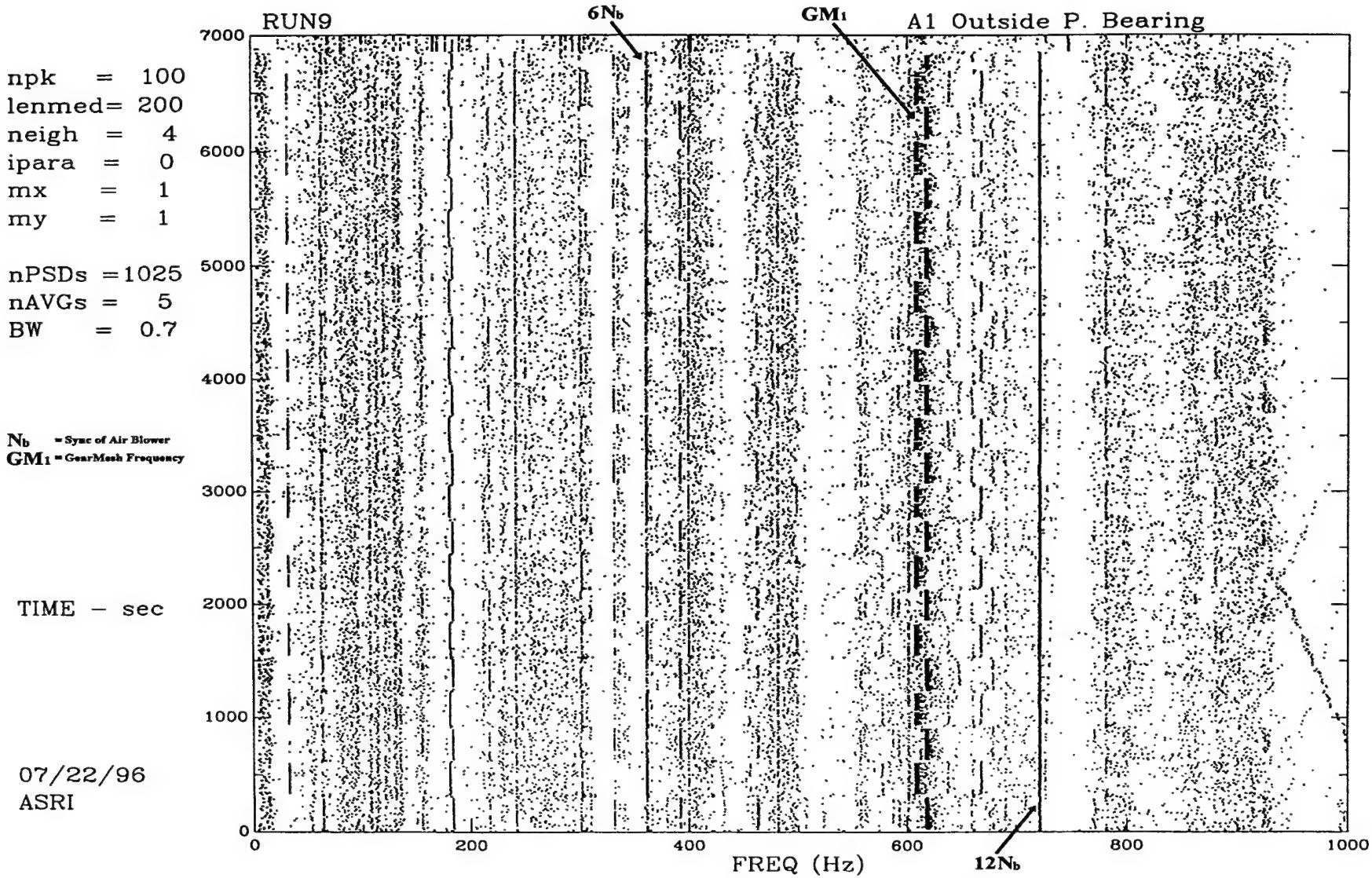

Figure 6: Joint Time/Frequency Spectrogram of Outside Pillow Block Accelerometer measurements over 22.5 full azimuth excursions

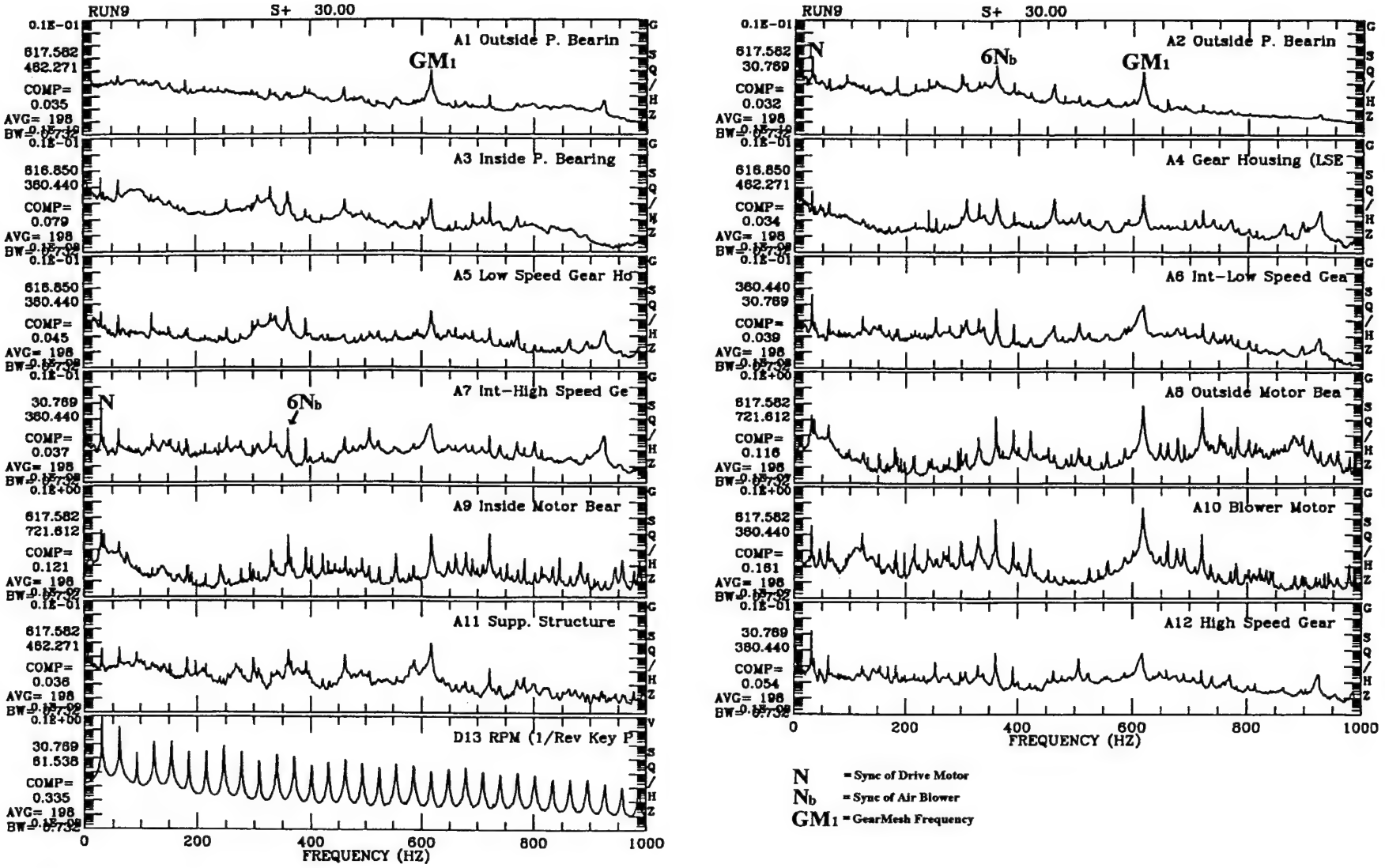

Figure 7: Power Spectral Density (PSD) functions of 13 MISA Drive measurements over one full azimuth excursion in CCW directions

2.4 Technical Problems and Unique Requirement/Consideration identified from MISA Test

As previously stated, one of the major objectives of this Phase I was to identify any unique requirement or consideration that would be critical for the development of a health monitoring system for the ALTAIR drive train. Based on the representative information obtained from MISA test data during antenna operations, the following four major requirements and considerations have been identified:

1. **Interference from RF radiation.**
2. **Interference and corruption due to air blower noise and vibration**
3. **Best method to generate frequency spectrum signatures of drive components.**
4. **Detection of Bearing Defect Signatures due to Nonlinear Interaction.**

These unique requirements and considerations play a significant role in the determination of the best method for generating frequency spectrum signature for health monitoring. As will be discussed in section 4.2, based on the Proof-Of-Concept study using the actual MISA test data, effective solutions have been identified which can deal with these special requirements and considerations in developing a reliable ALTAIR drive health monitoring system.

[3] GENERAL METHODOLOGY

Machinery failure prediction is based on observing and recognizing measurable phenomena that occur as a result of nominal system operation and those associated with components degradation. Most failures are generally preceded by growing tolerances, imbalance, bearing element wear, and the like, which may manifest themselves through subtle modifications in the waveform observed by vibration or acoustic measurements. The frequency content of the modified waveform usually contains valuable signatures for failure prediction and failure-mode identification. For this reason, signal analysis has become one of the most important elements in machinery diagnostics. Improving system reliability has required a more complete understanding of the vibration signals associated with various failure mechanisms.

The applications and limitations of ferrous debris magnetic collectors and non-ferrous spectrometric oil analysis diagnostic techniques are described in references 1 through 6. These articles indicate the need for analytical methods for determining the nature of fault signal generation and propagation in a faulty drive train. The fault signals generated are induced by rotational excitation, impact excitation, and shaft speed modulation (AM or FM) while fault signal propagation's are traversed by stress waves or acoustic waves. Additionally, the phenomena of mechanical resonance can be produced by the forced excitation of an objects natural frequency, gear disc or shaft. Candidates for computer based analytical diagnostics of impending fatigue failures in drive trains, for example, are listed in Table 3. The effectiveness of these diagnostic methodologies are degraded, by the following phenomena: noise contamination, signal isolation problems, dynamic frequency response limitations, transmissibility attenuation between excitation point and response point, or interactive damping masks. Slow moving components of the ALTAIR system pose unique problems, and also opportunities.

1) ACOUSTIC EMISSIONS ANALYSIS (PIEZOELECTRIC FILM COATING OR CRACK WIRE)
2) NATURAL FREQUENCY SIGNATURE ANALYSIS (NATURAL RINGING FREQUENCIES OF COMPONENTS)
3.) ACOUSTIC SIGNATURE ANALYSIS (ACOUSTIC SIGNALS FROM MICROPHONES)
4.) VIBRATION SIGNATURE ANALYSIS (BROADBAND DIRECTIONAL ACCELEROMETERS)

TABLE 3 CANDIDATES

ASRI's practiced experience in non-linear coherence diagnostic analysis methods (Ref. 7, 8), Bi-Coherence analysis (Ref. 9, 10) and Tri-Coherence analysis (Ref. 11, 12), directs that they can be utilized in ALTAIR fault detection, specifically, when tooth spacing errors or defects in gear sets and bearings cause impact events; these types of quasi-periodic oscillations result in AM and FM modulations. Non-linear analysis can determine the modulation contributions by examining the phase relationships in the sidebands and enhance the SNR by examining the coherence between corresponding side bands of different clusters.

This leads to determining whether the modulation frequency is sync, Ball/Roller train or structural natural frequency in origin, depending on the fault mechanism. Conjunctionally, ASRI has utilized Instantaneous Frequency Correlation (IFC) (Ref. 13, 14, 15), and Phase Synchronized Enhancement Method with Time Domain Average (Ref. 16, 17) to diagnose bearing fault conditions. The instantaneous frequency/phase (IF/IP) information derived by the IFC from the spectra can identify well-hidden modulation phenomenon associated with bearing defects.

The PSEM technique developed by ASRI utilizes the IF/IP information to transform the quasi-periodic sync component into a pure-tone discrete component. This process converts a signal with constant-time sampling into a constant-phase sampling interval; which is analogous to external sampling which adjusts the sampling rate with rotational speed variation. The Synchronous Phase Averaging (SPA) method, which by TDA averaging the PSEM signal, can improve the SNR of the spectra signal. This SPA is superior to classical synchronous time averaging (STA), because the complete cycle of data points within each ensemble is synchronized to the rotating shaft rather than just the first sample as for the case of classical STA. Such an ideal averaging process as SPA provides a superior SNR enhancement capability.

REFERENCES:

[1] Tandon, N. and Nakra, B. C. "Defect Detection in Rolling Element Bearings by Acoustic Emission Method", Journal of Acoustic Emission, Volume 9, NO. 1.

[2] Rose, H. J. "Diagnostic System Research Applicable to Helicopter Transmissions", 44th MFPG Meeting, Cavalier Hotel, Virginia Beach, Virginia. USA, April 1990.

[3] Gadd, P., "The Integration of health Monitoring Techniques for Helicopter gearboxes", eleventh European Rotor Craft Forum, London, England.

[4] Stewart, R. M. et al, "Monitoring of Rotorcraft Dynamic Systems". Stewart Hughes Ltd. Document SHL/162, February 1985.

[5] Astridge, D. G., "Helicopter Manufacturer's Requirements and Experience with Advanced HUM Systems on Westland Helicopters", MechEng Aerospace Industries Division Publication, Health and Usage Monitoring in Helicopter Mechanical Systems. April 1986

[6] Astridge, D. G., "Vibration Health Monitoring of the Westland 30 Helicopter Transmission - Development and Service Experience", 41st MFPG Meeting, NATC Patuxent River, Maryland, USA, October 1986.

[7] Broyles, W. R. and M. A. Deatt. "Analysis of bandpass Signal on the HP Fourier Analyzer", GE Technical Information Series, NO 80, POD3, 1980.

[8] Ktonas, W. R. and Nicola Papp. "Instantaneous Envelope and Phase Extraction from real Signal: Theory, Implementation, & Application to EEG Analysis", Signal Processing, Volume 2, NO. 4, October 1980.

[9] Jong J., Jones J., Jones P., Nesman T., Zoladz T., Coffin T., "Nonlinear Correlation Analysis for Rocket Engine Turbomachinery Vibration Diagnostics", 48th Meeting of the Mechanical Failure Prevention Group (MFPG). April 1994.

[10] Jong J. Y. and Coffin T., "Diagnostic Assessment of Turbomachinery by the Hyper-Coherence Method", NASA Conference Publication 2436, Advanced Earth-to-Orbit Propulsion Technology, May 1986.

[11] Jong J. Y. and Coffin T., "A Nonlinear Coherence Function and Its Application to Machine diagnostics", 110th Meeting of the Acoustical Society of America, November 1985.

[12] Jong J., Jones J., McBride J., "Some Recent Development in Turbomachinery Fault Detection", NASA Conference on Advanced Earth-to-Orbit Propulsion Technology, 1992.

[13] Dowling, Martin, AM and FM Digital Demodulation Technique for Electric Power. Final Report to Naval Ship Systems Engineering Station, FRC Project 5847-05, -13, Feb., 1984.

[14] Jong J., Jones J., McBride J., Coffin T., "Correlation Identification Between Spectral Components in Turbomachinery Measurements by Generalized Hyper-Coherence", 3rd International Machinery Monitoring And Diagnostic Conference, December, 1991.

[15] Jong J., Jones J., "Anomaly Identification for Space Shuttle main Engine Diagnostics" 48th Meeting of Mechanical Failure Prevention Group (MFPG). April, 1994.

[16] Mc Fadden, P. D. "Interpolation Techniques for the Time Domain Averaging of Vibration Data with Application to Helicopter Gear Box Monitoring", Aero Propulsion Technical Memo 437, AR-004-448, DOD S&T. Aeronautical Research Lab., Australia, 1986.

[17] Jong J., Jones J., "Phase Synchronized Enhancement Method for Space Shuttle Main Engine Diagnostics". NASA Advanced Earth-to-Orbit Propulsion Technology, 1994.

[4] Technical Approaches and Results

The major objective of this program is to develop a Phase Signature Antenna Drive Diagnostics System (PSADDS) utilizing innovative Phase Synchronous Analysis (PSA) techniques to achieve on-line health monitoring capability of the ALTAIR antenna drive systems. During Phase I of this SBIR program, a proof of concept (POC) study was conducted by analyzing the drive train system test data from a field test of the operational Millstone Hill Steerable UHF Antenna (MISA) in order to demonstrate the feasibility and effectiveness of the PSADDS. The results from these studies demonstrated that the phase signature analysis techniques within the PSADDS can successfully monitor critical bearing and gearbox signatures within the drive train and identify extraneous disturbances such as the noise interference from the air blower and rail joint impulses. Most important, these real-world hardware applications prove the feasibility of the PSADDS as a reliable health monitoring system for ALTAIR antenna.

In the following subsections, the technical approach for the design and development of the PSADDS system will be discussed. Section 4.1 discusses the software design of PSADDS for the ALTAIR drive train monitoring system and its three major subsystems. Based on the Proof-Of-Concept study by analyzing actual MISA test data, a number of special requirements and considerations that would be critical for the development of the ALTAIR health monitoring system have been identified. A number of proposed solutions which can effectively deal with these special requirements and considerations will be discussed in section 4.2. Several examples from MISA Antenna test data using PSADDS signal analysis techniques will be discussed to demonstrate the effectiveness of PSADDS's innovative phase signature analysis in dealing with these special considerations.

4.1 PSADDS System Software Design

The PSADDS is an intelligent drive train health monitoring system design for ALTAIR. The PSADDS provides a systematic approach to automatically capture, reduce, store and analyze dynamic data during ALTAIR antenna operation. The PSADDS analysis suite is composed of the following three modules:

(1) **Base-Line Data Base (BLDB) Module** - Establishes the base-line history of a drive train vibration signal's dynamic content.

(2) **Anomaly Detection (AD) Module** - Detects anomalous signatures through trend and similarity analysis by comparing a machine's present condition against its base-line history established in the BLDB module.

(3) **Anomaly Identification (AI) Module** - Verifies whether an anomalous signature detected in the AD module is a false-alarm or misinterpretation.

4.1.1 Base-Line Data Base (BLDB) Module

The most fundamental element of the PSADDS system is the Base-Line Data Base (BLDB) module. The purpose of this module is to establish the knowledge history of the basic mechanical characteristics of each machinery and/or drive train component to be monitored. During routine monitoring, test data will be reduced into several basic dynamic signatures. A data base with these dynamic signatures will provide valuable information for trend analysis which is a critical element in any predictive maintenance program. A fundamental dynamic signature data base, the PSD-BLDB, will be created in the PSADDS system. The PSD (Power Spectral Density) function contains important dynamic information about a vibration signal. During routine monitoring, the BLDB subsystem will automatically reduce the raw signal into PSD format for each measurement. The frequency of the PSD will first be normalized with respect to the Sync (shaft rotational) frequency (e.g. the Sync of the drive motor of ALTAIR). The PSD-BLDB is composed of the average PSD amplitude for each normalized frequency line, along with its associated standard deviation. Over a period of time, an inventory of PSDs will be created for each type of measurement under various

operational conditions. This inventory provides the foundation for trend and similarity analysis in anomaly detection subsystem.

The Proof Of Concept Study performed during Phase I of the MISA antenna test data has demonstrated that our Phase Synchronized Enhancement Method (PSEM) can automatically perform frequency normalization during antenna operation in which case the Sync frequency of the drive train would be highly nonstationary due to the acceleration, deceleration and reversed direction of the antenna. With this frequency normalization capability, the PSEM PSD would provide better signal-to-noise ratio (SNR) since PSD averaging over nonstationary period becomes feasible for low frequency analysis. In addition, such normalized PSEM PSD would provide a much higher frequency resolution for any sync-related spectral component, and as a result, discrimination from other independent noise interference such as the blower motor within the MISA drive train can be easily achieved. Such PSEM PSD thus provides the best spectrum signature for antenna drive component monitoring, and will be the recommended format to be stored in the PSD-BLDB.

Knowledge pertaining to the types of malfunction mechanisms which occur during the history of a drive train and their corresponding dynamic symptoms is of paramount importance for diagnostic purposes. These malfunctions include various bearing defects, bearing freeze, imbalance, gear defect, rotor instabilities etc. Dynamic signatures which best represent these defects will be recorded in the Defect Signatures Data Base (DSDB) for signature comparison purposes in the Anomaly Detection (AD) module. Fault symptoms for bearing-related defects are of primary interest to this SBIR program which will be briefly discussed below:

Rolling-Element Bearing Defects. Rolling-element bearing defects are the most common cause of failure in machine/drive-train systems. Several specific characteristic frequencies that result from bearing defects, such as cage frequencies, inner/outer race passing frequencies, and rolling element spin frequencies, can be easily estimated from bearing geometry and the speed of shaft rotation. These unique bearing defect characteristic frequencies serve as effective indicators in both failure detection and analysis. The base-line statistical histories of the PSD amplitudes at these frequencies will be monitored and established in the PSD-BLDB. Abnormal responses at these bearing frequencies will be detected and flagged whenever they deviate from the template statistics in the base-line data base.

While computation of bearing characteristic frequencies is straightforward, other factors can change the dynamic response of the system, and cause problems in detecting the bearing defect signatures. Previous studies of bearing defect signatures have shown that certain bearing failure mechanisms can modify a response spectrum by introducing additional bearing related components other than those associated with conventional bearing defect frequencies. Typical examples of these phenomena include modulation/sideband components resulting from bearing frequencies modulating other vibration responses. Another variation which occurs primarily in advanced stages of bearing degradation is the concentration of defect energy in higher harmonics of bearing characteristic frequencies. These phenomena will cause defect signatures at new frequencies rather than at the expected characteristic frequencies, and this often leads to mis-interpretation. Therefore, any spectral pattern representing a unique bearing defect configuration within a drive train will be recorded in the DSDB data base for future comparison.

4.1.2. Anomaly Detection (AD) Module

The baseline information recorded in the Base-Line Data Base provides the foundation for comparing a machine's present condition against its nominal states. A warning flag will be raised whenever key statistics or PSDs deviate from their nominal status. Two types of analyses are performed in the AD subsystem: the Similarity Analysis and the Trend Analysis. The operating technique and objective for each analysis are briefly discussed below:

Similarity Analysis. The AD module will continuously measure the similarity of a currently monitored PSD against an inventory of PSDs in the PSD-BLDB and DSDB, based on their statistical characteristics.

Similarity criteria are based on measuring the "distance" between two PSDs that are characterized by their individual statistics (mean, and variance). In other words, whether or not the two PSDs belong to the same class is determined. One of the most commonly used criteria available is the "divergence" measure, which can be considered as a dimensionless "distance" between two PSDs, each a random vector.

A PSD representing current operation conditions ($\mathbf{PSD}_N$) is compared to a bank of inventoried PSDs ($\mathbf{PSD}_j$, j=1 to N-1) that are stored in the PSD-BLDB. Through the similarity (distance) measure, a plot of divergence as a function of time can be displayed characterizing current machine operational status. Whenever a PSD deviates from its nominal status as recorded in the PSD-BLDB or conforms to a template defect signature in the DSDB within a pre-specified statistical confidence range, a red flag will be raised by the AD module. This red flag warning will then trigger the Anomaly Identification (AI) module for a detailed signal analysis inspection prior to a warning being issued to the machine operator.

Trend Analysis. Along with providing a similarity measure against the PSD-BLDB and DSDB, the AD module will also continuously monitor the trends of various critical spectral components in order to provide early warning of impending failures. From the PSD-BLDB, the AD module can retrieve the time histories of various statistics such as the composite-RMS values of all measured signals, the RMS values of the Sync component (RPM) and each of its harmonics, the RMS values of all bearing characteristic frequencies and their harmonics, the RMS of modulation/sideband bearing-defect frequencies (e.g. inner roller pass frequency plus 2 times of Sync frequency due to modulation), etc. Time histories of all these parameters or statistics will be monitored to allow quick detection of any trending. Redline threshold levels for the trend analysis will be continuously tuned and established based on the probability and statistical confidence interval associated with each parameter.

4.1.3 Anomaly Identification (AI) Module

In many health monitoring systems for industrial application, emphasis has been placed on the base-line data base and similarity/trend analysis aspects as discussed in the last two sections. With the monitoring of most critical dynamic information, these two subsystems when integrated with an expert system or artificial neural network can provide an effective solution for *unsupervised* health monitoring requirement. Such a system would be reliable and robust under certain isolated operational conditions. However, under other unique or complicated operational environments, this type of limited system could provide a high rate of false-alarms and mis-interpretations. Within the ALTAIR antenna drive system, many other vibration sources, such as structure vibration, the air blower and lube pump would contaminate the monitored signature and confuse the base-line data base for similarity/trend analysis. In addition, the various rotor/bearing/gear within the antenna drive train generate complex signals so that identification of physical cause of any anomalous spectral component would be difficult.

The innovative central feature of this PSADDS system is to provide an "intelligent" ingredient in the health monitoring system by including a unique Anomaly Identification (AI) module. Whenever an anomaly is detected and flagged by the AD module, the PSADDS will invoke the AI module to identify the source of the anomaly and determine if a fault mode is indeed present. The AI module will perform a detailed analysis and verification through a hierarchy of innovative phase signature analysis techniques. With the advanced diagnostic tools, the chance of false-alarms and mis-interpretations will be greatly reduced. These diagnostic signal analysis techniques can identify a specific type of signal characteristic which, in turn, provide valuable clues in identifying association with a specific fault mechanism.

The detection and understanding of anomalous signatures along with their physical implications is the most important function of the AI module. This AI function is highly dependent on the effectiveness of signal processing of the phase signature analysis techniques. As will be discussed in section 4.2 of the Phase I study, several phase signature analysis techniques have been proven to be highly effective for anomaly identification under the unique operation environment of MISA antenna. Table-4 lists more complete

anomaly detection/identification capabilities offered by PSADDS for diagnostic evaluation. **The Anomaly detection/identification algorithms will be imbedded within the AI module - providing an intelligence capability that is largely transparent to the operator so that the operator need not be concerned with the complexities of dynamic signal analysis and interpretation.**

- Detect Nonlinear modulation/sideband phenomenon associated with various bearing fault patterns.
- Detect wideband modulation phenomenon associated with cavitation (hydrodynamic) induced vibration.
- Identify feed-through or resonance from neighboring equipment
- Identify RPM/Harmonics interference/overlap within a multi-rotor system
- Discriminate Rotor-related vibration from independent non-rotor-driven source/noise.
- Identify Sync (RPM) modulated spectral component associated various nonlinear vibration mechanisms including mechanical-driven such as deadband interaction, and fluid-driven such as cavitation-induced asynchronous vibration, etc.
- Identify Pure-tone Electric Line Noise.
- Identify Structural/acoustical resonant mode.
- Detect Frequency Modulation (FM) Phenomenon associated with various FM vibration mechanisms such as shaft torsional vibration or gearbox transmission error.
- Identify signal source through time-delay estimation
- Improve the signal-to-noise ratio in the vibration measurement data corrupted by noise
- Enhance Spectral resolution for all RPM-related vibration components.

TABLE-4 PSADDS ANOMALY DETECTION/IDENTIFICATION CAPABILITIES

4.2 Proposed Solutions for the Unique Requirement and Consideration of ALTAIR Health Monitoring Based on MISA Field Test Data

As previously stated, one of the major objectives of this Phase I was to identify any unique requirement or consideration that would be critical for the development of a health monitoring system for the ALTAIR drive train. Based on the representative information obtained from MISA test data during antenna operations, the following four major requirements and considerations have been identified:

1. **Interference from RF radiation.**
2. **Interference and corruption due to air blower noise and vibration**
3. **Best method to generate frequency spectrum signatures of drive components.**
4. **Detection of Bearing Defect Signatures due to Nonlinear Interaction.**

These unique requirements and considerations play a significant role in the determination of the best method for generating frequency spectrum signature for health monitoring. In the following sections, the proposed solutions to effectively deal with these special requirements and considerations for developing a reliable ALTAIR drive health monitoring system will be discussed.

4.2.1. Interference from RF radiation

RF interference was so overwhelming during MISA UHF operations that any attempt to achieve total isolation of PSADDS from this interference is neither feasible or warranted. We propose to address this problem by restricting ALTAIR health monitoring to periodic "calibration" runs whereby azimuth and elevation drive systems would be operated through a prescribed duty cycle with UHF/VHF operations turned off. Data from these periodic "calibration" runs would constitute the historical data base for ALTAIR and would be subject to PSADDS analysis.

A second, important, reason to perform periodic "calibration" runs is to achieve a measure of stationarity in drive system operations. For example, MISA operations are highly non-stationary with azimuth and elevation drives operated in an intermittent or random manner over varying excursions. Operations of this type greatly complicate health monitoring analyses and could lead to a high percentage of false alarms or failure to detect faults. Controlled, periodic "calibration" runs will greatly simplify health monitoring diagnostics, and will lead to improved reliability and utility of the health monitoring system.

As will be shown in the following sections, the other special requirements can be effectively dealt with using the unique phase signature analysis techniques within the PSADDS. Description of two signal analysis techniques, the *nonlinear bi-coherence analysis* and *Phase Synchronized Enhancement Method (PSEM)* will first be discussed in detailed. In order to best demonstrate the effectiveness of these techniques, application examples for bearing/gearbox fault diagnosis using test data from Space Shuttle Main Engine (SSME) and Helicopter drive train system will also be presented. Actual application to MISA antenna test data will then be discussed to demonstrate their effectiveness for the development of the ALTAIR drive monitoring system.

4.2.2. Interference and corruption due to air blower noise and vibration

The results of test data analysis from the MISA drive train have indicated that most of the accel measurements across the drive train are subjected to strong interference from air blower noise and vibration. Therefore, it is critical to be able to identify any contribution from the air blower (as well as the lube pump for ALTAIR) in the monitoring spectrum so that false alarms can be reduced. The PSD in figure 8 shows strong sync/harmonics interference from the air blower at 6*Nb and 12*Nb. However, as will be shown later, many other spectral peaks in this PSD are also due to the air blower interference. Identification of such interference can be effectively achieved using two unique phase signature analysis techniques, the nonlinear bi-coherence analysis and Phase Synchronized Enhancement Method.

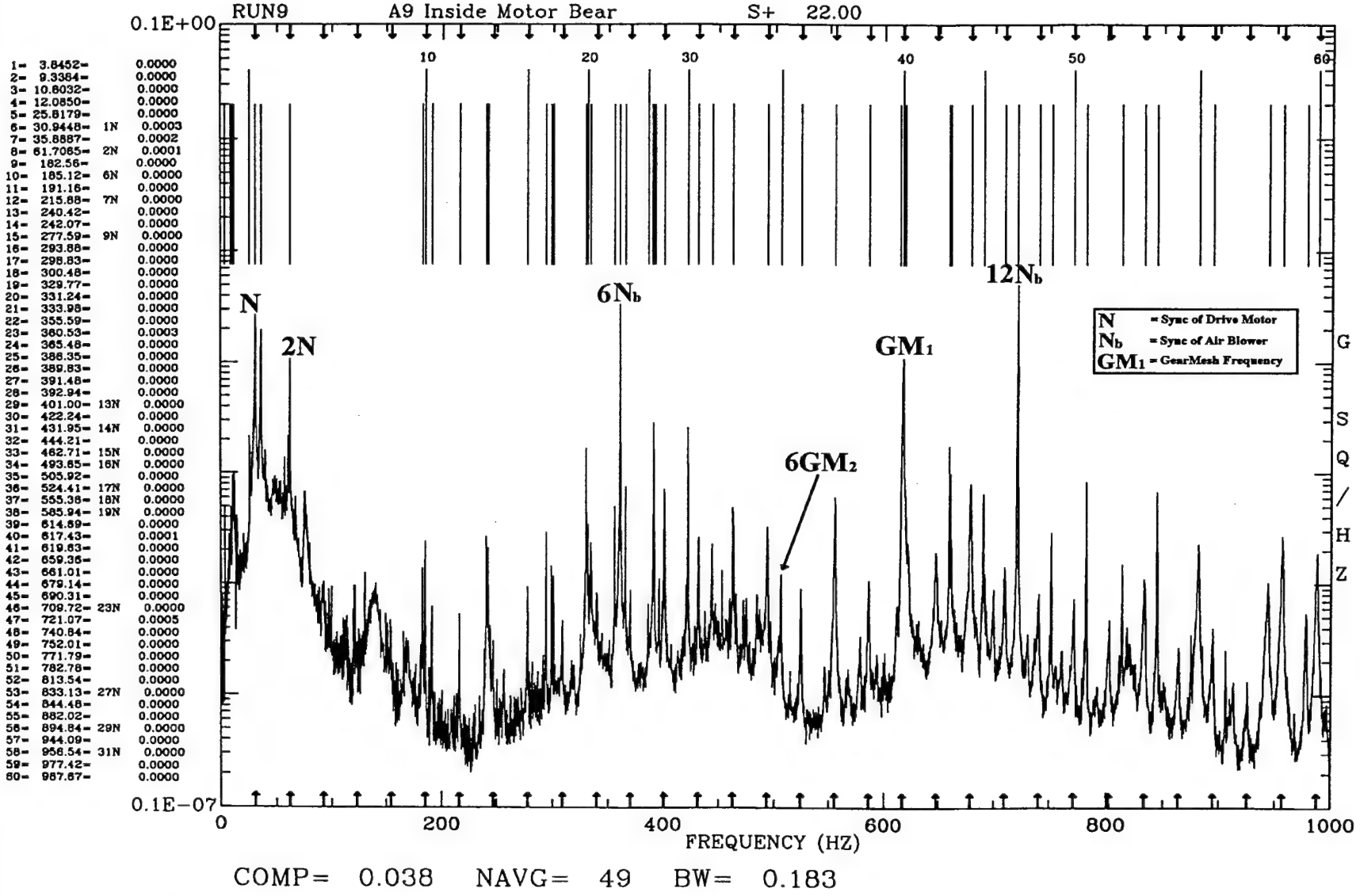

Figure 8: Detailed PSD of Outside Drive Motor Accelerometer Measurement A8

Proposed Solution: Nonlinear Bi-Coherence Analysis Method

The dynamic response of a rotating machine can exhibit nonlinear interaction phenomena primarily due to modulation between various rotational components and fluid/structure interactions. Amplitude modulation can be generated by at least six phenomena. Enrich and Eshleman have published works using analytical techniques to explain how these modulations are physically generated. The characteristics of such nonlinear interactions are usually reflected in a response waveform which can be identified by using the bi-spectral technique. The proposed nonlinear coherence analysis techniques can provide improved capability to investigate modulation/sideband phenomenon in rotordynamics by taking advantage of the deeply hidden nonlinear signature due to phase coupling. As the power spectral density (PSD) function is a second moment statistic of a random signal, the auto-bispectrum (ABS) represents the third joint moment among three different waves at frequencies w_1, w_2 and the sum frequency w_1+w_2, and can be estimated by:

$$B_{XXX}(\omega_1,\omega_2) = E[X(\omega_1)X(\omega_2)X^*(\omega_1+\omega_2)] \quad (1)$$

Where X(w) is the Fourier transform of x(t). The auto-bicoherence (ABC), a normalized bispectrum, is defined as:

$$b^2_{XXX}(\omega_1,\omega_2) = \frac{|B_{XXX}(\omega_1,\omega_2)|^2}{E[|X(\omega_1)X(\omega_2)|^2]E[|X(\omega_1+\omega_2)|^2]} \quad (2)$$

Bi-spectrum $B_{XXX}(\omega_1,\omega_2)$ is a function of two frequencies, ω_1 and ω_2, rather than a single frequency argument as with a PSD. Therefore, a three dimensional figure would be required to display a bi-spectrum since it is a function of two frequency arguments. However, to maximize the visualization effect, one of the bi-frequency arguments, ω_1, can be fixed at some particular frequency of interest (such as bearing characteristic frequency) while the other frequency argument, ω_2 , sweeps through the entire analysis frequency range.

By using Schwarz' inequality, it can be shown that the auto/cross bi-coherence is always bounded by zero and unity. Amplitude modulation process always involves three basic spectral components at frequencies ω1, ω2 and there sum frequency ω1+ω2. Even though a PSD might be able to identify the power distribution at these three particular frequencies, the existence of modulation can only be proven by identifying their coherent phase relationship. The phase information of the bispectrum in equation (1) can provide a unique way to identify such phase coupling. If the wave at frequency ω1+ω2 is really correlated to the waves at frequencies ω1 and ω2 due to some nonlinear process then a constant relative phase relationship will be identified in the bispectrum estimation, and as a result, its bicoherence will be equal to one. On the other hand, if the waves at frequency ω1, ω2 and ω1+ω2 are totally independent of each other, then the phase of bispectrum will remain a random phase, and its bicoherence will be reduced to zero.

SIMULATION EXAMPLE OF BICOHERENCE

The following simulation example can best describe the application process of bicoherence. Three time histories $x_1(t)$, $x_2(t)$ and $x_3(t)$ are generated as follows:

$$X_1(t) = \cos(\omega_a t+\Phi_1)+\cos(\omega_b t+\Phi_2)+\cos[(\omega_a+\omega_b)t+(\Phi_1+\Phi_2)]+N_1(t)$$
$$X_2(t) = \cos(\omega_a t+\Phi_1)+\cos(\omega_b t+\Phi_2)+\cos[(\omega_a+\omega_b)t+\Phi_3]+N_2(t)$$
$$X_3(t) = \cos(\omega_a t+\Phi_1)+\cos(\omega_b t+\Phi_2)+0.5*\cos[(\omega_a+\omega_b)t+(\Phi_1+\Phi_2)]$$
$$+0.5*\cos[(\omega_a+\omega_b)t+\Phi_3]+N_3(t)$$

where ϕ_1, ϕ_2 and ϕ_3 are independent random phase; $N_1(t)$, $N_2(t)$ and $N_3(t)$ are independent Gaussian White Noise, and the sum frequency $\omega_c = \omega_a + \omega_b$, is the frequency of the third sine wave. Each one of these time series is composed of three sine waves at frequency ω_a , ω_b and ω_c. The first two waves at ω_a and ω_b are identical for each of the time histories. But the third wave at ω_c is quite different. For $x_1(t)$, the phase at ω_c is equal to the sum of the phases at ω_a and ω_b, which represents perfect phase coupling. For $x_2(t)$, the random phase at ω_c indicates total independence among these three sine waves. For $x_3(t)$, 50% of the component at ω_c is phase coupled with ω_a and ω_b, and the remaining 50% with random phase independent of ω_a and ω_b.

Figures 9-a, 9-b and 9-c are the PSD (Power spectral density) for $x_1(t)$, $x_2(t)$ and $x_3(t)$. They are identical and cannot be discriminated. Figures 9-d, 9-e, and 9-f are their corresponding auto-bicoherence mappings. The x- and y-axes represent the bi-frequency arguments of $bxxx(\omega_1,\omega_2)$ and the surface elevation represent the bicoherence. In figure 9-d, there is a strong peak at bi-frequency (ω_a , ω_b) with amplitude close to one. This indicates the components at ω_a , ω_b and ωc in $x_1(t)$ are highly correlated due to strong phase coupling. For $x_2(t)$, since the phases at these three frequencies are independent random phases, no significant bicoherence peaks are apparent in figure 9-e. For $x_3(t)$, figure 9-f, the amplitude at bi-frequency (ω_a ,ω_b) is only 0.5 which indicates that only 50% of the power at ω_c is correlated with ω_a and ω_b, and the remainder is totally independent. Therefore, the bi-coherence analysis completely distinguishes these three time histories even though they have identical PSDs.

SSME Example of bicoherence analysis

In a complex machinery operational environment involving multiple rotational systems, spectral component feedthrough from one system to another could create many false-alarm anomalies. Such anomaly feedthrough due to linear and/or nonlinear mechanisms has been frequently encountered in the SSME test/flight history. With its unique ability in detecting nonlinear correlation within a complex signal, bicoherence is also an effective tool in identifying false alarm feedthrough anomaly in bearing diagnosis. A case encountered during an SSME hot firing test will be used to demonstrate how bispectral analysis can identify false-alarm signatures in the turbomachinery environment. Figure 10(a) shows a PSD taken from a SSME high pressure oxygen turbopump (HPOTP) external strain gauge measurement. The peaks marked "N", "2N", "3N", are the Sync (shaft rotational) frequency component and its harmonics. The peak marked " N' " is the Sync feed-through from the nearby high pressure fuel turbopump (HPTFP) whose PSD is shown in figure 10(b). This linear feedthrough can be easily identified using a conventional linear cross-coherence between these two measurements as shown in figure 10(c). The linear coherence indeed identifies a strong linear correlation at 600 Hz ("N'" component). This indicates that this N' component in the HPOTP signal is indeed a Sync feed-through from the HPFTP. Notice that there is an anomalous frequency component marked "OPB" or "4N+N' " present in the HPOTP measurement. This anomaly is coincident with the predicted outer ball pass (OBP) frequency corresponding to one of the HPOTP pump-end bearings. Therefore, an outer race defect was suspected as the source of the anomaly. Based on this assessment, a costly turbomachine would have been rejected for flight and been subjected to an in-depth hardware tear-down inspection. Cross-bispectral analysis discriminated this anomaly to be a false-alarm defect signature as described below.

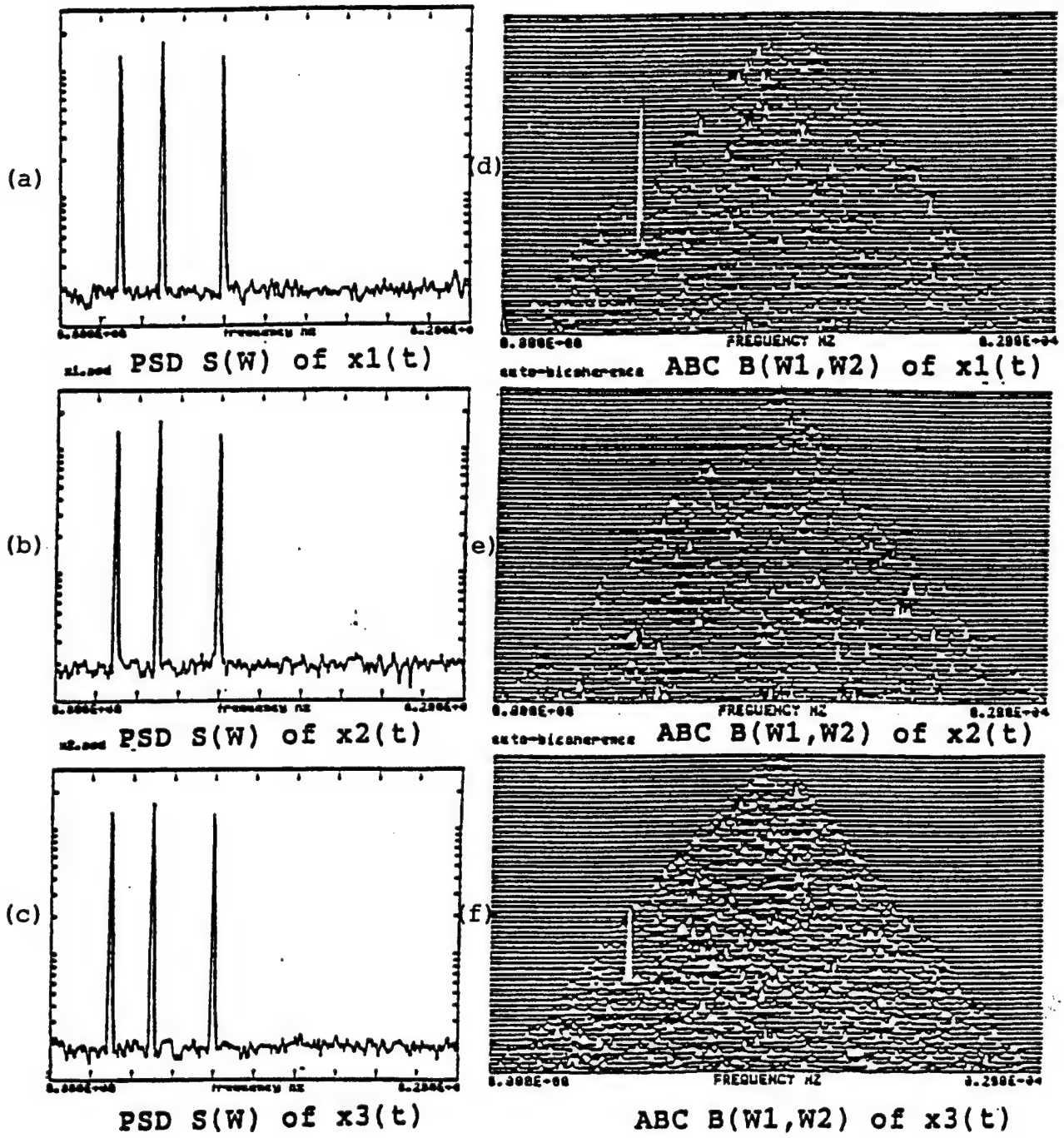

Figure 9(a), 9(b), & 9(c): PSDs for x1(t), x2(t) & x3(t).
9(d), 9(e), & 9(f): Auto-Bicoherence for x1(t), x2(t) & x3(t).

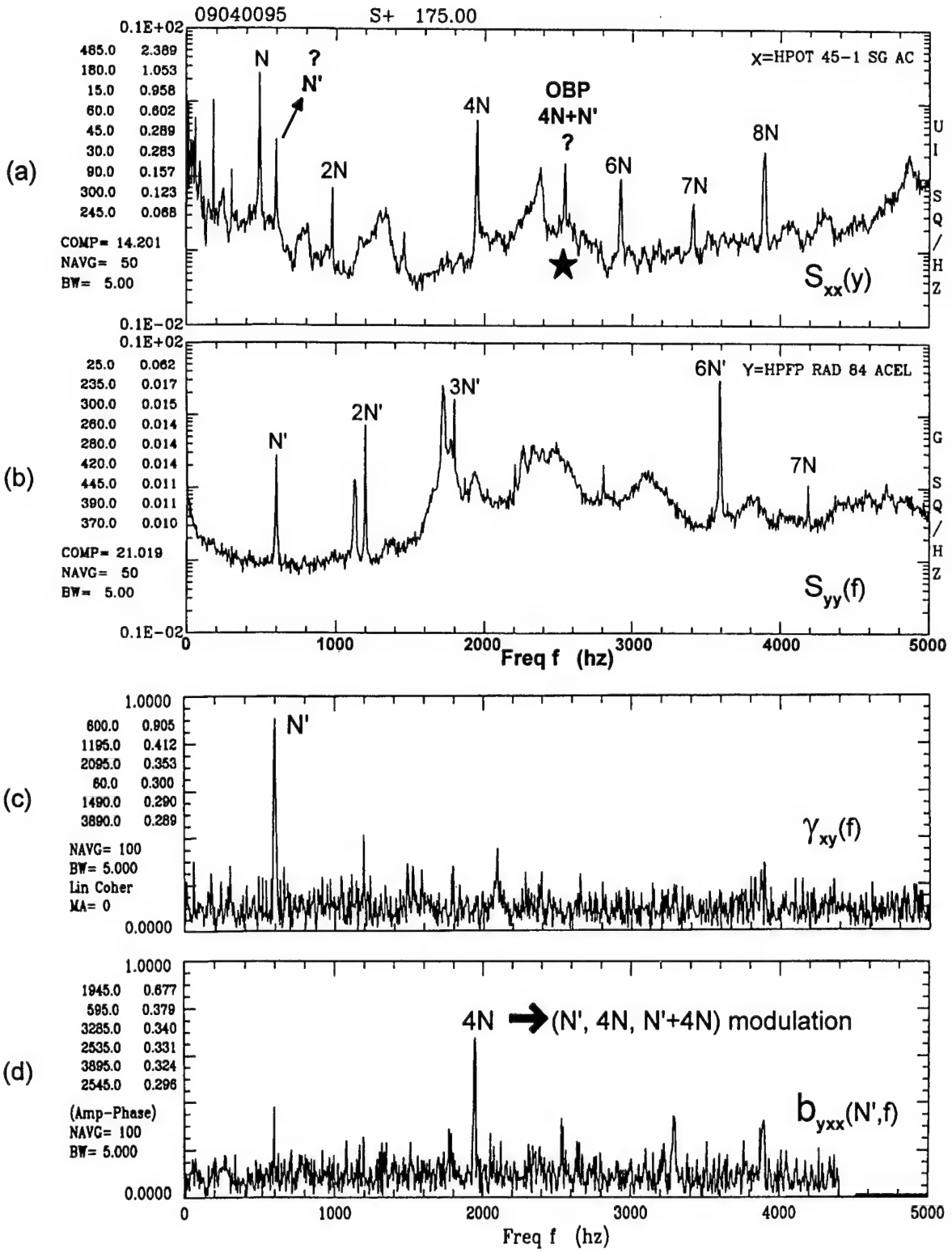

Figure 10 (a): PSD of SSME HPOTP Strain Gauge Measurement.
(b): PSD of SSME HPFTP Accelerometer Measurement.
(c): Linear Cross Coherence γxy(f) Between HPOTP & HPFTP
(d): Cross Bi-Coherence Byxx(N', f) Between HPOTP & HPFTP

By closely examining the frequency relationships of all these components, this apparent OBP anomaly was observed to be 4N plus the Sync feed-through (N') from the nearby HPFTP. Therefore, a new question was raised, that is, whether this OBP anomaly was truly an OBP defect signature or was it just the modulation between 4N of the HPOTP, and the Sync of the HPFTP. The latter phenomenon has been frequently observed in multiple machinery environments where two rotational processes interact with each other due to some nonlinear process. To answer this question, the nonlinear correlation between the frequency components emanating from the two separate pumps had to be determined through bispectral analysis. Figure 10(d) depicts the cross bi-coherence between the HPFTP and HPOTP measurements. A significant bicoherence peak is detected at the 4N frequency which corresponds to the bi-coherence function bxxx(N', 4N). This indicates that the N' and 4N components, along with their sum frequency, the OBP anomaly, are highly correlated with each other quadratically. Therefore, this OBP anomaly is actually due to the modulation between 4N of the HPOTP and the Sync the HPFTP (N'). In this case, the OBP anomaly turned out to be a false alarm rather than a true OBP defect signature as it appeared to be. Moreover, this finding exonerated a healthy multi-million dollar turbopump for flight purposes. This example demonstrates how the linear coherence and cross-bi-coherence analyses can identify the relationship among different rotational (RPM) components within a multi-rotor system. In the next section, it will be shown that the nonlinear interaction between the air blower and drive motor is the major source of interference in the MISA antenna drive train measurement, and bi-coherence analysis can be used effectively to identify such air blower interference.

Identification of MISA Antenna Drive Air Blower Interference using bicoherence analysis

Figure 11 shows the PSD functions of all the 13 measurements from 0 to 1,000 Hz frequency with the antenna stopped and the air blower in operation. A sequence of spectral peaks are observed in these PSD's which are corresponding to the Sync and harmonics of the air blower (Nb). Compared to the PSD's in figure 7 when the antenna is in rotation, it is evident that the sync and harmonics of the air blower feed through to many other measurement across the drive train. If these sync/harmonics are the only corruption from the air blower, then implementation of an adaptive notch/comb filter should eliminate or reduce such air blower interference.

However, as it turns out, such air blower interference is not just limited to the Sync/harmonics frequencies of the air blower, they can also show up in many other frequencies due to the nonlinear interaction between the drive motor and the air blower similar to the phenomenon discussed in figure 10. This makes a simple filtering approach for air blower noise removal not feasible. Therefore, a critical requirement for a reliable ALTAIR drive train monitoring system is having the ability to at least identify such contribution from air blower and lube pump in the monitored spectrum signature. The proposed nonlinear bi-coherence within the PSADDS provides this unique capability.

Figure 12(a) shows the PSD of the accel measurement A9 near the inside motor bearing. By closely examining the frequency relationships of all the components in the PSD, clear modulation/sideband patterns at 6*Nb+k*N1 and 12*Nb+k*N1 are observed which are due to the nonlinear interaction between the air blower and the drive motor. Since these patterns generate many spectral peaks whose frequencies could be close to or coalesce with some critical bearing defect signatures, they could cause false alarm. Therefore, any anomaly detected in the spectrum during monitoring must be further identified whether it was truly a defect signature or just an air blower interference due to such modulation (similar to the SSME example in figure 10). This identification can be achieved through bicoherence analysis. Figure 12(b) depicts the auto bi-coherence of the accel measurement with 6Nb (the 6th harmonic of the air blower) as the reference frequency. Many strong bicoherence peaks are detected at the modulation/sideband frequencies: 6*Nb+k*N1, 12*Nb+k*N1, and GM1+6*Nb. Each bicoherence peak establishes a nonlinear correlation with the air blower at three frequencies. For example, the bicoherence peak marked "6Nb+N1" indicates that the 6Nb+N1 (bicoherence peak) and 6Nb (reference) components, along with their sum frequency, 12Nb+N1 are highly correlated with each

other. Therefore, the spectral peak at 6Nb+N1 and 12Nb+N1 are actually due to the interaction with air blower. If the frequency 6Nb+N1 happens to be near a bearing defect signature such as 2*IRP+2N (IRP represents Inner Roller Pass), it would be a false alarm rather than a true defect signature as it appeared to be. The remaining bi-coherence peaks in figure 12(b) would lead to the identification of all the other components due to air blower interference, i.e. the PSD peaks marked "*". Figure 13 shows the bicoherence of all the 12 accel measurement with the same reference frequency (6Nb). Strong bicoherence is detected in most of the measurements. This indicates that the effect of the air blower interference is quite extensive across the drive train, and must be taken into consideration when developing the ALTAIR monitoring system. This example has demonstrated that, bicoherence analysis can provide a unique capability to identify air blower interference and will be incorporated into design of the ALTAIR monitoring system.

4.2.3. Best method to generate frequency spectrum signatures of drive components

The Proof Of Concept Study based on the MISA antenna test data has indicated the best method to generate a frequency spectrum signature of drive components should be a "Normalized" PSD with respect to Sync frequency rather than the "Raw" PSD. The basic reason is twofold:

1. Most of the bearing characteristic frequencies of MISA's Bogie wheel bearings are in a very low frequency region. For example, at a nominal motor drive speed of 1850 RPM, the Cage frequency (C), Roller Spin frequency (RS), Inner Roller Pass (IRP) and Outer Roller Pass (ORP) of the Outer Wheel Pillow-block bearing of the MISA antenna drive are at 0.0706 Hz, 0.675 Hz, 1.695 Hz, and 2.137 Hz. respectively (see Table 2). In order to provide better signal-to-noise ratio (SNR) for early detection of bearing defects in such low frequency region, it would be desirable to be able to perform PSD averaging over several nonstationary antenna operation period (CW, stop, CCW etc). Figure 14(a) shows a PSD of Outer Wheel Bearing measurement from 0 to 5 Hz over one full cycle of antenna excursion. Due to the limited amount of available low frequency data, PSD averaging cannot be performed and the contains of the spectrum become quite noisy.

2. The frequencies of most bearing/gear defect signatures are at ratio to Sync frequency (e.g. Inner Roller Pass frequency IRP=13.38N for outer wheel bearing) rather than fixed frequencies. Therefore, utilization of a frequency normalized PSD with respect to Sync frequency for monitoring "spectrum signature" for baseline database generation would allow a more robust and reliable detection of any subtle change due to defect.

The equivalent time domain effect of a normalized PSD with respect to sync is to have the sampling process vary as RPM changes. In other words, when RPM speeds up (or slows down), the sampling does also so that the time interval between samples varies, but the phase angle between samples is maintained absolutely constant. To achieve this, the original measurement signal with uniform sampling interval must be digitally transformed into another new signal with uniform phase intervals. This transformation process between constant time/phase sampling interval will effectively normalize the original PSD with respect to the Sync frequency. Since there exists some uncertainties of the antenna's RPM (for example, the RPM in CW and CCW are different as shown in the MISA test data), such frequency normalization procedure during monitoring must be highly automatic without relying on any human judgment and prior knowledge of the antenna operation RPM profile. Therefore, the straight-forward approach of re-scaling and interpolating the frequency scale of a spectrum will not be feasible. The proposed solution is to use the Phase Synchronized Enhancement Method.

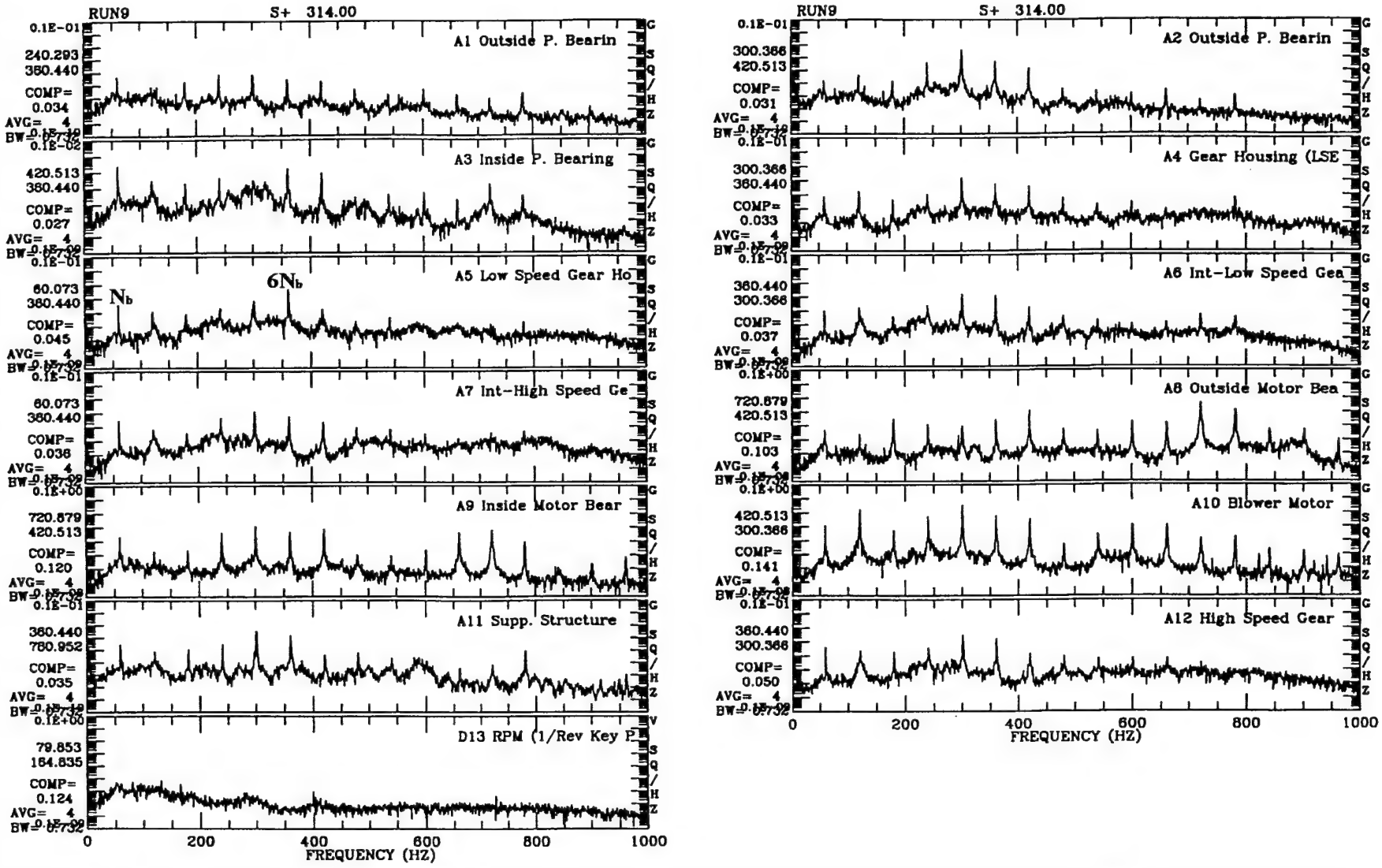

Figure 11: PSD functions of 13 MISA Drive Measurements with the antenna stopped and the air blower in operation

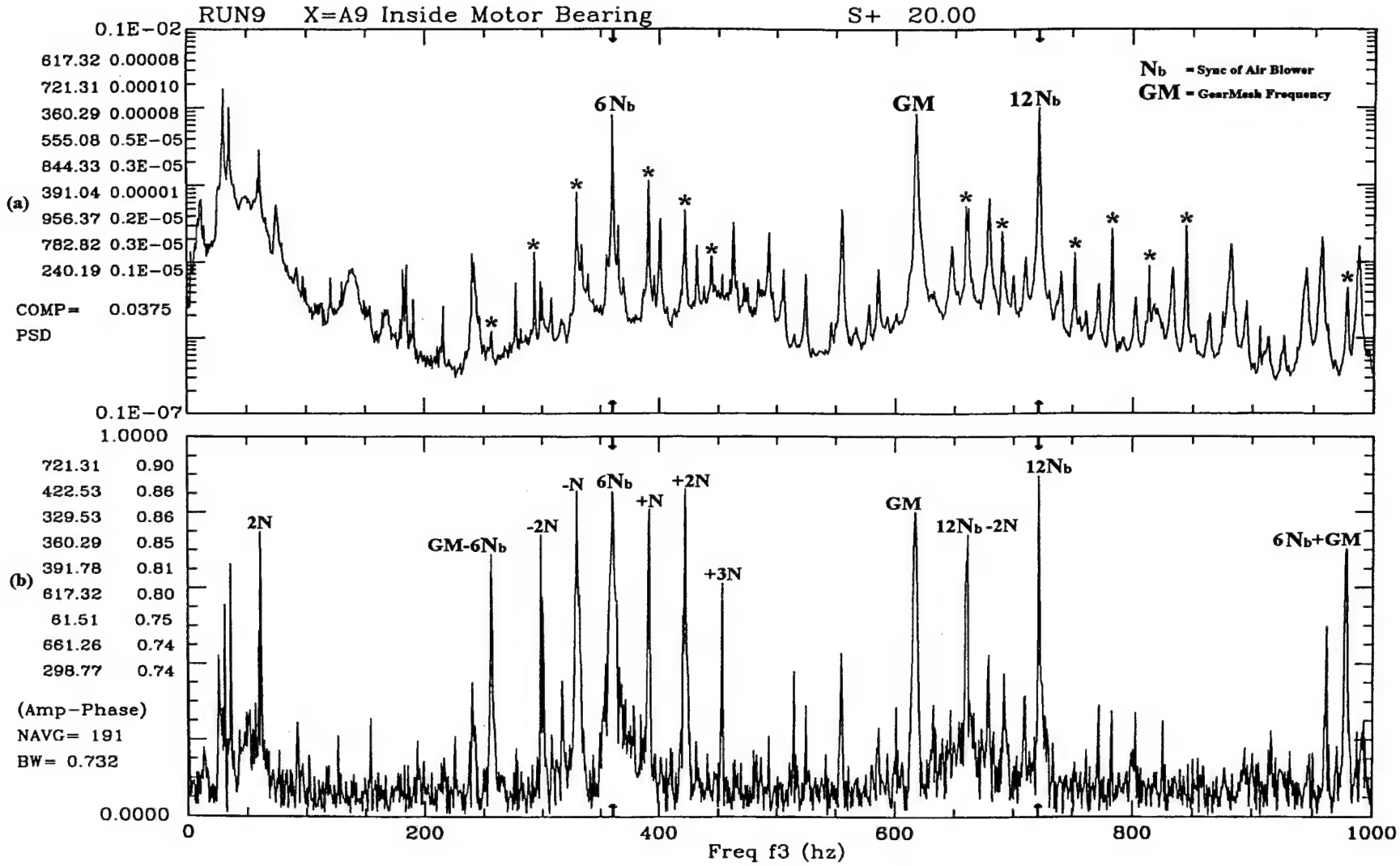

Figure 12: (a) PSD of accel measurement A9 near the inside motor bearing.
(b) Auto bi-coherence $b_{xxx}(\omega1=6*Nb, \omega2)$ of accel measurement A9 with $\omega1$ fixed at the 6th harmonic of the air blower

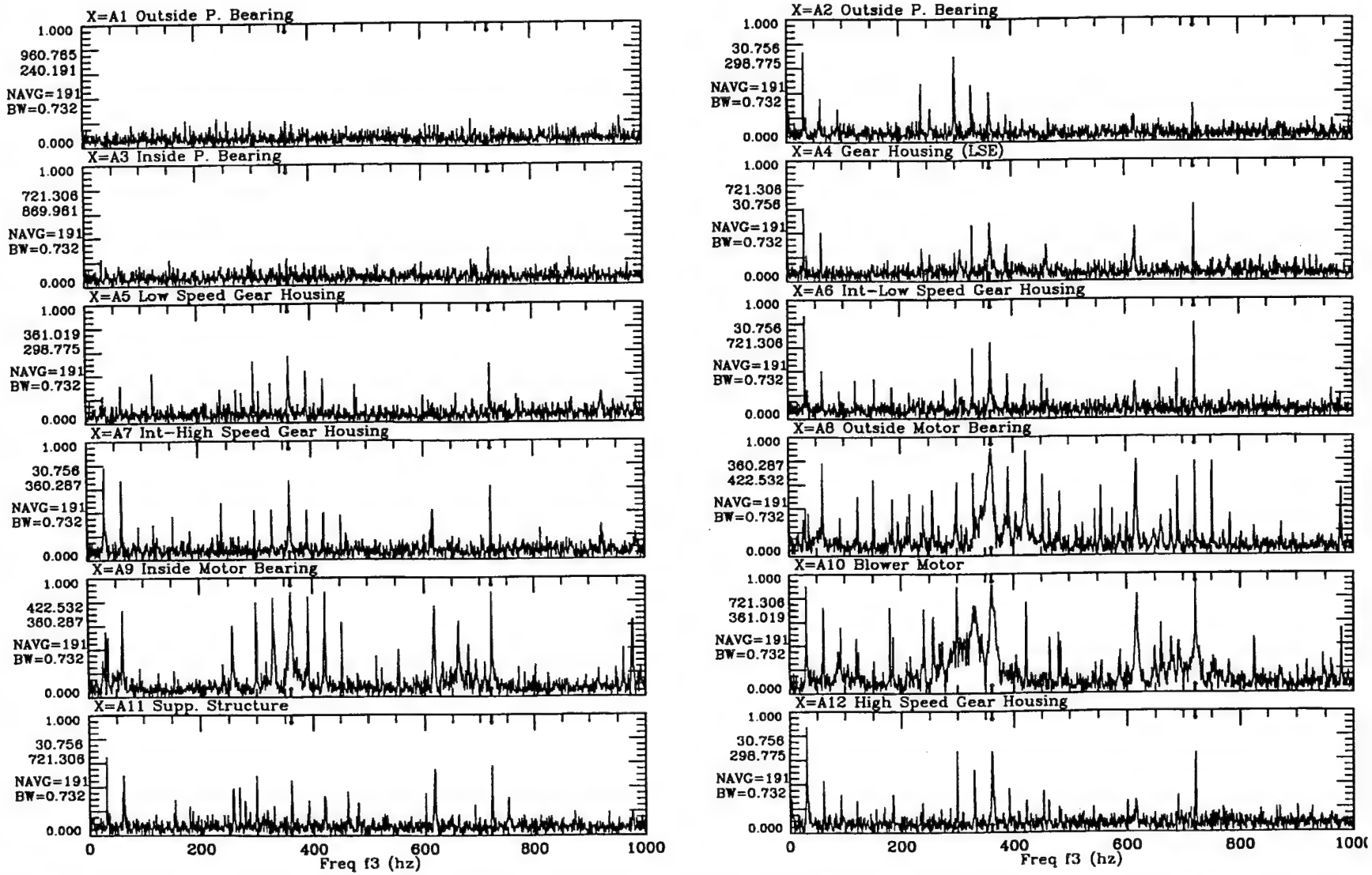

Figure 13: Auto-bicoherence $b_{xxx}(\omega 1=6*Nb,\omega 2)$ of 12 MISA Drive accel measurements with $\omega 1$ fixed at the 6th harmonic of the air blower

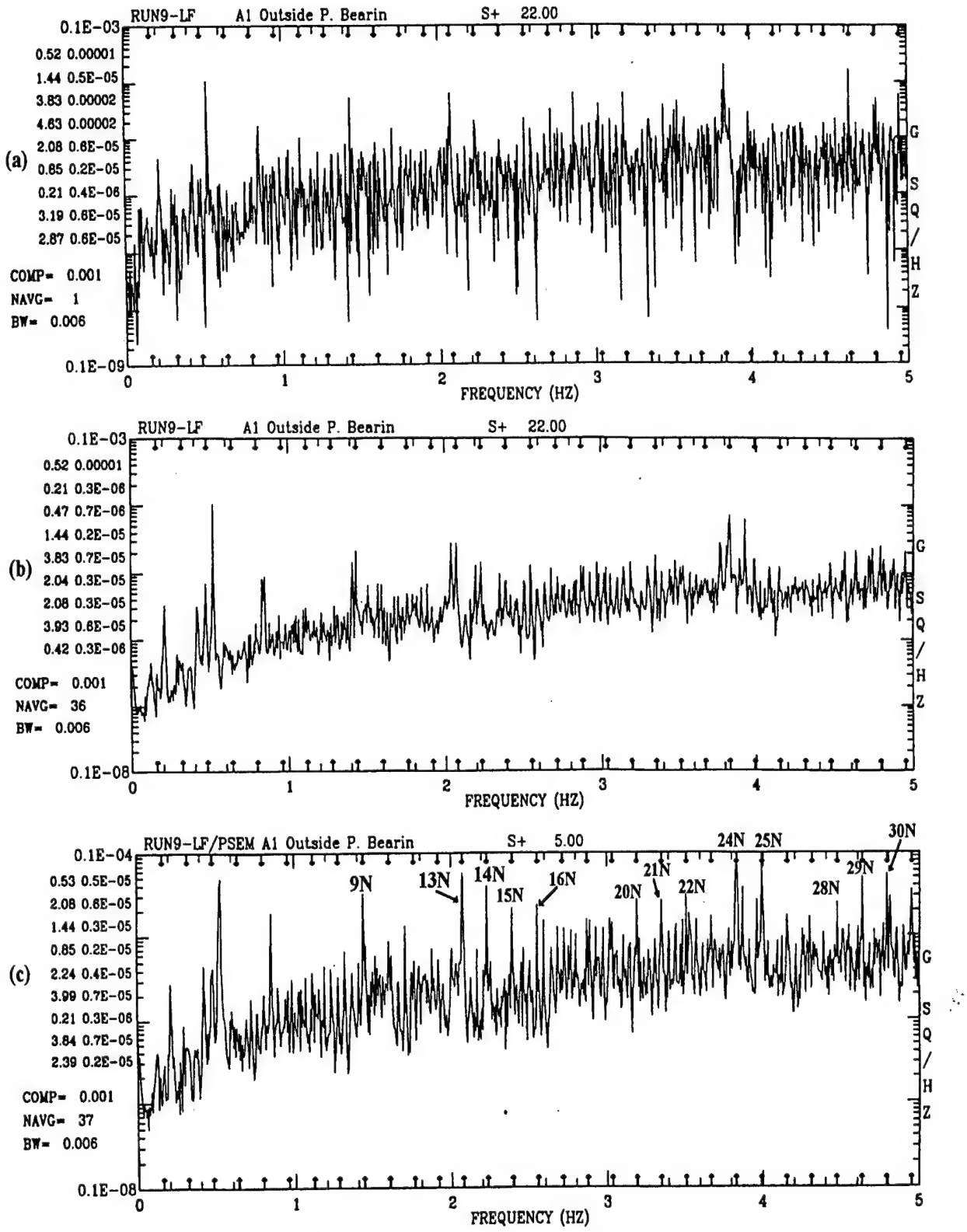

Figure 14: (a) Raw PSD of outer Wheel Bearing measurement over one cycle of antenna excursion
(b) Raw PSD Averaging over 22 cycles of antenna excursion
(c) PSEM PSD Averaging over 22 cycles of antenna excursion

Phase Synchronized Enhancement Method (PSEM)

The shaft rotational speed in a rotor system tends to momentarily speed up or slow down due to dynamic load variation. This micro-frequency variation phenomenon can be observed from the instantaneous frequency at Sync frequency using a Frequency Demodulation technique. With this instantaneous frequency, useful information for bearing/gearbox diagnosis can then be obtained using a novel method called the Phase Synchronized Enhancement Method (PSEM). The basic principle of the PSEM is to force the quasi-periodic Sync component whose frequency is slightly fluctuating around some center frequency into a pure-tone discrete component whose frequency is constant. PSEM, with its unique capability of transforming a quasi-periodic Sync into a pure-tone discrete component, generates a highly desirable effect on an entire diagnostic signal with all Sync-related components becoming discrete. With this enhanced frequency resolution, the PSEM signal can recover detailed spectral information useful in diagnostic evaluation. This method is especially useful for machinery diagnostics, in which case a quasi-periodic driving process (Sync) generates many other rotational components. These related components such as Sync harmonics, bearing element spin and passing frequencies, modulation and sideband components can provide useful information about a machine's operational condition. More importantly for ALTAIR application, the PSEM provides an effective method to normalize the original PSD with respect to the Sync frequency by digitally transforming the original measurement signal with uniform sampling interval into a new signal with uniform phase intervals. A brief discussion of the PSEM algorithm will be given first.

The signal model of a measurement signal in a rotor system can be formulated as:

$$x(t') = A\cos[\Psi(t')] + B\cos[\gamma * \Psi(t')] \qquad (3)$$

SYNC SYNC-RELATED

Where $\Psi(t)$ is the instantaneous phase of sync
γ is a constant

The first term A*cos[$\Psi(t')$] represents the Sync frequency component, while the second term B*cos[$\gamma * \Psi(t')$] represents a Sync-related component whose phase variation is synchronized with Sync. The sampling process of the original signal can be viewed as an observer traveling at a constant speed V(t) along the time-axis observing the waveform x(t'). If the observer is traveling at a time-dependent non-constant speed V(t), he will then observe a slightly different waveform y(t) as:

$$y(t) = x[t' = V(t)t] = A\cos\{\Psi[V(t)t]\} + B\cos\{\gamma * \Psi[V(t)t]\} \qquad (4)$$

This new waveform y(t) will generate new phase information for both the sync and the sync-related components. However, the new phase of the Sync-related component is still synchronized with the phase of Sync as shown in equation (4). This relationship indicates that phase correlation between two spectral components is independent of the sampling process.

The waveform of the Sync frequency component under a constant sampling rate is typically quasi-periodic. This sync component then can be discretized by resampling with a unique time-dependent sampling rate so that the newly-generated waveform will become periodic instead of quasi-periodic. This unique time-dependent sampling rate can be found from the instantaneous phase information of Sync. The signal model of Sync can be rewritten as:

$$x(t) = A(t)\cos[\omega_c t + \Phi(t)] \qquad (5)$$

Where: ω_c is the center frequency of Sync
$\Phi(t)$ is instantaneous phase variation

Since time and phase are directly related to each other, the resampling rate can be obtained through the following relationship:

$$\Phi(t) = \omega_c \Delta(t) \tag{6}$$

By replacing the instantaneous phase variation $\Phi(t)$ with $\omega_c \Delta(t)$, equation (5) becomes:

$$x(t) = A(t)\cos[\omega_c t + \omega_c \Delta(t)]$$

$$= A(t)\cos\{\omega_c[t + \Delta(t)]\} \tag{7}$$

Equation (7) states that, by treating the original quasi-periodic signal as a resampled signal represented by equation (7), the resampled signal will become periodic since the original phase variation is now transformed into its corresponding time variation $\Delta(t)$. Once the Sync frequency component becomes discrete in the resampled signal, all the other Sync-related components will automatically become discrete.

Figure 15 shows the PSEM algorithm. The input signal is composed of a reference Sync component along with several other Sync-related and non-Sync-related components. The band-pass filter first removes all the other spectral components in order to generated the time history of a quasi-periodic Sync component. The instantaneous phase variation signal $\Phi(t)$ of Sync is then estimated with the Hilbert Transform method. With the relationship between phase and time, this phase variation signal can now be converted into a realignment time signal $\Delta(t)$. The uniform sampling interval of the original signal is then remapped onto an array of non-uniform sampling intervals based on the realignment time. This realignment process will transform the original quasi-periodic signal into a periodic signal. An interpolator is then used to recover the uniformly sampled periodic signal from the non-uniformly sampled signal. Notice that, once the realignment time signal $\Delta(t)$ is identified, the remaining realignment process will be performed on the original signal rather than the band-pass filtered signal. As a result, all the other Sync-related components in the signal will automatically become discrete and synchronized to the RPM. When implementing the PSEM algorithm, such discritization or normalization can be directly performed with respect to any strong sync-related spectral component in the measurement signal. However if key phasor measurement is available, the PSEM normalization can be easily and automatically achieved with respect to the key phasor signal.

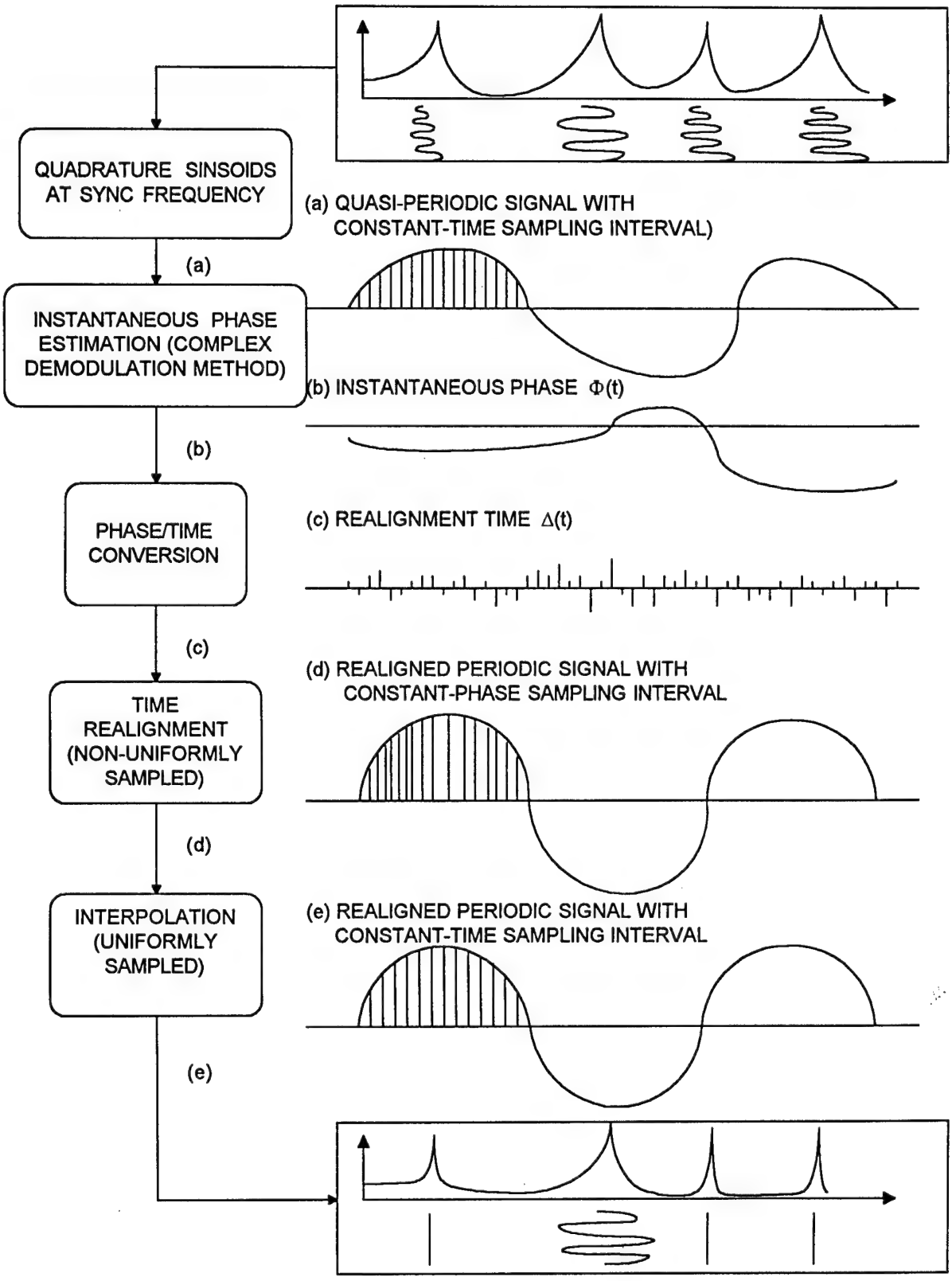

FIGURE 15 PHASE SYNCHRONIZED ENHANCEMENT (PSEM) ALGORITHM

PSEM SIMULATION EXAMPLE

A simple simulation example is used to demonstrate the PSEM technique. A quasi-periodic sine wave is generated at a sampling frequency of 10,240 Hz. The instantaneous frequency of the sine wave is fluctuating slightly around a center frequency of 1000 Hz. The amplitude of this quasi-periodic sine wave is then clipped at 0.2 of normalized amplitude level in order to generate higher harmonics at 2000 Hz, 3000 Hz, and 4000 Hz, etc. Figures 16-a and 16-d show the raw time history and PSD of this clipped sine wave. The fundamental frequency component at 1000 Hz can be treated as the Sync frequency component of a machinery component vibration signal with harmonics as other Sync-related components.

The PSEM algorithm first estimates the instantaneous phase of the raw signal at the fundamental frequency through the complex demodulation method. Figure 16-c shows the instantaneous phase variation of the fundamental frequency component. A resampling rate $\Delta(t)$ can then be obtained from the instantaneous phase variation. To recover the constant sampling time interval of the resampled signal, interpolation is applied to obtain the PSEM signal whose time history is shown in figure 16-b. Compared to the raw time history in figure 16-a, the PSEM signal is still very similar. However, since the fundamental frequency component has become discrete, the PSD of the PSEM signal as shown in figure 16-e is quite different than the raw PSD in figure 16-d. Notice that, in the PSEM signal, not only the fundamental frequency component becomes discrete, but also all the other correlated components (the harmonics and modulation components) become discrete. Therefore, the PSEM PSD provides an effective method to automatically synchronize all waves in a vibration measurement to the RPM, which not only achieves frequency normalization but also provides better frequency resolution useful diagnostic evaluation.

PSEM PSD - Sync Frequency Normalization of MISA Antenna Drive Test data

As previously discussed, the best method to generate a frequency spectrum signature of drive components should be a "Normalized" PSD with respect to Sync frequency rather than the "Raw" PSD. Such normalized PSD would provide not only a more "standardized" signature for monitoring but also better signal-to-noise ratio (SNR) for detection of low frequency antenna wheel bearing defect signatures since PSD averaging over nonstationary antenna operation periods would be possible. Due to the limited amount of data over one full cycle of antenna excursion, a noisy low frequency PSD for the MISA's Outer Wheel Bearing measurement is obtained in figure 14(a). To enhance the SNR, PSD averaging would be highly desirable.

Figure 14(b) shows the corresponding averaged PSD of the Outer Wheel Bearing measurement over 22 full cycle of antenna excursion by directly averaging the un-normalized "Raw" PSD. Even though the noise floor variation is improved, this PSD would provide erroneous spectral information due the RMP variation in CW and CCW directions. To overcome this, the PSEM normalization is first performed on all the raw measurement signals with respect to the key phasor signal (D13). As a result, the original measurement signals with uniform sampling interval are now transformed into new signals with uniform phase intervals. This PSEM transformation process thus effectively normalizes the original PSD with respect to the Sync frequency. Figure 14(c) shows the normalized "PSEM PSD" of the Outer Wheel Bearing measurement averaged over 22 full cycles of antenna excursion. Despite the nonstationary antenna operation, the SNR is improved in this PSEM PSD with all Sync/harmonics of the wheel rotation (N4=0.1597 Hz) clearly identified. It should be pointed out that , in actual application, the 22 averaging shown in this example would not be realistic since it represents a long period of time at such low frequency. However, this example has demonstrated the ability to deal with nonstationarity by utilizing the normalized PSEM PSD when averaging over nonstationary antenna operation periods is required.

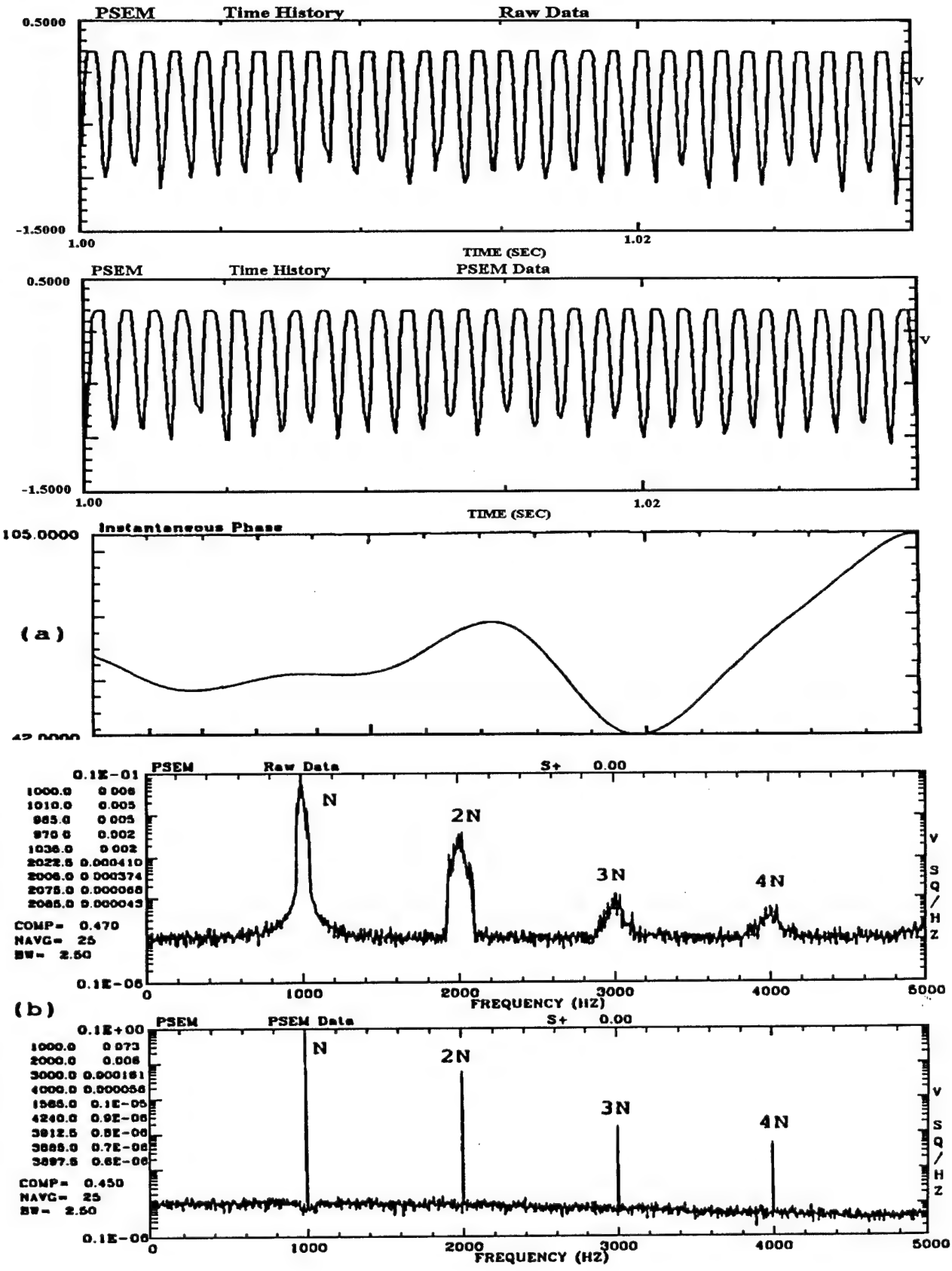

Figure 16: PSEM Simulation Example
(a), (b) show the raw time history of Simulation Signal
(c) Instantaneous Phase Variation of the Reference Component (N)
(d), (e) Raw PSD and PSEM PSD of Simulation Signal

Detection of rail track gap using PSEM signal

As mentioned before, it was not possible to plant seeded faults into the MISA drive train during Phase I field test. Therefore, the MISA test data does not provide the "best" example in demonstrating the wheel bearing fault detection capability in the low frequency region using the PSEM PSD. However, the example shown in figure 14(c) has at least demonstrated that any low frequency bearing defect signature, if exists, will be detected by the PSEM PSD just like most of the Sync and harmonics are clearly detected in this PSEM PSD. In addition, the rail track gap on the MISA antenna is used here to demonstrate the detection of an anomalous low frequency signature since seeded fault is not present in the wheel bearing. Figure 17 shows the time history of six measurements over one full azimuth excursion in the CCW direction. A sequence of spikes corresponding to the impact motion due to the rail track gaps of are clearly observed in most of these accel measurements. The frequency of the rail gap signature is at a low frequency of 0.045 Hz. Even though its signature is clearly observable in the time history, it would be more robust to monitor this signature in the frequency domain for unsupervised monitoring. Figure 18 shows its corresponding envelop PSD from the normalized PSEM signal. The fundamental rail gap impact component (0.045 Hz) along with its harmonics are clearly observable in this PSD. Deterioration and/or change of condition of the rail gap can be monitored by trending the amplitude of these rail gap signatures. Consequently, PSADDS offers the capability to monitor rail gap integrity.

SSME Example of PSEM analysis

Other than the critical advantage of overcoming the nonstationary problem by normalizing the PSD with respect to Sync frequency, the PSEM discretization process will also generate a highly desirable effect for signal enhancement. Once a signal is synchronized to RPM, all the other Sync-related components within the entire signal will automatically become discrete. With this enhanced frequency resolution, the PSEM signal can recover detailed spectral information useful for diagnostic evaluation since most defect signatures such as Sync Harmonics, Inner Ball Pass, modulation and sideband are all sync-related. Test data from an application example on the SSME ATD High Pressure Fuel TurboPump is used to demonstrate the signal enhancement capability of PSEM. During a sequence of developmental testing of ATD HPFTP, strong 6N sideband anomaly was consistently observed. The presence of this anomaly severely impacted the schedule of this shuttle main engine development. Figure 19(a) shows a typical zoomed PSD of this anomaly. The peak marked "6N", is the 6 harmonic of Sync frequency. The two strong peaks marked $6N\pm\alpha$ around 6N are the 6N sideband anomalies whose frequencies are equal-spaced from 6N. Since the left sideband, $6N-\alpha$ is right around the predicted Outer Roller Pass (ORP) frequency, and the right sideband $6N+\alpha$ is on the Inner Roller Pass (IRP) minus 2N (IRP-2N) frequency, this 6N sideband anomaly has been labeled as a possible bearing-related Defect signature. Based on this assumption, several tests have been designed and conducted in order to investigate this anomaly.

The PSEM method provided valuable insight concerning this anomaly. The Figure 19(b) shows its corresponding enhanced PSEM PSD. The 6N component indeed becomes discrete as expected. However, there is another discrete peak that became enhanced and begins to show. Notice that, in the lower frequency region of the PSEM PSD (not shown in the frequency range of figure 19), it also recovers the fundamental bearing cage frequency component and its harmonics. Since this is a 14 roller bearing system, the true ORP frequency can be pinpointed to be at the 14th harmonic of Cage. It was apparent, the 14th harmonic of cage is exactly located at the newly recovered discrete peak. This indicates that, this newly-recovered discrete peak is the true ORP frequency component. Therefore, the original strong 6N left sideband anomaly is not the ORP component as was thought before. The true ORP component is the smaller discrete peak at a different frequency very close to the 6N left sideband anomaly. Based on this finding, anomaly investigation of the ATD HPFP has changed direction to identify other vibration sources. This example has demonstrated that the PSEM can also improve the signal-to-noise ratio and recover critical signature for diagnostic evaluation and source identification. An example from MISA test data will be discussed next to demonstrate source identification from air blower interference in the PSEM PSD.

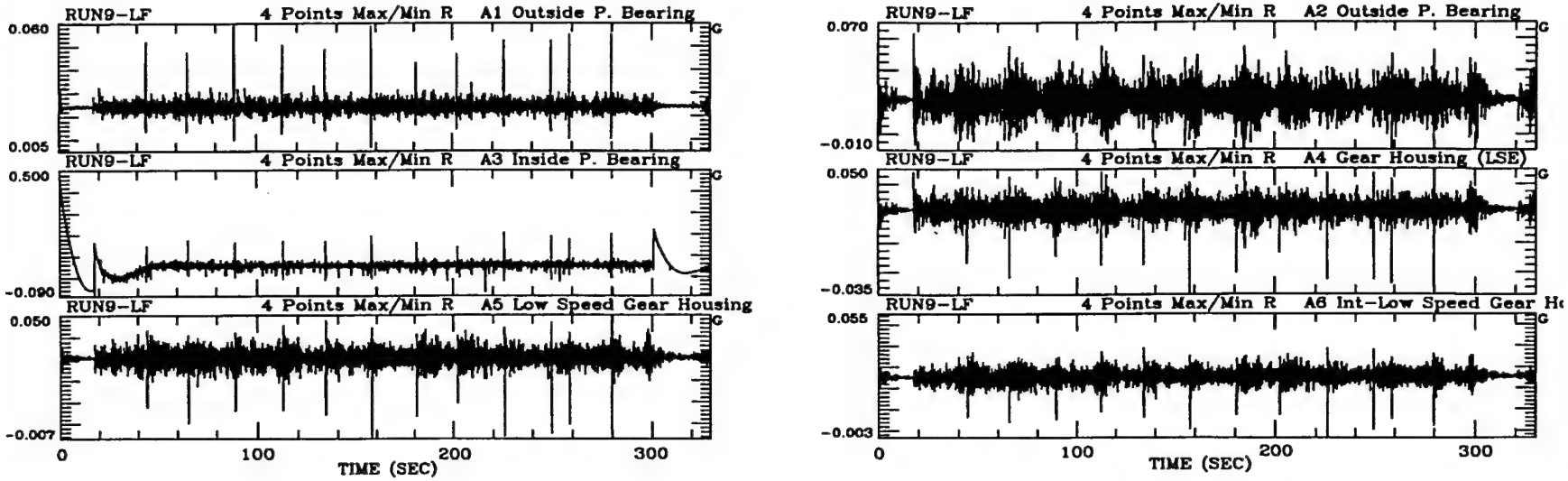

Figure 17: Time Histories of six MISA Drive measurements showing the rail gap impact responses over one full azimuth excursion

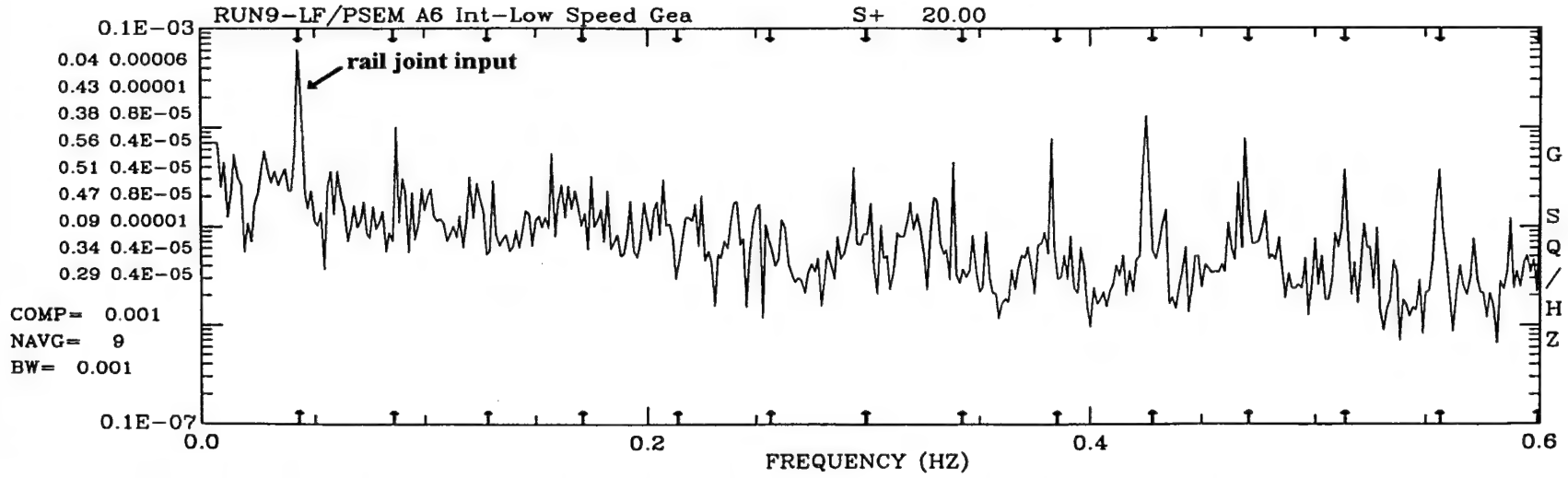

Figure 18: Envelop PSD of PSEM signal showing the fundamental rail gap impact component (0.045 Hz) along with its harmonics

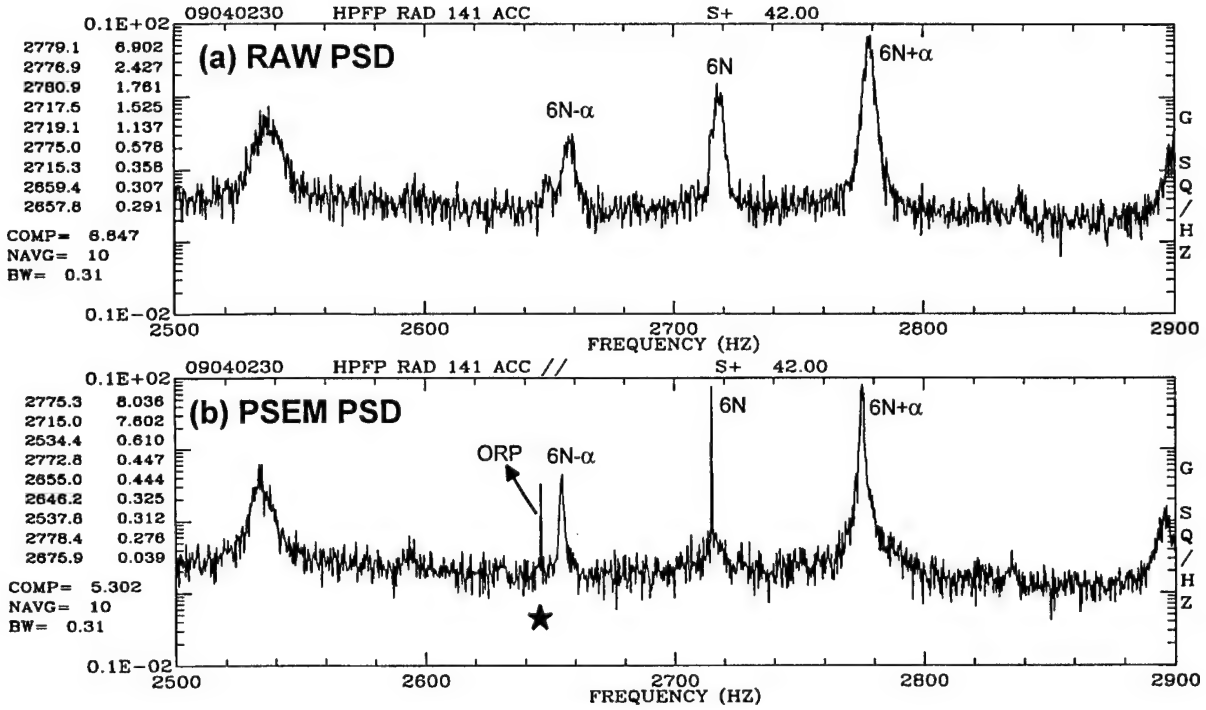

Figure 19 (a) Raw PSD of ATD HPFTP Accelerometer Test Data.
(b) PSEM PSD of ATD HPFTP Accelerometer Test Data.

Identification of MISA Antenna Drive Air Blower Interference using PSEM Analysis

As shown in last section, the PSEM will discretize all the sync-related components. On the other hand, for a non-sync-related component such as structural mode or an independent feedthrough from other nearby machinery such as an air blower or lube pump, PSEM spectral peaks will remain broad in spite of this discretization process. This leads to another powerful property of PSEM for anomaly identification, in which case we want to identify whether a spectral component is a sync-related and a non-sync-related component within a rotor system.

Figure 20(a) shows the raw PSD of the MISA's inside motor bearing measurement in the frequency range of 650 Hz to 950 Hz. Most peaks are the nominal Sync/harmonics of the drive motor (N1=30.8529 Hz) at 22N, 23N, 24N, ,30N. The strongest peak in this PSD at 721 Hz is the 12th harmonic of the air blower. The frequencies of the remaining peaks do not directly correspond to any bearing/gearbox characteristic frequency. For diagnostic evaluation purpose, it would be critical to identify whether these anomalies are sync-related or not. A non-sync-related component would indicate its vibration source is independent of the drive motor's shaft rotation process such as the air blower or other neighboring equipment. On the other hand, a sync-related component would indicate it is directly generated within the drive motor and therefore, should be further studied. From this raw PSD, it would be difficult to identify whether these anomalies are Sync-related or not since they all have similar spectral peak bandwidths. However, it would become very clear after the PSEM discritization process forces all the sync-related components to become discrete.

Figure 20(b)shows the corresponding PSEM PSDs. First, it will be noted that the Sync harmonics such as 22N, 23N, 24N, ...,30N have become discrete as we expected. However, a sequence of anomalies marked "12Nb-N," "12Nb+N," 12Nb+2N," ..., "12Nb+4N" still remain broad in spite of the PSEM discretization process. This indicates that these anomalies are non-sync-related components (i.e. independent of the drive motor). They are not synchronize with the shaft rotational motion of the drive motor. Since the spacing frequency between these anomalies is the sync frequency of the drive motor, the anomalies should be due to the nonlinear interaction between the air blower and the drive motor. Also notice that, the two anomalies marked "A1", and "A2" in figure 20(a) have become discrete, they should be sync-related components. As will be proven in the next section, even though the frequencies of these two anomalies are not at bearing characteristic frequencies, they turn out to be bearing related signatures. **This example has demonstrated that the PSEM is a very powerful tool in discriminating between a sync-related and a non-sync-related components. And such discrimination can provide critical insight for Anomaly Identification.**

4.2.4. Detection of Bearing Defect Signatures due to Nonlinear Interaction.

Faults in bearings will tend to generate characteristic frequencies. The magnitude of the signal generated will depend on the defect's proximity to the load zone. Monitoring of these bearing defect signatures at their characteristic frequencies would be the fundamental requirement for bearing health monitoring. Even though the computation of bearing characteristic frequencies is straightforward, other factors such as nonlinear interaction can cause problems in detecting the bearing defect signatures. As will be shown in this section, bearing defect signatures can be generated at different frequencies than bearing characteristic frequencies. For example, the two anomalies "A1" and "A2" in the PSD in Figure 20(a) are not directly corresponding to any bearing characteristic frequency, they still represent important bearing signatures. In addition, under the complicated MISA antenna operation environment, the spectral content of a measured PSD is quite complex due to multiple vibration sources such as the drive motor, air blower, GearMesh components within gear train and, the interaction/modulation among various components. The complexity of the spectral content presents some difficulty in detecting and identifying bearing defect signatures.

Bearing modulation Sideband Fault Pattern

As a fault in an inner race moves into and out of the load zone within each revolution, it can cause amplitude modulation with a modulating frequency of Sync (once per rev), and a carrier frequency of Inner Race Defect (IRD) frequency. Similarly, as a defect on a rolling element moves into and out of the load zone, as well as the line of contact, it will also cause amplitude modulation with a modulating frequency of Cage (ball/roller train frequency), and a carrier frequency of ball/roller spin frequency. These nonlinear interactions among various frequency components provide important signatures for bearing fault diagnostics. Such bearing faults with their associated nonlinear modulations will typically generate modulation/sideband patterns as shown in figure 21, which are composed of a fundamental and its harmonics of some bearing characteristic frequency, plus a family of sidebands around each. For example, the fundamental frequency components could be IRD or Ball/Roller Spin Frequency, and the modulating frequency (the spacing between sidebands) could be Sync frequency, the Cage frequency, or a structure's natural frequency, depending on the fault mechanism.

Due to the lack of phase relationship information among different frequency components, conventional linear spectral analysis is not able to describe or identify such nonlinear phenomena. In linear spectral analysis, the time series of any fluctuating physical quantity is regarded as the superposition of statistically uncorrelated waves and can be described, in part, by its PSD which shows the power distribution in the frequency domain. However, if nonlinear interactions occur, some coherent phase relationship exists among different frequency components. As a result, the information content of harmonics and sidebands for machinery fault diagnostics is usually not fully exploited. Furthermore, the analytically predicted bearing fault patterns are often confused with the noise corruption and signal interference from the operation environment. Under these conditions, bearing diagnostics based on PSD analysis would not be effective and could lead to false alarm identification.

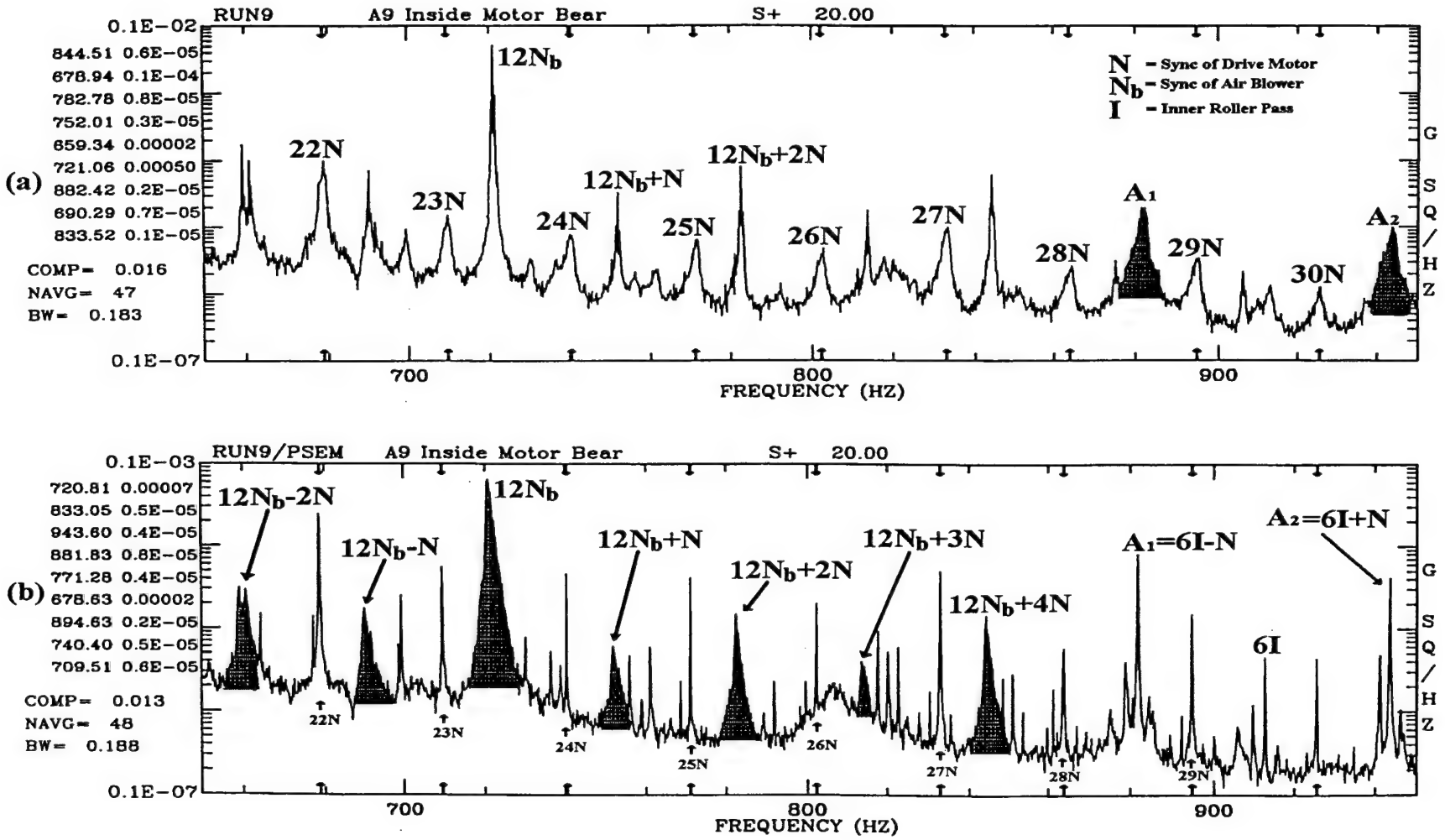

Figure 20: (a) Raw PSD of inside motor bearing measurement
(b) PSEM PSD of inside motor bearing measurement
Discrete peaks indicate sync-related
Broad peaks indicate non-sync-related (e.g. due to air blower)

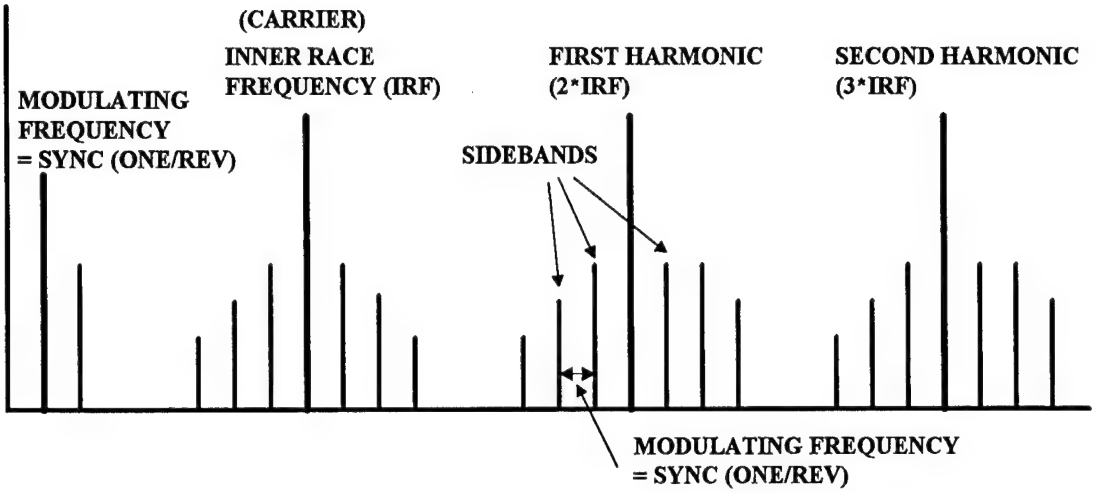

FIGURE 21. TYPICAL BEARING INNER RACE FAULT PATTERN TEMPLATE

SSME Example of Bearing Modulation Sideband Fault Pattern

An example of from the Space Shuttle Main Engine (SSME) test data will be discussed here to demonstrate the importance of such bearing modulation/sideband defect signature. Figure 22(a) shows the PSD of a SSME High Pressure Oxygen Turbopump (HPOTP) internal Strain Gauge measurement recorded during an engine hot firing. The peaks marked "N", "2N", "4N", etc., are the synchronous frequency component and its harmonics. The other peaks marked "C" and "2C" are the cage train frequency component and its second harmonic, and are normally seen in such internal measurements. However, a strong anomalous component, marked "A", is observed around a frequency of 8.5N. The frequency of this anomaly does not correspond to any bearing characteristic frequencies. In order to assess if this anomaly is an indication of a bearing related defect, the correlation between "A", the ball cage train frequency, and synchronous must be determined.

By examining the frequencies of these components, the component at 8.5N is observed to be equal to 14N-12C, or 12(N-C)+2N. This implies that the 8.5N component might be caused by the modulation between the inner ball pass component (for a 12-ball bearing set), which is at a frequency of 12(N-C), and the second harmonic of Sync. If the existence of such modulation could be proven, then the anomalous 8.5N component would represent a bearing related defect signature. However, the potential modulating harmonics at 14N, 12C and the inner race frequency, 12(N-C), do not exist in the PSD. Therefore, nonlinear spectral analysis techniques are not applicable in identifying whether such a modulation creates the anomaly 8.5N.

Instantaneous frequency if information provides an alternative way to identify such correlation between fundamental rotor and bearing components by matching the appropriate integer multiple of each fundamental IF signal corresponding to each of the modulating components. In this example, the IF signals are first estimated at the cage frequency "C", the SYNC frequency "N" and the anomalous frequency "A", as shown in figures 22(b), 22(c) and 22(d) respectively. Figure 22(e) shows the summation of negative twelve times the IF signal of "C" and 14 times the IF signal of "N". If modulation does exist, this composite IF signal in figure 22(e) should be equal to the IF signal of the anomaly "A" at frequency IRD+2N. Comparison of the reconstructed composite waveform Figure 22(e) with the IF signal of "A" Figure 22(d) reveals a strong correlation between the two figures. Therefore, anomaly "A" is a true bearing defect signature. It is both a Sync and cage related component being generated from the modulation of the

inner ball pass frequency at 12(N-C) with 2 times Sync. A later hardware teardown inspection indeed indicates uneven wear on the inner race of the bearing. In this case, the turbopump was a developmental unit which was used for continued testing following identification of the anomaly. However, if the unit had been in the flight inventory, the turbopump would have been rejected for flight. This example has also demonstrated that it is critical for any bearing health monitoring system to monitor and identify such nonlinear modulation/sideband pattern since a bearing defect may not generate signatures at bearing characteristic frequencies.

Helicopter Example of Bearing Modulation Sideband Fault Pattern Using Bi-coherence

An application example from a helicopter drive-train system is utilized to demonstrate the performance of the bispectral techniques for bearing diagnostics. The test data were captured from externally mounted accelerometers at the output end of a 42 degree gearbox which is a component in the H-46 helicopter drive train and couples to the tail rotor gearbox. Both input pinion and output gears have 27 teeth. The shaft rotational frequency (RPM or Sync) is running at approximately 71.667 Hz during the tests. The content of these tests included nominal and induced fault conditions within the transmission systems. Figure 23 shows the raw PSDs of 4 sets of tests of the accelerometer measurements. These spectra are cluttered with a gamut of discrete signals. Some of these components could represent critical bearing defect signatures, while others may be nominal system responses or tail rotor feedthrough. The complexity of the spectral content makes it very difficult to extract the analytically predicted bearing fault patterns (modulation/sideband patterns) depicted in figure 21. In addition, a sequence of spectral peaks matching the sideband pattern does not ensure that such a pattern is indicative of a fault-generated modulation sideband.

Bicoherence analysis provides an effective way to identify the bearing fault patterns since the cluster of sidebands around various carrier frequencies (e.g. IRD+k*N, and 2IRD+k*N,..) are nonlinearly correlated with each other. Therefore, a bearing fault pattern due to an inner race defect can be identified using bicoherence with the first frequency argument (1 fixed at the IRD frequency, while the second frequency argument, (2, sweeps through the entire analysis frequency range. Figure 24 depicts a bicoherence with (1 fixed at 510 Hz, the IRD frequency of the ball bearings, for the 4 sets of gearbox test data. Notice that first, spectral information in this bi-frequency domain appears "cleaner" than the PSD. In addition, a clear pattern identical to the inner race fault pattern template is immediately identified for test 3. In the bicoherence function for test 3, two clusters of sidebands are shown. The carrier frequency of the first cluster is the IRD frequency, and the carrier of the second cluster is the second harmonic of IRD (i.e. 2*IRD). The spacing frequency between the sidebands within each cluster is equal to the Sync frequency. The identification of this fault template clearly indicates that an inner race defect is present in the ball bearing of test 3. Notice that the bicoherence for test 2 also picks up strong coherence at N and it harmonics but without the presence of rich sideband clusters. This modulation phenomenon between the IRD and the Sync/harmonics also indicates a ball-bearing related fault. Later discussion with test representatives confirmed that the bispectral analysis correctly identified seeded bearing faults in tests 2, and 3.

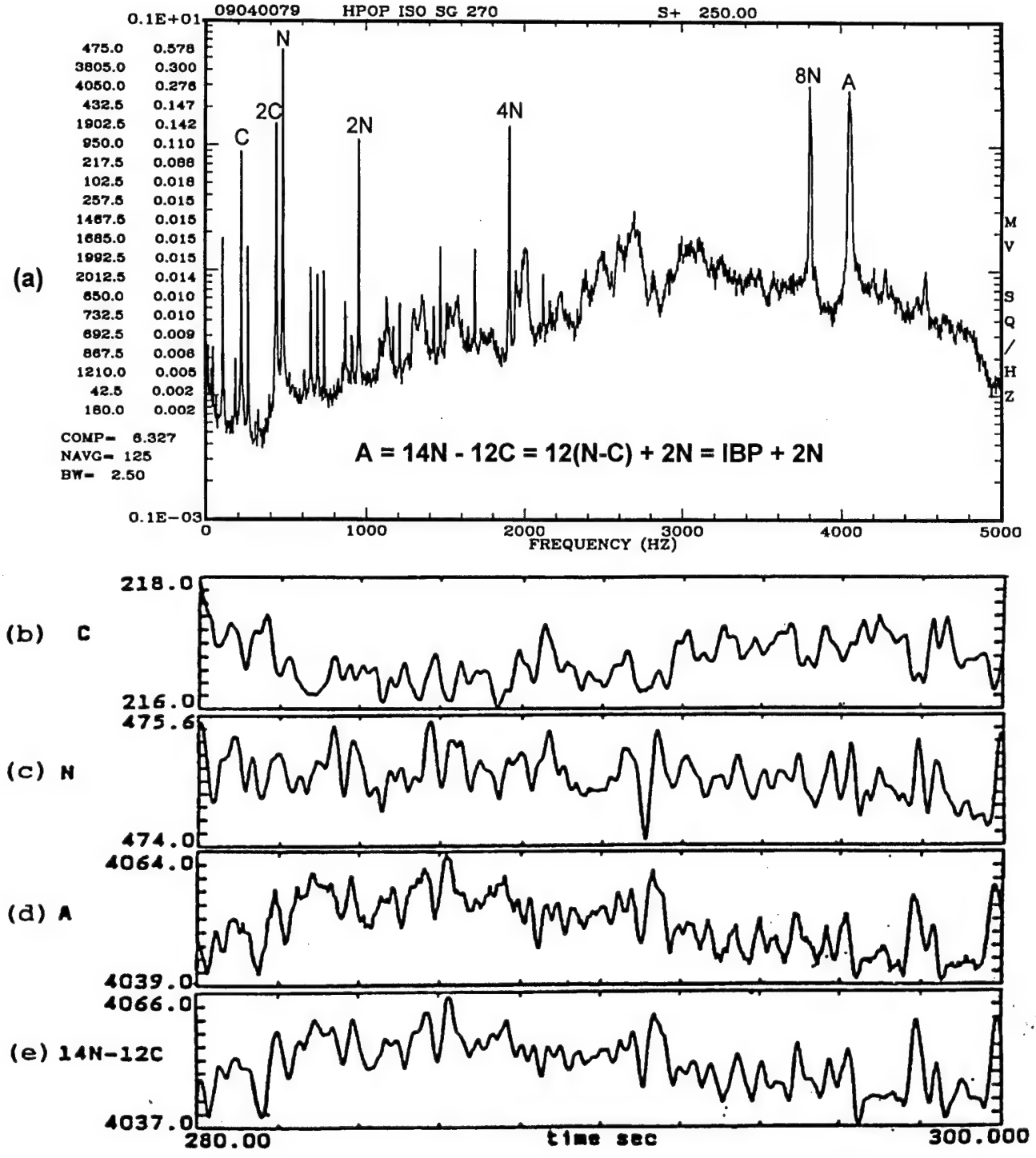

Figure 22 (a) PSD of HPOTP Strain Gauge Measurement.
(b) Instantaneous Frequency (IF) of Cage (C).
(c) Instantaneous Frequency (IF) of Sync (N).
(d) Instantaneous Frequency (IF) of Anomaly (A).
(e) 14 times of IF Signal of N (Figure 5-c) minus. 12 times of IF Signal of C (Figure 5-b).

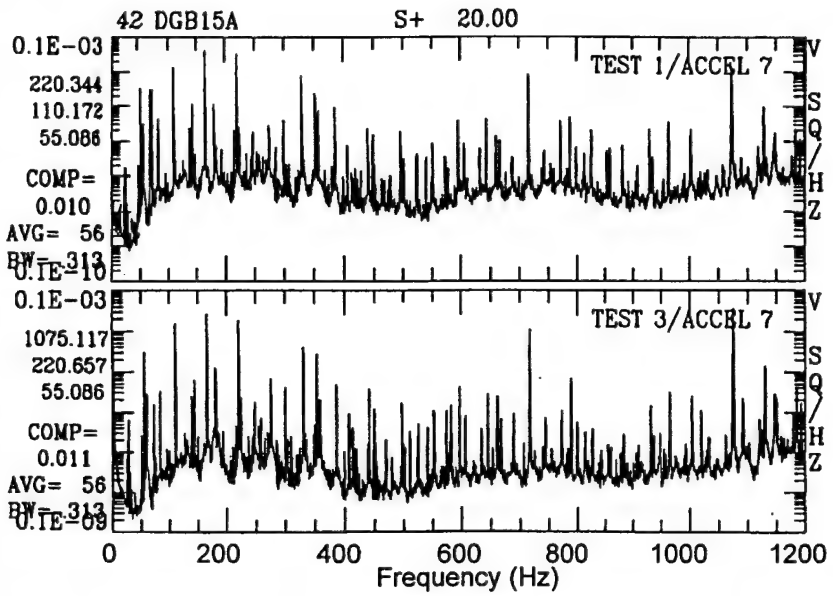

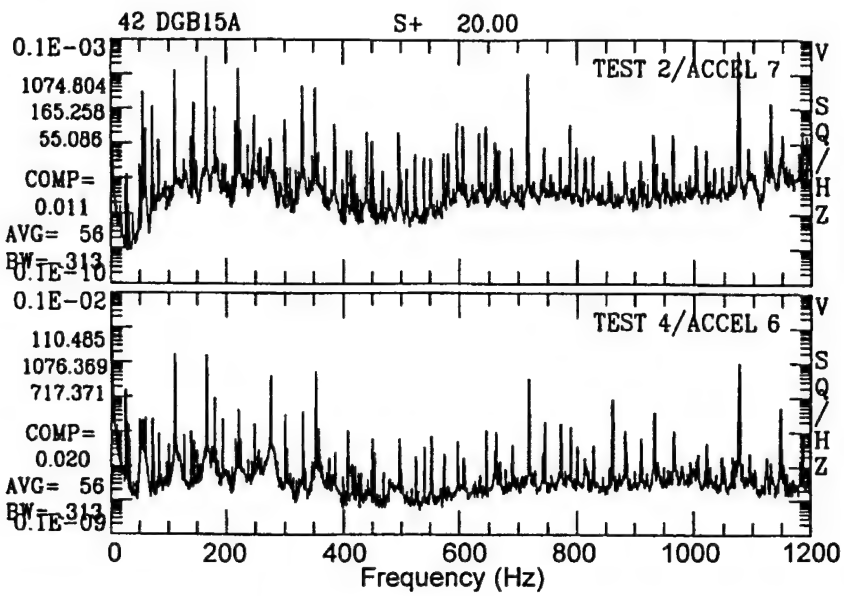

Figure 23 PSDs of 4 Sets of 42 Degree Gearbox Tests Data (0 to 1,200 Hz).

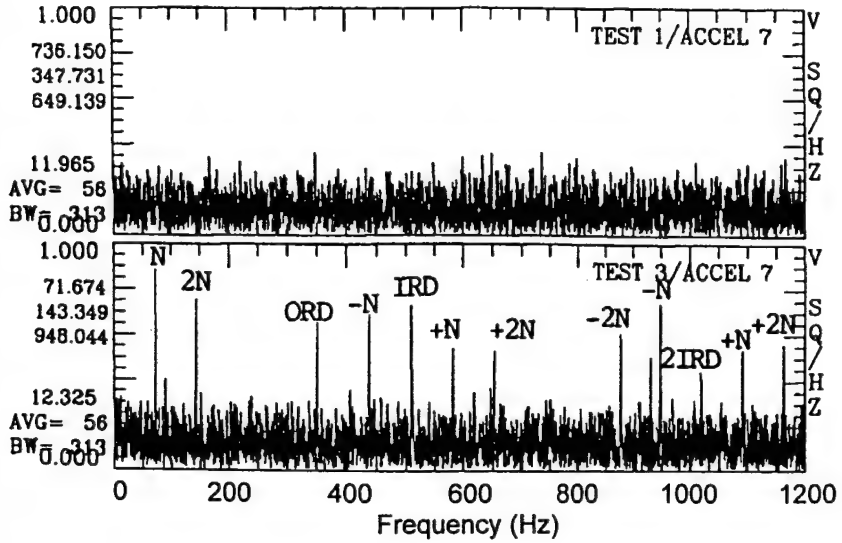

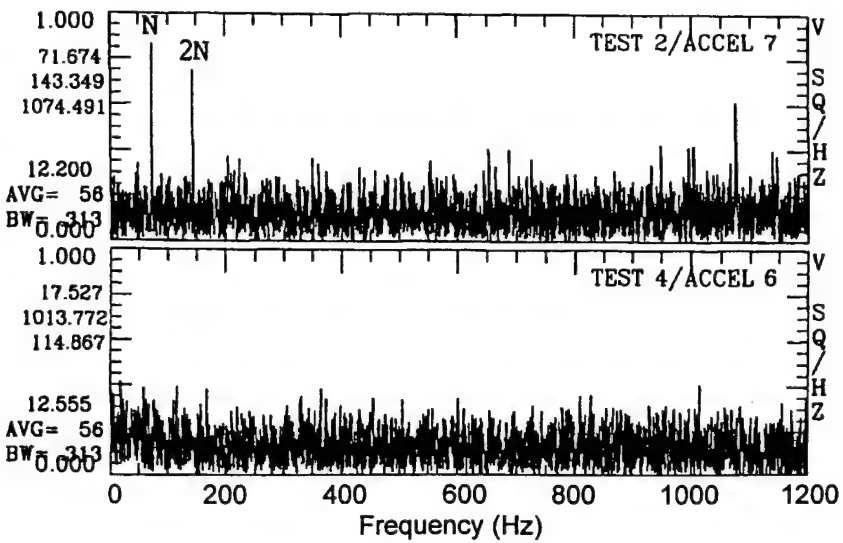

Figure 24 Auto Bi-Coherence Bxxx(510 Hz, f) of 42 Degree Gearbox Tests Data.

MISA Example of Bearing Modulation Sideband Fault Pattern Using Bi-coherence

An application example from MISA test data is utilized here to demonstrate the performance of the bicoherence analysis techniques for bearing diagnostics. Figure 25(a) shows the raw PSDs of the inside drive motor bearing accelerometer measurements. These spectra are again cluttered with a gamut of discrete signals including drive motor sync/harmonic, air blower sync/harmonics, interaction between drive motor and air blower, and possibly some critical bearing signatures.

Figure 25(b) shows the bicoherence with the first frequency argument (1 fixed at the IRP frequency, while the second frequency argument, (2, sweeps through the entire analysis frequency range. Again, spectral information in this bi-frequency domain appears "cleaner" than the PSD since only the components that are correlated with IRP will be shown in this bi-coherence function. Several modulation/sideband patterns are clearly identified. In this bi-coherence function, four "partial" clusters of modulation/sidebands are detected with carrier frequencies at 3I, 4I, 5I and 6I, (I=IRP = 151 Hz, see Table 3), and spacing frequency between the sidebands equal to the Sync frequency. Each one of these bicoherence peaks will lead to the identification of three IRP-related spectral peaks in the PSD. For example, the bicoherence peak at 5I+N= 761.21 Hz, which corresponds to the bicoherence function bxxx(I, 5I+N; 6I+N), indicates that three spectral peaks: I , 5I+N, and their sum frequency, the 6I+N component, are highly correlated with each other since they all belong to the same modulation/sideband pattern. Notice that, the frequency of 6N+I at 944 Hz is corresponding to the anomaly "A2" in the PSD in figure 20(a). This anomaly "A2" has been proven to be a sync-related component by the PSEM PSD in figure 20(b). The bicoherence analysis here further identifies it to be a bearing-related, or more specifically Inner-race-related signature. The other anomaly "A1" at 882 Hz, which also is sync-related in the PSEM PSD, turns out to be another member of the IRP modulation/sideband pattern at 6I-N. It should be pointed out that, the presence of this bearing signature may not indicate an immediate or severe gearing defect since a good bearing could also generate these bearing signature depending on the load condition. **However, this example demonstrates that it is important to monitor and identify such nonlinear bearing modulation/sideband fault patterns for the ALTAIR drive monitoring system since a growth in spectral amplitude at the sideband frequencies would indicate bearing degradation and defect development.**

4.2.5 Gearbox Monitoring of MISA Antenna

The gear box is another important component within the antenna drive train to be monitored. In this section, gearbox monitoring using MISA test data will be discussed. Time domain averaging (TDA) is a well-known and powerful technique for extracting periodic signals from noisy or complex waveforms. For this process to be coherent, it requires that the period (T0) of the signal to be extracted be known or assumed. It is based on averaging points one period apart, where the period is that of the signal to be extracted. It can be shown that, the TDA process is equivalent to a comb filter with center frequencies of Kf0, (f0=1/T0; K=1,2,3...). Figure 26 shows a typical shape of the transfer function |H(f)| of a TDA comb filter. The filter is formed by side lobes in addition to the main lobes centered around Kf0. As the number of averaged ensembles (N), increases, so does the sharpness of the main lobes. For machine diagnosis, the quasi-periodic nature of shaft rotational speed does not allow direct application of TDA. Therefore, TDA is usually performed by utilizing a trigger-pulse synchronous signal (such as once per rev signal) in order to synchronize the averaging process with the shaft rotational motion. Such synchronous time averaging (STA) is generally considered to be a key method for analyzing gear behavior .

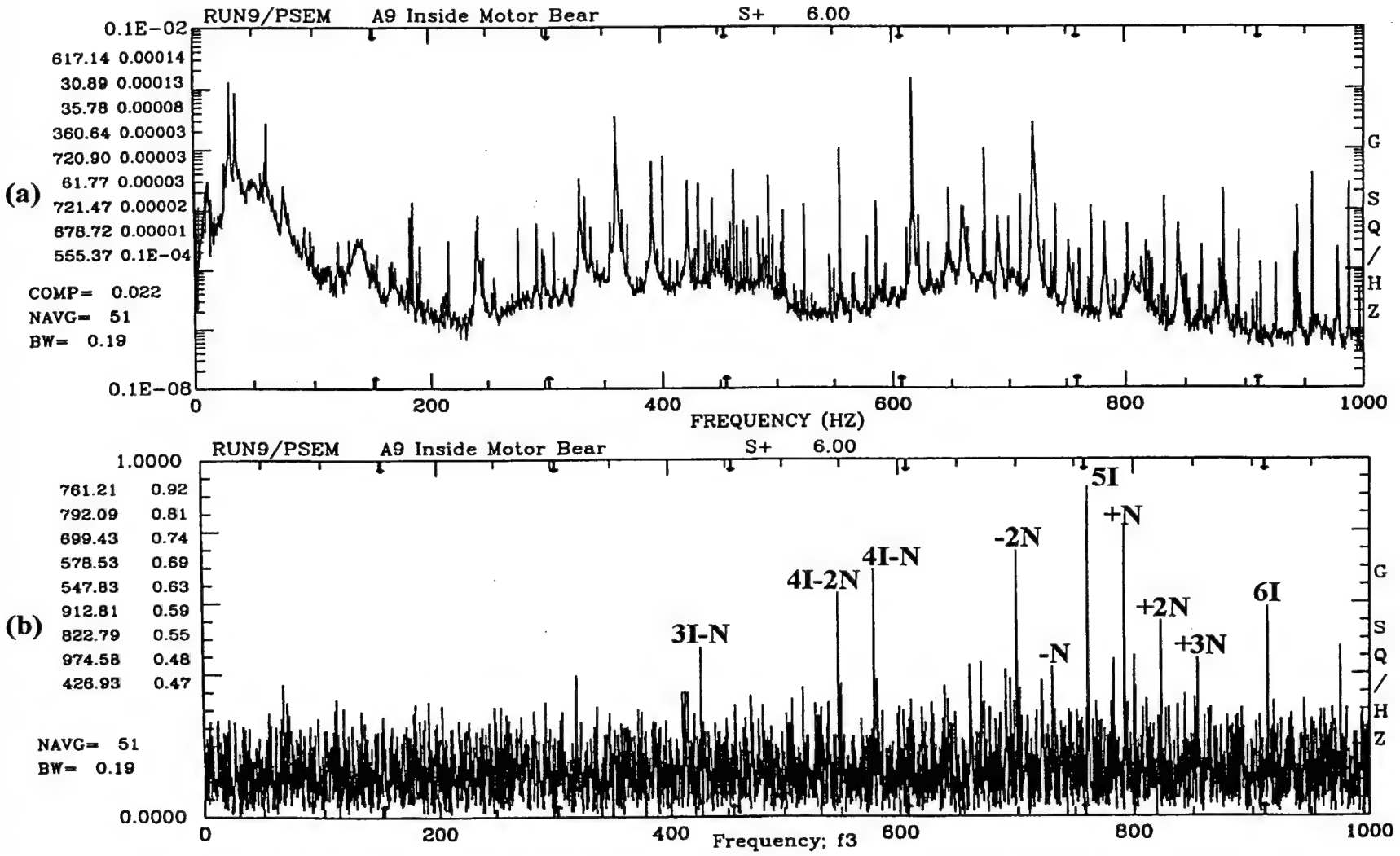

Figure 25: (a) PSDs of the inside drive motor bearing measurement A9
(b) Bicoherence bxxx(w1=IRP, w2) of measurement A9 with w1 fixed at Inner Roller Pass (IRP) Frequency

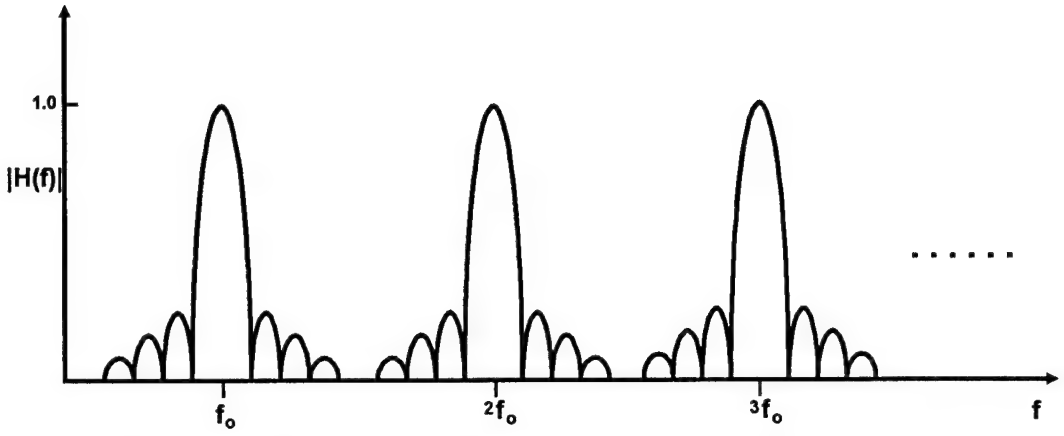

FIGURE 25 TRANSFER FUNCTION OF TDA COMB FILTER

Helicopter Gearbox Example for Gear Fault Detection

Application examples from helicopter gearbox test data with seeded gear faults are utilized to demonstrate the STA techniques for gearbox diagnostics. The test data were captured from accelerometers at the output end of a 42 degree gearbox. The 42 degree gearbox is a component in the H-46 drive train which couples the H-46 engine to the tail rotor gearbox. Both input pinion and output gears have 27 teeth. The shaft rotational frequency is running at approximately 72 Hz during the tests, therefore, the predicted gear mesh frequency is approximately 1935 Hz (27N). All analog accelerometer channels were sampled at 10,240 Hz. The content of these tests included nominal and induced fault conditions within the transmission systems.

Six sets of test data from the 42 degree gearbox are used to demonstrate this STA application. Figure 27 shows the raw time history of an accel measurement for these six sets of gearbox data during one revolution of shaft rotation. The waveforms of the raw signal are all corrupted by background noise. Notice that, in this example, the key phasor information is not available, therefore, the STA is performed differently by performing TDA on the PSEM signal. Figure 28 shows the resulting STA (or TDA/PSEM) signals each over a full cycle of shaft rotation for the six tests. The number of ensemble averages performed in the analysis is 500. Within this full cycle of shaft revolution, an enhanced signal with 27 cycles of oscillation is observed which corresponds to the tooth mesh waveform. In examining the smoothness of this waveform, a noticeable discontinuity or irregularity is readily observed in tests 6 and 7 at the 26th oscillation cycle. This discontinuity repeatedly shows up in the SPA enhanced signal at other time periods within the test. This indicates a gear tooth fault at the 26th gear tooth within the hardware used in tests 6 and 7. Subsequent discussion with the helicopter drive train test representative revealed that the SPA analysis indeed successfully identified seeded faults in the 42 degree gear boxes of tests 6 and 7.

MISA Antenna Drive Example for Gear Fault Detection

Test data from the MISA drive gearbox measurements are used to demonstrate this STA application. Figure 29 shows the raw time history of the key phasor and five other accel measurements of MISA test data during three revolutions of drive motor shaft rotation. The waveforms of these raw signal are all corrupted by background noise. Figure 30 shows the resulting STA signals each over a full cycle of drive motor shaft rotation. The STA waveforms on the left column are corresponding to three different full excursions in the CCW direction for the outside motor bearing measurement (A8); while the STA waveforms on the right column are for the air blower measurement (A10). The number of ensemble averages performed in the analysis is 8600. Within one full cycle of shaft revolution of the drive motor, an

enhanced signal with 20 cycles of oscillation is observed which corresponds to the tooth mesh waveform of the high speed gear. Strong similarity among different excursions is clearly evident in these STA waveforms. This indicates that a statistically "stable" STA waveform can be generated from the measurement as the "gear signatures" for monitoring. Gearbox health monitoring can then be performed by closely monitoring any deviation of current gearmesh waveforms from such gear signatures. Any significant deviation such as discontinuity or irregularity could indicate gear-related fault.

[5] IMPORTANT FINDINGS AND CONCLUSIONS

The proof of concept study conducted during Phase I of this SBIR program has successfully demonstrated that the development of the PSADDS system as an effective ALTAIR drive train health monitoring system is highly feasible. Based on the representative information obtained from MISA test data under actual antenna operations, several requirements and considerations critical to the development of the ALTAIR drive health monitoring system have been identified. These include (1) RF interference (2) Air blower noise interference, (3) Frequency normalization due to nonstationary operation, and (4) Detection of nonlinear modulation/sideband bearing defect signature. These unique requirements and considerations play a significant role in the determination of the best method for generating frequency spectrum signatures for health monitoring. Since the MISA antenna should adequately replicate the ALTAIR drive system, any reliable ALTAIR health monitoring system should take into account these special requirements identified from MISA antenna test data. Several actual application examples have been shown to demonstrate the significance of these considerations along with the effectiveness of our proposed solutions in developing the ALTAIR drive monitoring system. Based on these special requirements and considerations, a PSEM PSD is identified as the best format to represent monitoring signatures for the drive train component since such signatures can (1) identify non-sync-related anomalies due to air blower noise interference, (2) identify sync-related anomalies due to bearing defects, and (3) provide a frequency normalized PSEM PSD which is more desirable under nonstationary antenna operations.

The results from the Phase I feasibility study demonstrates that with the incorporation of a hierarchy of diagnostic signal analysis techniques for anomaly detection and identification, the PSADDS can successfully identify critical bearing and gearbox defect signatures/anomalies along with their underlying causes. In addition, with this Anomaly Identification capability, the PSADDS will greatly reduce mis-interpretation/false-alarm rates, and improve system reliability. This study using the real-world examples from the MISA antenna reinforces the feasibility of the development of PSADDS as a reliable ALTAIR drive health monitoring system. The Phase I results have demonstrated that the development of the PSADDS is highly feasible, and can fully justify the Phase II continuation in completing the design, development and testing of the antenna drive health monitoring system for both the DOD and other industrial application.

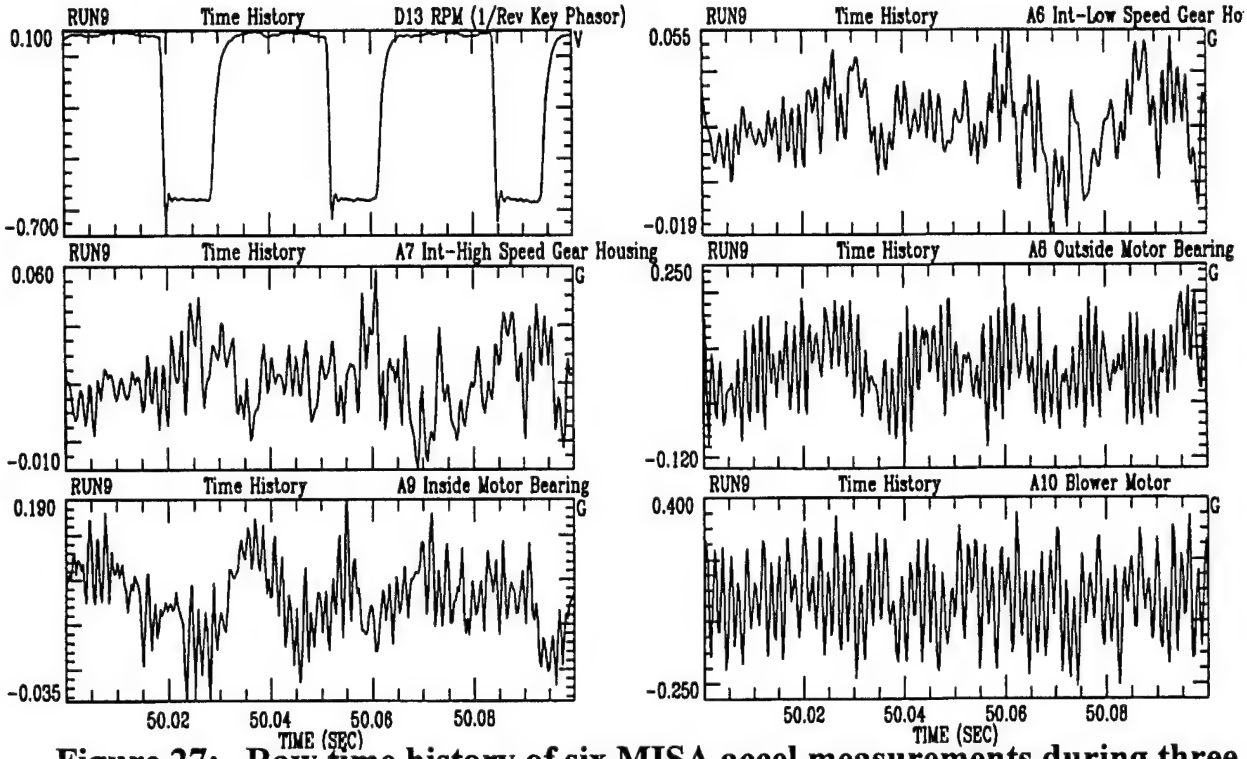

Figure 27: Raw time history of six MISA accel measurements during three revolution of shaft rotation

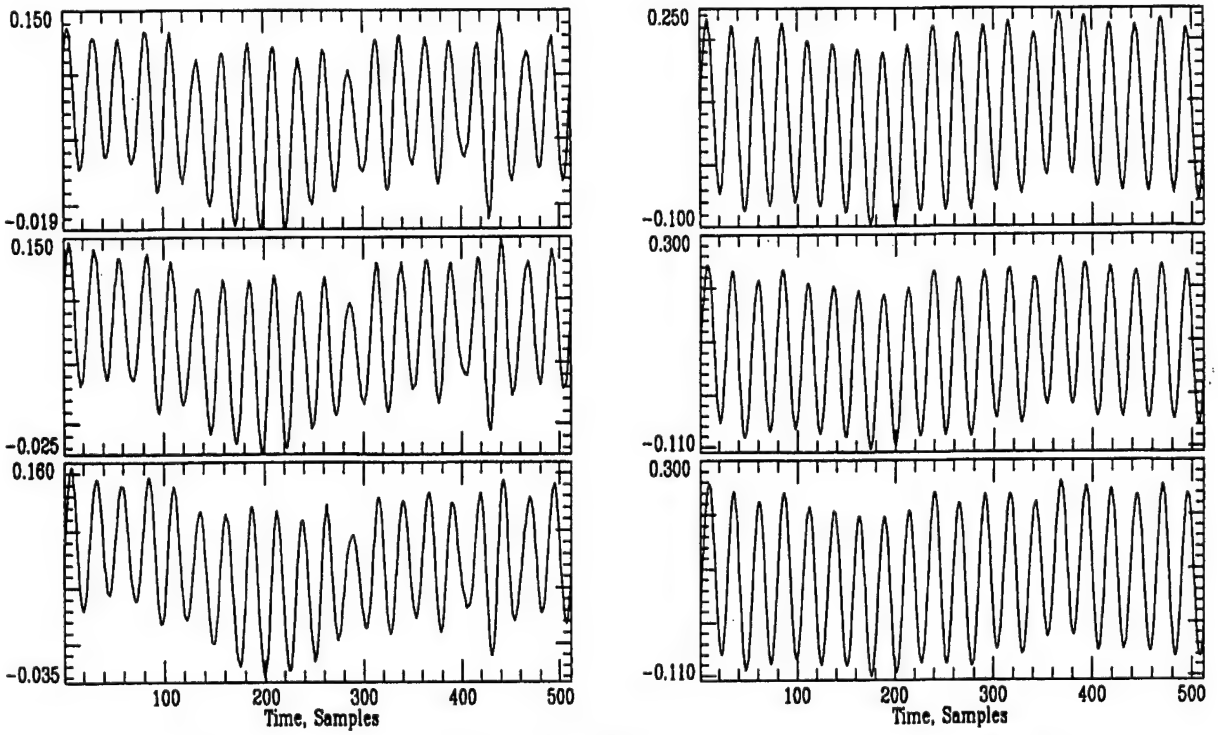

Figure 28: Enhanced STA GearMesh waveforms of six MISA accel measurements over a full cycle of shaft rotation

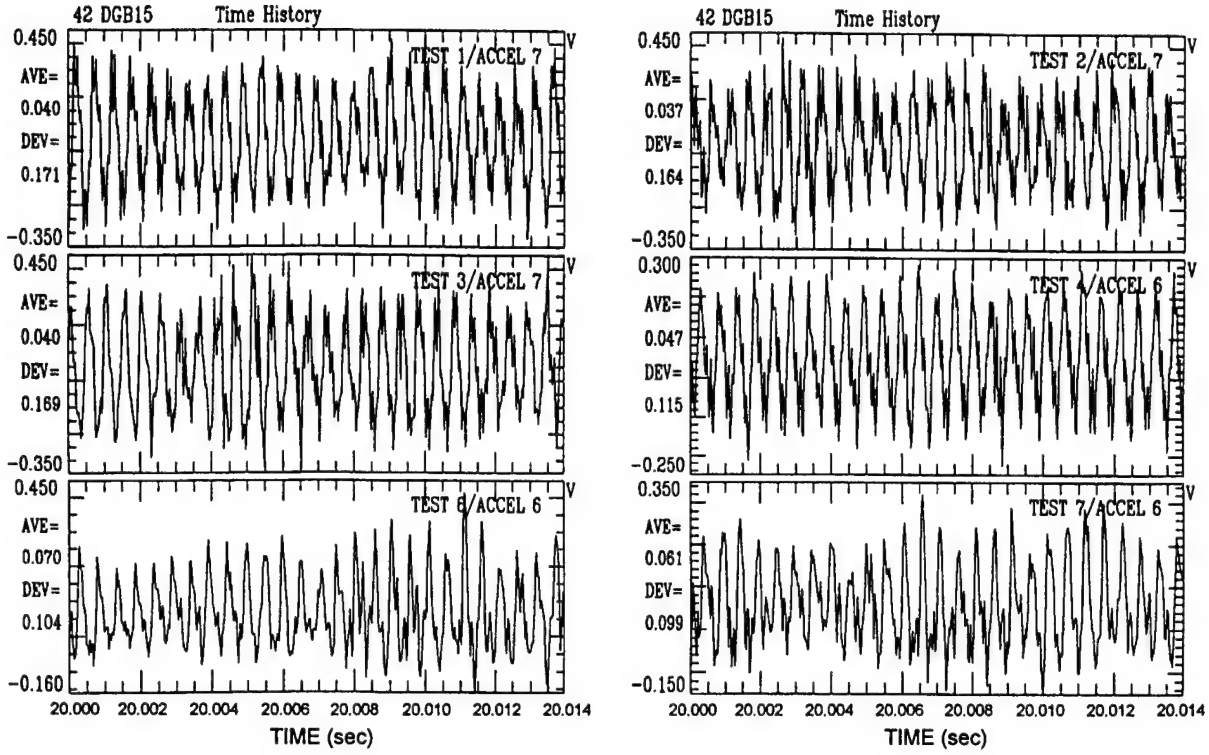

Figure 29: RAW Signal of 42 Degree Gearbox Data with 500 Averages (Fundamental Frequency=Sync)

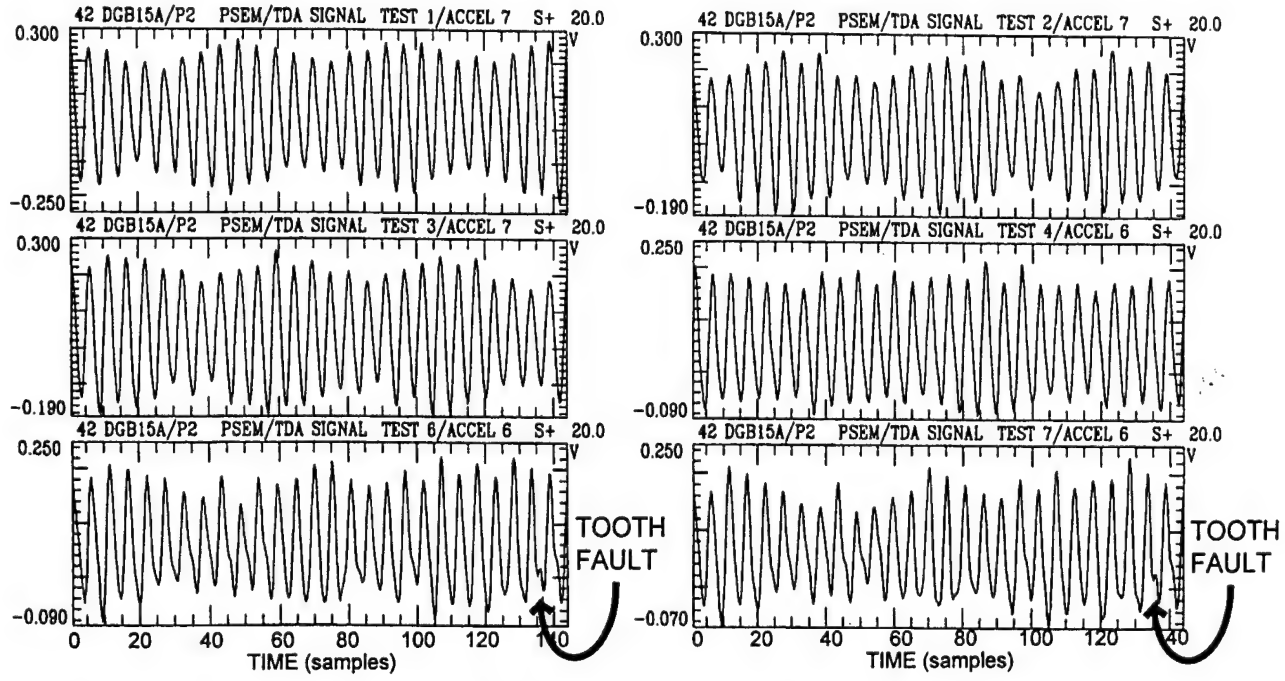

Figure 30: SPA Signal of 42 Degree Gearbox Data with 500 Averages. (Fundamental Frequency=Sync)

[6] IMPLICATIONS FOR FUTURE RESEARCH

An on-line PSADDS System for drive train diagnostics will have considerable commercial potential outside DOD, particularly in the air traffic control radars and weather radars in the commercial transportation industry. In addition, power generation industries and manufacturing process sectors could all benefit from an effective on-line diagnostics system. Such systems will allow plant operators to initiate appropriate corrective action, and provide efficient scheduling of maintenance and repair activities. With this in mind, there exists significant commercial potential for a low-cost, high-performance machinery health monitoring system. Our approach would greatly increase client system reliability by automating the signal intelligence monitoring and identification task, thereby reducing costs associated with system monitoring. Once the technology is demonstrated to be highly promising, ASRI plans to jointly exploit the potential commercial market with our subcontractor who will supply development and marketing support for the introduction of this product to a selected industrial market. The currently unrealized commercial demand for such a system is significant due to the tremendous cost savings and productivity enhancement it can offer.

The scope of work planned for the Phase II program will consist of the following tasks aimed at PSADDS development, delivery and commercialization planning:

Task 1 - Prototype Design and Development
Task 2 - Field Test and Verification
Task 3 - Performance Analysis and Refinements
Task 4 - Systems Installation and Acceptance Testing
Task 5 - Commercial Implementation Planning

Figure 31 illustrates the flow of work between tasks leading to the major program deliverables: 1) An operational PSADDS for ALTAIR with integrated software and supported by demonstrations and training, 2) a Commercial Implementation Plan that will establish the basis for a Phase III commercialization program, and 3) a final Report that documents the total Phase II program. A brief discussion of work to be performed under each task follows:

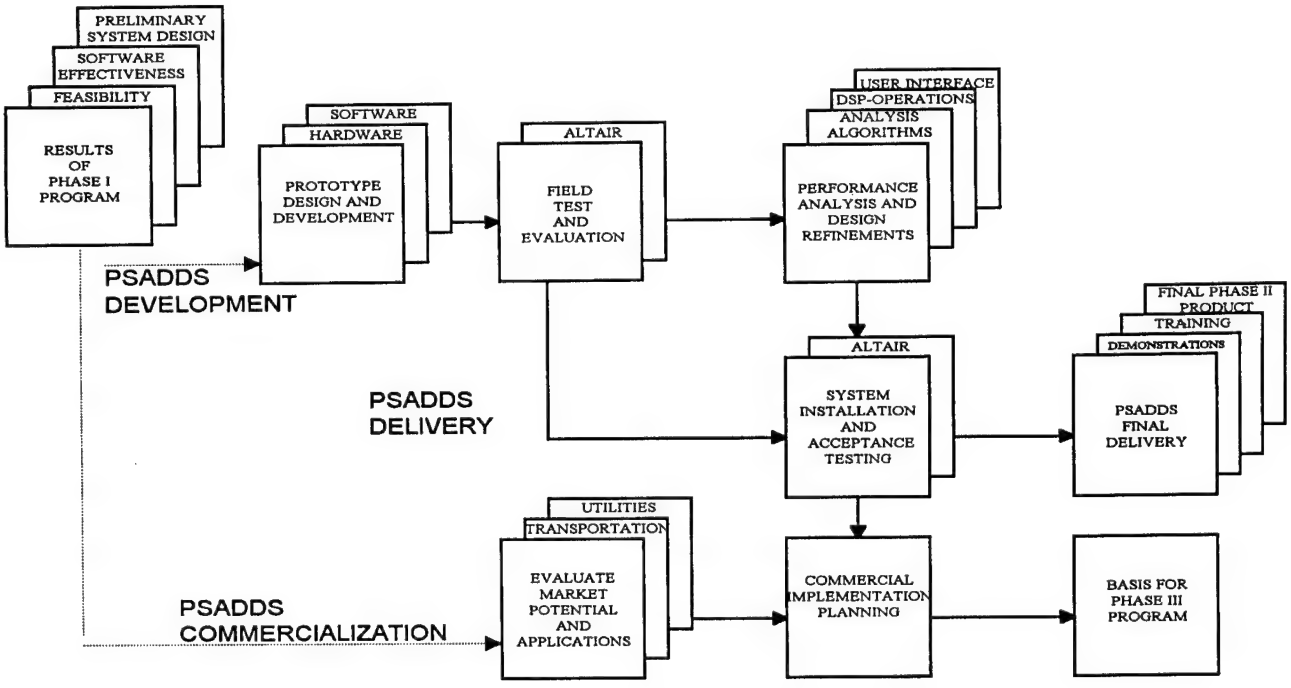

Figure 31: Phase II Program Work Flowchart

6.1 TASK 1 - PROTOTYPE DESIGN AND DEVELOPMENT

A preliminary design of the PSADDS was developed under the Phase I program and a brief description is presented in this report. Major functional subsystems have been identified and generic specification are defined. Under this task, the preliminary design and specification will be refined and detailed to facilitate the development of a prototype PSADDS for test and evaluation. ASRI'S concept for the PSADDS consists of a hierarchical set of computer hardware and software, integrated to achieve real-time machinery health monitoring, in general, and ALTAIR drive system fault detection and diagnostics, in particular. The computer hardware shall be expandable in terms of data channels with an open architecture that will accommodate advanced developments. Similarly, the PSADDS signal analysis capabilities will be designed to accommodate a family of analysis algorithms that can be readily updated as future developments warrant. The design of the prototype PSADDS under this task will address all elements of the system including:

- Sensor Selection and Location

  1) Compatibility with operational environment
  2) Protected installation and long term reliability
  3) Analysis technique sensitivity and bandwidth requirements
  4) Safety

- Signature detection/identification methodology and its Signal Processing Algorithm. Criteria for the evaluation of candidate diagnostic detection algorithms will include:

  1) Fault detection/false alarm discrimination (statistical reliability)
  2) Sensitivity to extraneous noise
  3) Failure mode isolation
  4) Fault growth identification (incipient detection)
  5) Simplicity and reliability of implementation

- Platform/hardware system components and performance range.

  1) Embedded automatic operation
  2) Open architecture
  3) User friendly interfaces and operation
  4) Commercial availability

The design of the PSADDS prototype shall be a functional prototype of the final system to be installed on the ALTAIR. The prototype PSADDS will serve as a pathfinder for a future commercial product that will be pursued under a subsequent Phase III program. A major goal of the prototype design effort is to configure the prototype so that transition to a commercial configuration can be accomplished with minimum scaring of the design. This approach places emphasis on the use of an open architecture, compliance with industry standards, and maximum utilization of commercial off-the-shelf components and software where possible.

The core of the PSADDS development program is the application of signal analysis techniques to achieve fault detection and identification via pattern recognition. This requires the application of both statistical-based, dynamic data reduction algorithms in combination with pattern recognition algorithms based on analytical models of machinery dynamic characteristics. Success in fault detection and identification is a sequential process involving first, the identification of an anomaly; second, an assessment of causality; and third, determination of severity. Several signal analysis algorithms may be involved in this process. Our experience has shown that one algorithm is optimal for a particular application and failure mode. However, screening of the data through several signal analysis techniques may be required to identify the optimum technique.

6.2 TASK 2 - FIELD TEST AND EVALUATION

Field testing of PSADDS to evaluate capabilities and to demonstrate effectiveness as a machinery health monitoring and diagnostics system will be performed in two steps. First, the prototype PSADDS will be installed on one or more of the ALTAIR drive system "bogies" and a comprehensive field test program will be performed during the first year of the Phase II program. This initial test and evaluation program will be performed under this task. Following analysis of field test data, refinement will be made to the PSADDS as required (under Task 3) and the final PSADDS tailored to ALTAIR requirements will be installed and acceptance testing performed under Task 4.0 during the second year of the Phase II program.

Our approach to the initial field tests of the prototype PSADDS will draw upon lessons learned from our Phase I experience with the MISA antenna at the MIT Haystack Observatory. As a minimum, we plan to thoroughly instrument one the ALTAIR azimuth drive system "bogies" by installing non-intrusive, surface mounted sensors to major drive components such as: bearing assemblies, gear trains, drive motors, air blowers and other components that are either critical components in the drive train or that may produce dynamic signals that could corrupt critical component signatures. It would also be desirable to thoroughly instrument representative drive components in the antenna elevation drive train if accessible and permitted by ALTAIR operational constraints. In addition, microphones will be located in the vicinity of the antenna to record, in the audible frequency range, noise radiation from the antenna. It may be possible to detect both drive system characteristic noise as well as defect signatures - particularly for drive system components on the high speed end of the drive train (prior to gear reduction). The microphones will also provide insight into background noise from blowers and other sources that would tend to mask important component signatures.

We expect that ALTAIR operational constraints may preclude the introduction of defective components with known, seeded faults into the drive systems. If this is the case, our field test will be limited to definition of baseline dynamic characteristics for "as installed" conditions which may or may not contain component defects. However, our prototype PSADDS should be fully capable of 1) establishing baseline dynamic characteristics for future trend analysis and 2) identifying any defects that may be present as in the case of a "blind" test.

One interesting feature of the ALTAIR is the presence of rail joints at approximately eleven equal intervals around the azimuth circular track. The joints introduce discrete dynamic inputs into the ALTAIR structure as each wheel passes over a joint in transient around the track. In effect, these impulses serve to simulate anomalous defects in the drive train and will be used to demonstrate PSADDS fault detection capabilities. Also, rail joint deterioration is of importance to ALTAIR maintenance personnel, and PSADDS will be evaluated as a means of monitoring and assessing rail joint integrity.

6.3 TASK 3 - PERFORMANCE ANALYSIS AND DESIGN REFINEMENTS

Following the field testing of the prototype PSADDS using the ALTAIR, a thorough analysis of test data will be performed. Data analysis will identify frequency characteristics of normal, baseline dynamic signals and any anomalous non-linear characteristics indicative of defects. As previously noted, there will be no attempt to introduce known, seeded faults into the ALTAIR drive system since we anticipate that our initial testing may piggy-back off normal antenna operations. However, we expect to fully characterize normal, baseline dynamic characteristics in the presence of extraneous background noise, to identify individual sources of disturbances, and to detect and identify, if present, anomalous non-linear signals attendant with any component defects such as rail joints. ASRI has submitted an application under the DOD SBIR "Fast Track" Program, and proposed an Interim Task to analyze wheel bearing data provided to us by the Association of American Railroads (AAR). These data provide accelerometer and microphone measurements for bearings with a range of known seeded defects operating under various load and speed conditions. Analysis of these data will provide valuable insight into the capabilities of PSADDS

technology to identify and characterize bearing defects, in particular, and drive train component anomalies, in general.

Based on extensive analysis of ALTAIR field measurements, related data such as the AAR faulted bearing data, and lessons learned regarding adaptation to the natural and induced environments, a final design iteration will be made for PSADDS. The design will be configured for final installation and acceptance testing on ALTAIR.

6.4 TASK 4 - SYSTEMS INSTALLATION AND ACCEPTANCE TESTING

Under this task, the final design of PSADDS for ALTAIR will be delivered and installed, and acceptance testing will be performed. We anticipate that the final system will have an array of sensors that will detect component vibration signatures for all critical drive system components including wheel bearings for the azimuth load - carrying bogies and the pivot bearings for the elevation axis. In addition, we anticipate making integrated system dynamic measurements such as 1) noise radiation from azimuth and elevation drive systems and 2) motor current for azimuth and elevation drive motors. Finally, it may be necessary to install special purpose instrumentation, such as stress-wave acoustic emission (AE) sensors to monitor quasi-static load carrying members such as the wheel bogie pivot bushings. AE sensors would detect any binding due to fretting or galling in these quasi-static bearings.

A major challenge for the final system installation is wire management and the protection of instrumentation from the adverse natural elements on Kwajalein. ASRI will use ruggadized instrumentation where possible and take special care to protect instrumentation - particularly sensors and wiring - by using protective covers and conduit. In addition, system design will employ modular systems for signal conditioning and multiplexing where possible to minimize the number of cable runs from the sensors to the data acquisition and analysis system. One of our subcontractors for the Phase II project will explore the possible use of a "wayside" measurement station in lieu of (or in combination with) surface mounted sensors.

Final acceptance testing will consist of a comprehensive shake-down test to verify the end-to-end performance of the installed system. In addition, operational tests will be performed to baseline the characteristic signatures for critical drive system components and to establish the historical data base for setting limits and performing trending analysis. The PSADDS will function as an intelligent on-line machinery monitoring and diagnostics system which will provide a systematic approach to automatically capture, reduce, store and analyze transient and steady state dynamic data in a variety of formats during the daily operation or testing of ALTAIR. Key analysis modules are:

1) Baseline Data Base module - Establishes the baseline history of ALTAIR drive system dynamic characteristics.
2) Anomaly Detection module - Detects anomalous signatures through similarity and trend analysis by comparing ALTAIR'S present condition against its baseline history.
3) Anomaly Identification module - Verifies whether an anomalous signature detected is a false alarm or misrepresentation and, if not, identifies the most likely cause of the anomaly.

Acceptance testing will demonstrate the capabilities of these key analysis modules.

6.5 TASK 5 - DEVELOP COMMERCIAL IMPLEMENTATION PLAN

The final task under the Phase II program will be to develop a detailed plan for the commercial launch of the PSADDS. The interest of our two subcontractors in PSADDS and their contribution will be key to the successful introduction of a commercial PSADDS into the marketplace. The ASRI team will identify commercial applications, in general, and specific niche markets, in particular. This team actively markets

products and services to the aerospace/defense, transportation and electric utilities industries. Many of our products and services involve equipment operation, safety and reliability. Machinery health monitoring and diagnostics is a complementary addition to the team portfolios. Our market assessment will focus on the automotive and railroad transportation industries and the electric utility industry. The Commercial Implementation Plan will focus on niche markets that require the unique capabilities of PSADDS to detect drive system component faults in rotary dynamic systems operating in noisy environments. It is anticipated that more conventional machinery monitoring and diagnostic systems using conventional accelerometers, displacement sensors, etc., and standard PSD analysis techniques provide adequate coverage for most industrial machinery health monitoring requirements. Although our PSADDS could be used as a general-purpose health monitoring system, the unique, value added capability of the PSADDS will be primarily in two areas: 1) the capability to detect faults in rotary system components in the presence of high-level background noise that would otherwise mask the fault-related signal and 2) improvement in the reliability of fault alerts i.e. increasing the probability that a fault does exist when the PSADDS indicates a fault and thereby reduce the occurrence of false alarms.

6.6 DELIVERABLES

At the completion of the Phase II program, a Final Report will be submitted together with the fully operational PSADDS. The Final Report will describe the results of all tasks performed during Phase II. In addition, documentation that describes the operation and maintenance of the PSADDS will be submitted with the system and a brief training of ALTAIR personnel will be conducted. Finally, a Commercial Implementation Plan will be submitted that describes ASRI plans for the development and marketing of a commercial PSADDS. This plan will form the basis for a Phase III commercialization program.

[7] SIGNIFICANT HARDWARE DEVELOPMENT

ASRI proposes an open system architecture for PSADDS that consists of a hierarchy of commercial-off-the-shelf sensors, signal conditioning electronics and computers integrated with the essential signal processing algorithms to achieve reliable health monitoring and fault diagnostics of the ALTAIR azimuth and elevation drive systems. Our design approach provides the best platform to fulfill requirements for long term, on-line monitoring and diagnostics in a cost effective manner. The preliminary layout of this design is presented in Figure 32. It will be noted that PSADDS has a distributed architecture that employs remote modules at five stations on the antenna and a host module located at the ALTAIR control room. Each of the four azimuth drive stations and the elevation drive station have a dedicated remote module. The five modules are essentially identical in their basic architecture with the elevation drive module configured somewhat differently to account for the unique diagnostic requirements of the elevation drive system. Each of the five modules will be comprised of the following subsystems:

1) Sensor and Amplifier Subsystem (SAS)
2) Data Acquisition and Digital Signal Processor Subsystem (DADSPS)
3) Remote Computer Subsystem (RCS)

The DADSPS will be integrated I/O boards that interface with the ISA bus of the remote computers.

The Host Module will consist of the following subsystems:

1) Host Computer Subsystem (HCS)
2) Graphical User Interface Subsystem (GUIS)

The HCS receives and archives all data downloaded from the remote modules and provides the operator interface with PSADDS in the ALTAIR control room. A description of remote and host modules are described in the following subsections.

7.1 Remote Modules

Remote modules are to be located as near as possible to their respective drive stations in order to minimize cable runs between sensors, amplifiers, and the data acquisition system. The elevation drive module will likely be located near the pintal bearing since sensor locations for this system are more widely distributed than for each of the azimuth drive systems. Consequently, individual sensor cabling will have to be routed over antenna structure to the elevation remote module. All remote modules will be housed in ruggadized containers and conditioned for the natural and induced environments on the antenna. The following discussions present our preliminary selections of remote module subsystems.

1) <u>Sensor and Amplifiers Subsystem</u>

Sensors will include accelerometers, microphones, and possibly, acoustic emission (AE) transducers for dynamic signal measurements and other measurement devices, such as proximity sensors for drive shaft speed/phase data and instrumentation to measure motor electrical load. We anticipate a broad application of surface-mounted accelerometers for most drive system components; however, certain components may require AE sensors for signature definition due to the quasi-static nature of their operation. A good example is the "bogie" pivot bushings in the azimuth wheel-rail systems. Typical sensors and power amplifiers are identified below:

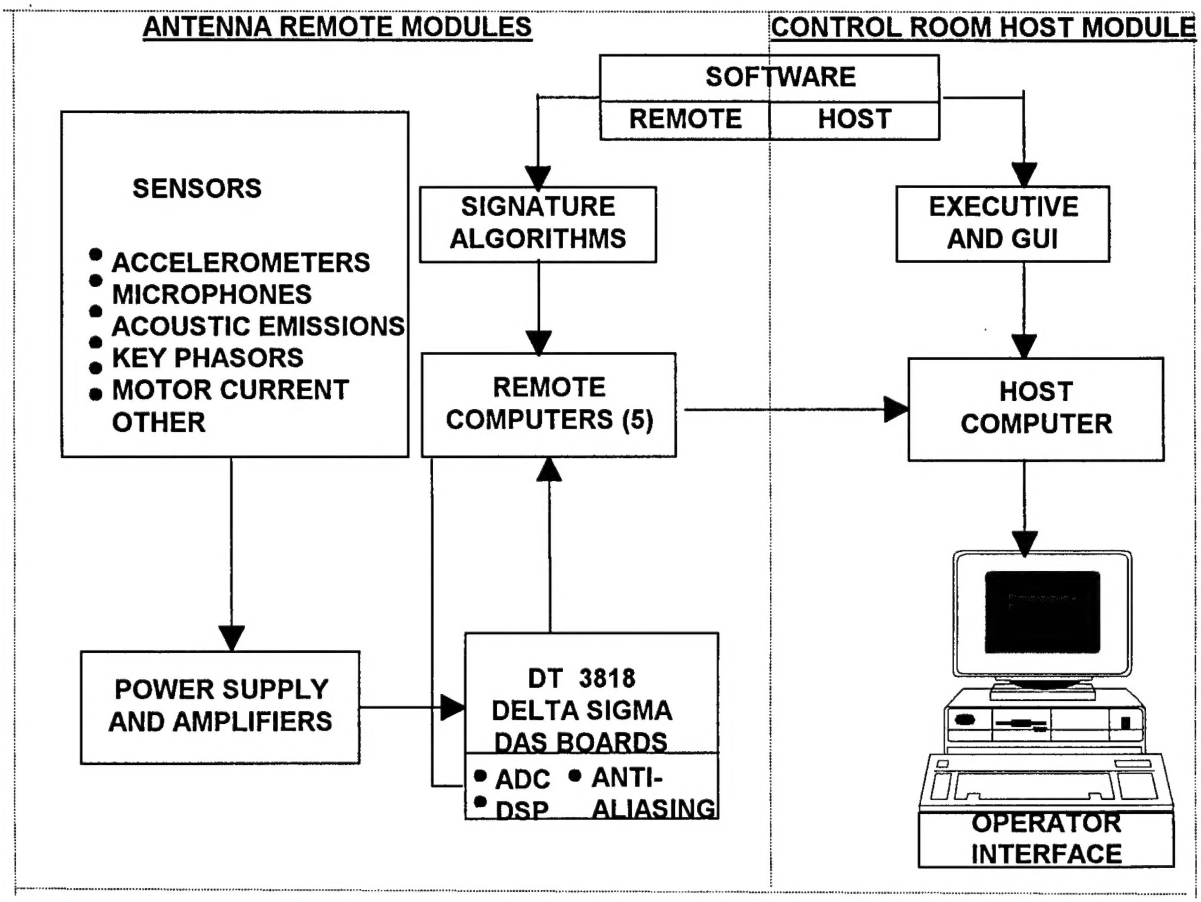

FIGURE 32 Preliminary PSADDS Architecture Showing Remote and Host Modules.

SENSORS

B&K 5958 Accelerometers

The B&K 5958 accelerometers are rugged sensors used for permanent vibration monitoring installations. The accelerometers can be used in a variety applications in wet, submerged, oily, or sea water environments. They can even be mounted underwater down to 400m depth.

The accelerometers come with permanently mounted integral cable and integral preamplifier built-in. The case is insulated and internally shielded. An integral coaxial cable of 10m is supplied standard. Since the cables are integral, these accelerometers are ideal for use in the harsh corrosive environment of the ALTAIR applications.

B&K 4189 Microphones

The microphones will be mounted on the bogies or the sides of the tract to pick up acoustic signals due to vibration. The signals will be composed of several bearings, motor, fuel pump, and the gear box. The signal will be more difficult to analyze than accelerometer signals at each bearing. However if the signal could correlate with the accelerometer signals, the simplicity of the microphone setup could lead to a very efficient, integrated monitoring system.

The 4189 Microphones are general purpose ½" condenser microphones. The 4189 microphones require Type 2671 preamplifiers.

Digital Wave B1025 AE Transducers
Digital Wave's B1025 transducer exhibits a flat response over a frequency range of 50 to 2000 kHz. These sensors are specifically designed to measure the extensional (in-plane) and flexural (out-of-plane) modes. The ¼ inch aperture provides a reasonable compromise between high frequency phase cancellation and wave mode sensitivity.

Proximity Probes
8mm proximity probes to be used for the key-phasor at the driving motor. The key-phasor will be permanently mounted adjacent to the drive shaft and the proximity probe measures the shaft motion. The key-phasor signal is important not only to synchronize the phase with the driving signal but also to differentiate the direction of the motion.

Power Amplifiers
All the above sensors require power amplifiers. Rack-mounted 5956 mainframes will be used for mounting the power supplies. Each mainframe can accommodate 12 WB1328 amplifiers and signal conditioners. Each WB1328 module consists of three channels. The modules will be added as needed.

2) **Data Acquisition and Digital Signal Processor Subsystem (DADSPS)**

The DADSPS will be configured to achieve high speed dynamic performance in the conversion and analysis of the dynamic signals from the various sensors of the SCS. The sequence of events to be performed by the DADSPS is:

1) Analog to Digital Conversion (ADC)
2) Anti-Aliasing Filtering
3) Signal Analysis using ASRI's Software Algorithms

We have tentatively selected the following integrated DSP-based data acquisition boards to serve the functions of the DADSPS.

Fulcrum Delta Sigma DT 3818 DSP-Based DAS
The DT 3818 provides .8-channel signal processing using Delta-sigma A/D converters, digital anti-aliasing filters, and a TIC40 digital signal processor (DSP) Throughput is up to 52 kHz/channel for each of eight differential inputs. The DT 3818 provides sufficient speed and computing power to achieve real-time signal analysis for the dynamic measurements that will be produced by the sensor subsystems.

3) **Remote Computer Subsystem, RCS**

The real-time data acquisition and digital signal processing will occur in the DADSPS subsystem previously discussed, however, they cannot be used as stand-alone computers. The DADSPS boards will be installed in the ISA bus of IBM compatible PCs. Software management of DADSPS operations will be performed by the RCS and the RCS hard drive will provide digital data storage and retrieval in support of DSP operations. Selection of a specific PC has not been made for the preliminary design, however, the specifications for the RCS will identify both computational and data storage requirements as well as the packaging constraints imposed by the natural and induced environments for their remote operation.

7.2 Host Module

The host module integrates the total PSADDS and provides the operator interface to the total system. The two subsystems that comprise the host module are described in the following subsections:

1) Host Computer Subsystem (HCS)

The tasks of displaying already processed data in real time, and recording the results of the extensive real-time signal processing algorithms to permanent storage, are best met through the use of a general purpose host computer. It can also serve as the software development platform. We propose to use a general purpose desktop PC type computer with high performance interface bus. While a vast array of desktop PC computers are available, an IBM PC clone is selected as the PSADDS development platform and host for the following reasons:

1) Cost effectiveness and wide hardware availability
2) Wide use throughout the engineering and business communities
3) Availability of ruggedized hardware as needs arise
4) Operating system flexibility, including a widely used GUI (Microsoft Windows)
5) Wide range of software development tools
6) Multitude of hardware/software vendor sources

The recommended PC platform for hosting these subsystems is a current state-of-the-art PC: A Pentium based computer running at a processor speed of 200 MHz, 2 Gbytes hard disk, 32 Mbytes of memory, and all the necessary storage and video support hardware. In addition, we plan to provide a large data storage backup system using either optical disks, removable magnetic disks, CD writer, or tape.

2) Graphical User Interface Subsystem (GUIS)

The graphical user interface subsystem will be developed in the Windows operating system. A user friendly system allowing future expansion is critical for this development. The GUIS should allow an operator to access on screen help for all the operating questions. Development of this on screen help capability shall not burden the storage requirement and speed performance. Care shall also be exercised to allow future updates and expansion of the interface software. Less important commands shall be grouped in optional menus.

[8] SPECIAL COMMENTS

One of the major objective of the SBIR Phase I program is to Identify the best method to generate a frequency spectrum of antenna drive components as diagnostic signature for on-line ALTAIR health monitoring. The field test data taken from the MISA antenna drive-train system has demonstrated that most vibration measurements across the MISA drive train are subjected to strong interference from air blower noise and vibration which would affect the effectiveness and reliability of fault detection and identification. The Phase I study using actual MISA test data has identified a unique PSEM PSD as the best format to represent best frequency spectrum as diagnostic signature for the drive train component. The PSEM PSD can (1) identify non-sync-related anomalies due to air blower noise interference, (2) identify sync-related anomalies due to bearing defects, and (3) provide a frequency normalized PSEM PSD which is more desirable under nonstationary antenna operations. In addition, a nonlinear coherence analysis techniques has been demonstrated to be highly effective in identifying and discriminating air blower interference.

The conventional linear spectral analysis (power spectrum, correlation/coherence functions, etc) has been used extensively for machinery/drive train health monitoring and fault diagnosis. However, phase information of machinery vibration signals can play a significant role for fault diagnostics and better identifies well-hidden defect symptoms which are often unidentifiable using conventional spectral analysis. The Phase I feasibility study utilizing MISA test data has shown that due to the lack of phase information among different frequency components, these conventional spectral analysis techniques would not be effective either in representing the best frequency spectrum as diagnostic signature nor in detecting and discriminating the noise interference from air blower.